Final Report

BUILDING ENVELOPE THERMAL AND DAYLIGHTING ANALYSIS IN SUPPORT OF RECOMMENDATIONS TO UPGRADE ASHRAE/IES STANDARD 90

R. Johnson, R. Sullivan, S. Nozaki, S. Selkowitz,
C. Conner, and D. Arasteh

Energy Efficient Buildings Program
Lawrence Berkeley Laboratory
University of California
Berkeley, California 94720

prepared for:

Battelle Pacific Northwest Laboratories
Richland, Washington 99352

September 1983

The data base definition and procedural guidelines for this report appear as Lawrence Berkeley Laboratory Report, LBID-801.

ERRATUM

to

BUILDING ENVELOPE THERMAL AND DAYLIGHTING
ANALYSIS IN SUPPORT OF RECOMMENDATIONS TO
UPGRADE ASHRAE/IES STANDARD 90

Some of the weather data used in the DOE-2 runs for Las Vegas, Medford, Albuquerque, Boise, Nashville, Los Angeles, and New York City have been found to be in error. Results for the basic five climates are not affected. The climate-generalized results, derived from the full 14-climate data base, incorporate the DOE-2 results generated with erroneous weather data. This is expected to have some influence on peak cooling values and small effect on annual cooling and heating values. Results affected include data presented in Tables 6.18 and 6.19 and Figures 6.1 through 6.42.

Vol. I

Table of Contents

Abstract

Fenestration design can greatly affect the energy requirements for space conditioning and electric lighting in buildings. The net annual effect greatly depends on the effectiveness of daylight utilization with specific results being a complex function of the interaction among building design features, building operating characteristics, and climate.

The object of this study was to isolate the energy effects of fenestration and electric lighting design, quantify these effects, and develop simplified analysis tools for compliance use in the building envelopes section of ASHRAE/IES Standard 90.

In this study, envelope thermal conductivity, fenestration design, and electric lighting characteristics are parametrically varied through a wide range of values and in a diversity of climates. For these parametric variations, annual energy consumption is calculated with the DOE-2.1B energy analysis program. The numerical results are collected and stored on tape. From this data base statistical analysis is performed using multiple regression techniques leading to simplified correlation expressions among important building and climatic variables. These expressions characterize annual energy performance trends for cooling, heating, and cooling peak so that users can easily ascertain the energy implications of design options for fenestration, daylighting, and electric lighting.

1.0 Introduction

As a part of the project managed by Battelle Pacific Northwest Laboratory to upgrade ASHRAE/IES Standard 90-75A (Energy Conservation in New Building Design), the need was recognized to accommodate building design using daylighting as an energy conservation feature. The Windows and Daylighting Group at Lawrence Berkeley Laboratory was contracted to develop the technical basis on which daylighting could be made an integral part of the building envelope criteria of the standard. This effort evolved into a large-scale parametric study done in collaboration with the Building Energy Simulation Group at LBL and covering the major variables in fenestration and daylighting design and providing a fenestration energy performance data base for developing building envelope design criteria.

Developing the results of this study into criteria recommended for adoption by ASHRAE was the responsibility of other members of the PNL project team, in particular the Technical Evaluation Committee (TEC) chaired by Jerold W. Jones. While the initial intent of the project was to develop some form of daylighting credits that could be applied to existing envelope criteria, it was subsequently recognized that a complete restructuring of the envelope criteria was necessary. Agreement

on this issue was reached with project management and the TEC, and LBL staff was asked to recommend approaches to developing new criteria. This mid-project shift in emphasis will be encountered in the development of rationale described in this report.

Using DOE-2.1B [1][2][3] as the analysis tool, a parametric study was originally designed to include those variables specifically relevant to daylighting energy impacts. To these the overall building envelope thermal conductance was added as a variable parameter, thus expanding the study to include all the pertinent variables under consideration in the ASHRAE envelope criteria.

The completed DOE-2.1B parametric runs produced a voluminous data base. By applying statistical analysis procedures, it was possible to develop from this data base functional correlations having high levels of agreement with individual computer simulations. First, highly accurate correlations, consisting of a large number of terms including exponentials, were generated. This form, because of its complexity, was cumbersome and did not use terms or a format that practicing engineers would have easily recognized. Practical considerations of the needs and expectations of the design community led to the request that LBL develop functional correlations that were linear, and explicitly described envelope design parameters, and were climate-generalized. Substantial additional analytic effort achieved these ends. The results are those recommendations presented in this report.

While the Windows and Daylighting Group and the Building Energy Simulation Group were engaged in the fenestration aspects of this problem, colleagues in the LBL Passive Solar Group collaborated in an examination of the effects of building mass. They developed mass correction factors compatible with our recommended envelope criteria. The results of their efforts are reported separately.[4]

2.0 Objectives

The principal objective of this study was to define the effects of building envelope design on net annual energy performance as a function of thermal conductivity, fenestration design, daylight utilization, electric lighting power density, and climate. This definition will then provide the basis for developing a simplified methodology by which the related design variables can be responsively accommodated in the building envelope criteria of ASHRAE/IES Standard 90.

The principal issue is appropriate accounting for solar radiation through glass. Solar thermal gain can provide energy benefits by offsetting winter heating loads, but imposes a penalty in cooling loads. Use of daylight, however, can drastically alter the energy consumption patterns of a building by reducing the requirements for electric lighting. Of further importance is the potential for using daylighting to

reduce cooling load by utilization of daylighting. Concurrent reductions in electric lighting load and cooling load can result in important peak electrical load reductions. Realization of the potential energy benefits to be derived from fenestration requires a careful consideration of the trade-offs among the energy flows in the context of an operating building.

3.0 Technical Approach

Considering that the number of possible combinations of building design, building operation, and climate variables is very large, the problem first had to be defined in terms of a manageable number of variables. Second, an adequately large and accessible data base had to be generated within these limits, and third the necessary and important correlations of energy interactions had to be developed from this data base.

3.1 Project Organization

The project was organized into three overlapping phases addressing the three requirements given above.

3.2 Strategy and Assumptions

It was clearly recognized that this study could not define energy performance for all buildings in all climates or provide adequate prediction thereof. The objective was, rather, to characterize energy performance as a function of building envelope influences over an extensive range of parameters. It was assumed that, based on a sufficiently large parametric range, such characterization could be extended to a broader range of building types not specifically treated in this study.

The structure of Standard 90, in which building envelope and HVAC systems are treated independently, limited the ability to consider the interaction of HVAC system operation and building envelope design. Because the standard disregards these interactions, the study therefore attempts to arrive at system-independent effects by limiting energy considerations to zone coil loads. It was then assumed that reducing energy requirements at this level, through refinements in envelope design, could offer a basis for reducing energy use in the building.

This approach is discussed in detail below.

3.3 Methodology

The first phase of the project required formulating a definition of realistic limits to the problem. This required defining both the physical building geometry and the parametric limits which in turn led to development of a prototypical building module in which fenestration effects could be isolated and characterized. Conceptual development of the module was facilitated by prior experience in similar studies using

prototypical modules. Certain parametric limits necessary to satisfy requirements for the standard were defined by the TEC. Within these bounds uncertainities were resolved through a sensitivity study; agreement on parameter definition was then reached with the TEC.

Concurrent with the development of the parametric study design, improved algorithms were written and incorporated into the DOE-2.1B program and post-processing capabilities were developed specifically for this project.

During the second phase, the design of the parametric study was finalized and implemented. Parametric runs were completed, with results stored on tape and subsequently processed into data files for analysis.

The third phase consisted of data analysis and the development of functional correlations.

3.3.1 Building Module Concept

The need to generate results that could be generally applied to a wide range of building types and configurations led to using a prototypical building module in which the important energy use patterns could be characterized on a unit area basis as a function of orientation and then applied to other configurations. Prior experience in similar studies[5] has demonstrated the viability of using a building module consisting of a single story of a multistory building with a square floor plan. Use of a prototypical building module for generalized analysis met the approval of the TEC. Certain design constraints were then imposed by the TEC in order to satisfy predetermined ASHRAE requirements. The basic module evolved from prior experience cited above. Final details of the new module were determined by a sensitivity study that considered ASHRAE objectives.

The new basic module consists of four perimeter zones of identical geometry surrounding a one-hundred-foot-square interior zone (Fig. 3.1). For modeling vertical windows, identical fenestration consisting of continuous strip windows is used in the exterior wall of each perimeter zone. For modeling skylights the perimeter zones are eliminated and skylights are uniformly distributed over the roof. Vertical windows and skylights are treated independently and not modeled simultaneously.

In order to isolate the energy effects of interest, thermal transfers were selectively constrained. For the fenestration studies the important issue is the orientation-dependent flows through the exterior wall and window system. For this reason, the floor and the ceiling are modeled as adiabatic (i.e., no heat transfer) surfaces, which is a realistic assumption for multistory buildings. The walls at each end of the perimeter zones are also modeled as adiabatic surfaces in order to limit envelope effects to the fenestrated exterior wall. The envelope effects

can thus be considered analogous to those in an individual office in a series of contiguous offices. Normal building thermal interactions include small transfers between core and perimeter. This interaction was accounted for by modeling thermal transfer through a conventional gypsum board partition wall.
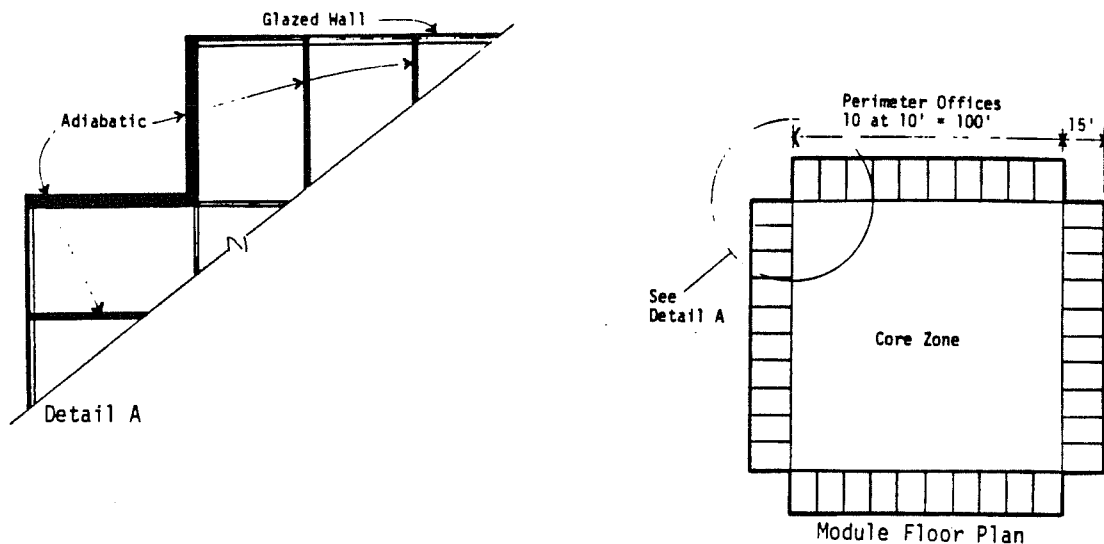

FIGURE 3.1 MODULE CONFIGURATION

For the skylight studies the roof/skylight system is the element of interest. In the skylight model, the exterior walls and the floor were modeled as adiabatic surfaces, thus limiting envelope energy flows to the roof and skylight system.

With building geometry so defined, orientation-dependent loads calculations in the DOE-2 program are reported for each zone. Since the loads calculation in DOE-2 are made at a constant interior temperature, calculations must be carried to the system level to realistically determine loads, given the variables of thermostat night set-back and other operating strategies. Consideration of all the variations and nuances of different HVAC systems was beyond the scope of this envelope study, and it was accepted that analysis would be based on zone coil load comparisons using a single consistent system type. Ideally, the coil loads should somehow be independent of system type, but this is not possible because some type of system must be simulated in order to obtain the loads. To isolate zone loads from building system interactions, a separate single-zone system was assigned to each zone. Under these conditions a simple-constant volume variable temperature system was considered acceptable for determining coil loads in response to envelope design. Thus in the five-zone building five separate single-zone,

constant-volume variable temperature systems are simulated. Building operating and occupancy schedules were based on the Standard Evaluation Technique (SET) standard profiles.[6] With the basic modules as described, an extensive sensitivity study was conducted to determine details of the final module design and to establish the limits of parametric consideration. The sensitivity study is described in the following section; a detailed description of the final building module and parametric variations follows.

3.3.2 Design of the Parametric Study

3.3.2.1 Sensitivity Study

In designing the parametric study, first a sensitivity study was done to establish the importance of considered variables, bound the limits of consideration, and define the details of the building module. Issues for consideration were established collaboratively by members of the project TEC and members of the LBL staff and are summarized below. The sensitivity issues were studied with weather data from Madison, Wisconsin, and Lake Charles, Louisiana, these being the climate extremes of the five climates originally selected for the study. At this point in the study the emphasis was placed on developing a "daylighting correction factor" to be applied to the thermal resistance criteria in standard 90. The sensitivity issues were then considered primarily as they affected what was perceived as daylighting-related performance.

The sensitivity issues and results summarized below have been previously presented in detail in progress reports.

3.3.2.1.1 Issue: Lighting Control Strategies

The study covered five types of control strategies to reduce electric lighting output in response to daylight levels in the interior spaces. With lighting power density at 1.7 W/ft^2 and a requirement to maintain 50 footcandles (fc), electric lights were controlled by continuous dimming, three-level switching, two-level switching, and one-level (on/off) switching.

Results: Daylight utilization primarily affects cooling load and electric lighting load. The effects are largest on orientations exposed to direct solar radiation and with a large glass area [window/wall ratio (WWR) = 0.5]. In these cases the energy performance with the five different approaches tended to group closely. Deviation from this close grouping occurs as the daylight contribution is reduced by reducing either the shading coefficient/visible transmittance or the window area. As daylighting contribution is diminished, the relative effectiveness of multistep and dimming controls increases relative to on/off control.

Conclusion: Lighting control systems can be limited to two types in the parametric study. Continuous dimming will provide maximum responsiveness. A multilevel stepped system, with the number of levels related to power density, will provide comparative performance.

3.3.2.1.2 Issue: Off-Normal Orientation

Energy performance was studied in relationship to the four cardinal points of the compass (N,S,E, W) and at 45° intermediate points (NE, NW, SE, SW) using WWR = 0.5 to maximize solar effects.

Results: Energy performance of E, SE, S, SW, and W tended to group within fairly narrow limits. Energy performance for NE and NW was intermediate between N and E or N and W.

Conclusion: The energy performance at off-normal orientations can be reasonably interpolated.

3.3.2.1.3 Issue: Interior Mass Effects

Interior mass was varied by increasing floor slab thickness from 4 in. to 8 in. The thermal response factor was varied by modeling the floor with tile and with carpet.

Results: The difference in annual energy performance among these configurations was very small.

Conclusion: Interior mass need not be included among parameters in this portion of the study. Detailed mass studies will be done by others.

3.3.2.1.4 Issue: Exterior Wall Mass Effects

The exterior wall configuration was studied as a "quick" wall (instantaneous thermal response), a light curtain wall, and a 6-in.-thick concrete wall.

Results: Energy performance differences between the quick wall and the curtain wall are negligible. Significant differences occur between heavy mass wall and the light mass walls. Changes in energy performance due to daylighting are, however, of similar magnitudes in all three configurations.

Conclusion: Glazing performance dominates the exterior wall performance and should govern the parametric study. Daylighting effects are of similar magnitude regardless of mass. Lightweight curtain walls dominate commercial construction and should serve as the basis for the parametric study model. Detailed mass studies will be done by others.

3.3.2.1.5 Issue: Interior Equipment Load

Energy performance was compared with interior equipment load at 0.25, 0.5, and 0.75 W/ft^2.

Result: Within this range, variations in interior equipment load resulted in small differences in annual energy performance.

Conclusion: Within these limits interior equipment load is a relatively small component of total load and can be considered at a single value, 0.5 W/ft^2, for the parametric study.

3.3.2.1.6 Issue: Perimeter Zone Depth

Energy performance was compared between a 15-ft-deep perimeter zone and a 30-ft-deep one.

Result: The change in thermal energy performance, on a unit area basis, due to daylighting was not significant.

Conclusion: Effective daylighting may be attainable in deep perimeter zones and may be a viable design strategy if properly and carefully considered. Even so, for the larger percentage of conventional building design, good daylighting performance cannot be assured in deep zones. Daylighting design in deep zones would typically require more critical design considerations that may exceed the scope of currently normal design practice and the present intent of the standard. The parametric study should thus be limited to presently realistic expectations and concentrate on the 15-ft depth. Deeper daylighting penetration should be a consideration in future revisions of the standard, assuming design practice will then accommodate such considerations.

3.3.2.1.7 Issue: Importance of Plenum Effects

Energy performance was initially modeled with 3.5-ft plenum in a 12-ft floor-to-floor configuration and compared to no plenum at 12-ft floor-to-floor and no plenum at 8.5-ft floor-to-floor. No other changes were made to the model.

A second set of comparisons was made between the 12-ft floor-to-floor with plenum and the 8.5-ft floor-to-floor without plenum. In this set the overall thermal conductivity $(UA)_0$ remained constant. Infiltration was also adjusted to be constant for both models.

The model for the sensitivity study originally included minimum humidity control. This was eliminated from the final model since it was not being used in the 10 test buildings. Minimum humidity control remained in the sensitivity model for the first two sets of comparison runs. Therefore, a third set of comparisons was made using the models from the second set with minimum humidity control deleted.

Results: In the first set the absolute magnitude of energy performance varied appreciably with and without the plenum. The relative effect of the daylighting contribution was fairly consistent.

Performance of the plenum and nonplenum models was brought into closer correspondence in the second set. Heating energy increase with shading coefficient increase in the south zone necessitated further study.

Elimination of minimum humidity control in the third set resulted in very close correspondence in energy performance between the two models. Heating and energy performance properly responded to increased solar gain in the south zone.

Conclusion: Modeling the plenum space doubles the number of zones and therefore the computer time and cost for marginal improvement in results. Considering limits on the computer budget, this time could be better spent extending the data base on variables having greater influence on daylighting-related performance.

3.3.2.1.8 Issue: Fixed Exterior Shades—Overhangs and Fins

Energy performance without overhangs was compared to performance with three overhang depths on all orientations. The overhang depths were calculated to provide full noon-time shading on the south side for June, May/July, and April/August.

Vertical fins were modeled projecting up to 3 ft from the fenestration and perpendicular to it.

Results: Overhangs produced small effects on the north elevation. On the south, overhangs affect cooling performance substantially, with the largest effects from June shading. Extending the overhang length generates small incremental effects. The difference in performance between fins and overhangs on the east and west elevations was small.

Conclusion: Overhangs should be included at least on the south elevation. The June shading depth should be included for all climates and selectively supplemented with April/August shading depth. Proper consideration of fins would require a separate optimization study which is beyond the scope of this project. Overhangs on east and west elevations should be included in this parametric study.

3.3.2.1.9 Issue: Operable Exterior Shades

Energy performance was modeled with operable exterior shades using the same management algorithm as used for interior shades.

Result: Operable exterior shades offer the opportunity for substantial improvements in energy performance over interior shades or fixed exterior shades.

Conclusion: Substantial investigation is necessary in the general area of operable exterior shading, which is beyond the scope of this project. Since these devices are increasing in popularity and have major savings potential, they should be considered for inclusion in future work. It should be possible to extend the present approach by developing an equivalent fixed shading coefficient for each type of operable and operating system.

3.3.2.2 Description of Final Building Module and Parametric Variation

Analysis and conclusions from the sensitivity study were reviewed with the TEC and agreement was reached on the final building module and parametric variables as described below. As previously discussed, the module configuration differs between the fenestration study and the skylight study. For the fenestration study the module is a single intermediate story of a multistory building with four perimeter zones. For the skylight study the module is a top story with perimeter zones deleted. In order to account for variations in building types, three sets of operating schedules, occupancies, and internal loads as selected by the TEC were used. These three types, A, B, and C, are based on conditions for office, retail, and apartment, respectively.

Fenestration area was limited to a window to wall ratio (WWR) that varied from zero to 0.5 where WWR is based on the floor-to-floor dimension. Visible transmittance values of the glass were modeled at two-thirds the value of the shading coefficient. This provides a good approximation for a wide range of the most popularly used tinted glasses. Interior operable shades are modeled on all orientations to automatically close when the direct solar radiation penetration through the glass exceeds 20 Btu/hr-ft^2. This is based on the assumption that direct beam radiation through the glass onto the work surface will create a discomfort glare condition and that blinds or drapes will be drawn to modulate the direct beam radiation. The shade was assumed to have a shading coefficient multiplier of 0.65 and a visible transmittance multipler of 0.35. These values are representative of a wide range of products in common use.

Details of the final building module and parametric variables are summarized below.

Site Conditions

Site: Flat, unobstructed with no adjacent shading
     elements.
Orientation: Cardinal compass directions.

Architectural

Core zone: 100 ft x 100 ft open space, $A = 10,000$ ft.^{2}

Perimeter zones: Fenestration model only,
                 Ten contiguous offices each 10 ft wide
                 and 15 ft deep; zone area = 1500 ft^2;
                 total perimeter area = 6000 ft.^{2}

Height: Total height 12 ft.

         Fenestration model,
         Floor to floor   12 ft nominal
         Floor to ceiling 8.5 ft nominal
         Plenum   3.5 ft nominal
        Actual DOE-2 input includes the 8.5-ft conditioned space but
        excludes the plenum space. Exterior wall U-values are
        adjusted so that $(UA)_o$ is equivalent to that of the full 12-ft
        height. Infiltration input values are similarly adjusted.

        Skylight model: Floor to ceiling 11.5 ft.

Partition walls: Stud wall with gypsum wall board both sides.
                Surface visible light reflectance of 0.5.

Floors: Adiabatic surfaces consisting of carpeting over
         4-in.-thick, 80 lb/ft^3, concrete slab.
         Surface visible light reflectance of 0.2.

Ceiling: Fenestration model only,
         Adiabatic surface consisting of acoustical tile and
         4-in.-thick concrete floor slab above it.
         Surface visible light reflectance of 0.7.

Roof: Skylight model only,
         Configuration with $(UA)_o$ determined to satisfy
         heating degree day criteria of ASHRAE 90 and then
         parametrically varied at (0.75) $(UA)_o$ and (1.5) $(UA)_o$.
         Mass effects are part of a separate study.[4]

Exterior wall: Fenestration model,
            100-ft-long face a no-mass quick wall with $(UA)_o$
            values assigned to satisfy heating degree day criteria of

ASHRAE 90 and then parametrically varied at (0.75) $(UA)_o$ and (1.5) $(UA)_o$. 15-ft-long end walls of perimeter zones are adiabatic. Mass effects are part of a separate study.[4]

Skylight model,
Adiabatic walls.

Fenestration: Continuous strip windows in 100-ft-long
   exterior face.
   Glazed area parametrically varied at 0, 15%, 30%, and 50%
   of 12-ft high wall area.
   Shading coefficient varied at 0.4, 0.6, 0.8, 1.0.
   Visible transmittance varied at 2/3 of shading coefficient.
   Thermal conductance varied from that of single to triple
   glazing as required to satisfy $(UA)_o$ criteria discussed above.

Skylights: Square skylights,
   Evenly distributed over roof on 12-ft centers.
   Glazed area parametrically varied from 0 to 5% of
   total roof area
   Shading coefficient varied from 0 to 0.8.
   Visible transmittance times well factor varied from 0 to 0.8.
   Glazing consists of one layer of diffusing translucent
   white and one layer of clear.

Exterior shading: Fenestration model only,
   Modeled with and without continuous, fixed, horizontally
   projecting, opaque overhangs.
   Overhangs modeled on all four orientations.
   Overhang projection from window head parametrically varied
   to a maximum projection of 0.6 times window height.

Electric Lighting

Type: Fluorescent evenly distributed.

Power density: 0.7, 1.7, 2.7 W/ft^2.

Maintained light level: 50 fc.

Daylighting controls: 1) None.
                       2) Continuous dimming from full light
                           output at 100% power to zero light
                           at 10% power.
                       3) Stepped switching from full light output at
                           100% power to zero light output at zero
                           power.

Daylighting control point:
        Fenestration model;
        10 ft in from window, 30 in. above floor.
        Skylight model;
        At diagonal intersection of four skylights 30 in. above
        floor.

Building Operation

Occupancy density: Type A;   100 ft^2/person
                              Type B;   50 ft^2/person
                              Type C;   300 ft^2/person

Schedules:
  Occupancy: Type A;   SET Standard Profile No. 1 (modified)
                    Type B;   SET Standard Profile No. 12
                    Type C;   SET Standard Profile No. 2

  Lighting: Type A;   SET Standard Profile No. 43
                    Type B;   SET Standard Profile No. 54
                    Type C;   SET Standard Profile No. 44

Infiltration schedule: Mirror of fan schedule, i.e., infiltration at
           specified rate when fans are off and zero infiltration when
           fans are on.

Infiltration rate: 0.6 air changes/hour

Window management: For fenestration model only,
                    Interior shades are
                    automatically deployed when transmitted direct
                    solar radiation exceeds 20 Btu/hr-ft^2.
                    Shade has shading coefficient multiplier of 0.6 and
                    visible transmittance multiplier of 0.35.

HVAC Systems

Type: Single-zone constant volume variable temperature,
      each zone with its own system.

Thermostat schedules:
 Heating
   Type A
      Weekday hours 7 to 18: 72°F; 19 to 6: 63°F
      Weekends and holidays all hours: 63°F

   Type B
      Weekday and Saturday hours 7 to 21: 72°F; 22 to 6: 62°F
      Weekend and holiday hours 7 to 19: 72°F; 20 to 6: 62°F

Type C
    All hours: 74°F

Cooling
  Type A
      Weekday hours 7 to 18: 78°F; 19 to 6: 90°F
      Weekends and holidays all hours: 90°F

  Type B
      All days hours 7 to 21: 78°F; 22 to 6: 99°F

  Type C
      All hours: 78 °F

Fan schedule
  Type A
      Weekday hours 7 to 18: on; 19 to 6: off
      Weekends and holidays, all hours: off

  Type A
      Weekday and Saturday hours 7 to 21: on; 22 to 6: off
      Weekend and holiday hours   7 to 19: on; 20 to 6: off

  Type C
      All hours: on

Night-cycle control: Fans cycle on during normally off periods when
  heating or cooling is required.

Humidity control: None

Economizer limit temperature: 62°F

Outside air requirement: 5 cubic feet per minute/person

3.3.2.3 Weather Data

The daylighting study requirements called for analysis with WYEC weather
data from the same five climates which had been selected previously for
general use in the standards project. In particular, these five cli-
mates were to be used in the 10 test buildings project; it was intended
that the climate-specific daylighting results would be used in that pro-
ject.   These five climates are Lake Charles LA; Madison WI, Washington
D.C; Seattle WA; and El Paso TX.

It was recognized that climate-generalized results would be of even
greater value to the TEC for use in formulating the standard. The LBL
staff considered the five-climate data base inadequate for generating
climate-generalized results having satisfactory levels of confidence.

We, therefore, elected to expand the data base using WYEC tapes from nine additional climates. These were chosen to expand the climate diversity and geographical coverage of the data base. The added climates are Albuquerque NM; Bosie ID; Dallas TX; Las Vegas NV; Los Angeles CA; Medford OR; Nashville TN; Omaha NE; and New York NY.

3.3.3 Modifications to DOE-2.1B Building Energy Simulation Program

A minor modification was made to the DOE-2.1B program to enable the generation of 20 output variables (2 from LOADS and 18 from SYSTEMS) in a special post-processor file. The file contains parameters related to heating and cooling energy; these were used for presentation purposes (both written and graphic) and also to form the foundation of the data base used in the regression analysis. Reference 7 should be consulted for a more complete discussion and listing of the output variables.

3.3.4 Development of Post-Processor Data Handling

In addition to the special post-processor file mentioned above, a general-purpose post-processor file was also generated for each DOE-2.1B run. The general file contains all the information present on the DOE-2.1B reports requested on input. This information is written in a format which can be easily accessed. Either particular quantities such as cooling energy or complete DOE-2.1B reports can be obtained. This file therefore permits discretionary DOE-2.1B output. However, it should be mentioned that the complete DOE-2.1B output is also available for each run. All the formatted DOE-2.1B reports requested can easily be obtained simply by disposing the output file to an appropriate printer. The general-purpose post-processor file, on the other hand, requires the use of certain utility programs to generate the desired DOE-2.1B output. Reference 8 contains the necessary information for selecting and printing this file.

3.3.5 Development of Computer Graphics Data Display

Graphics output was generated through the development of three FORTRAN utility programs. Two of these routines were responsible for reading the special DOE-2.1B output file and creating a new input file for use by the third program, which controlled the plotting sequence calls to the IDDS (Integrated Data Display System) plotting package. Reference 7 contains more details regarding the plots generated and listings of the above FORTRAN programs.

3.3.6 Statistical Analysis with Multiple Regression

In this study a large integrated data base was created, then a series of multiple regressions were undertaken to define coefficients for selected configuration variables that could accurately predict energy usage. Multiple regression is a statistical analysis procedure in which

relationships between different variables are established mathematically using a least-squares approach. Generally, sets of independent variables are defined from which a dependent variable is predicted.

A decision was made early in the program to perform the regression analysis for each climate independently. It was reasoned that with only five climates being simulated a correlation using climatic variables would be difficult. Climate generalization/configuration interface is discussed in the next section of this report. Thus, distinct expressions were generated for each climate and use pattern. Heating peak was not considered in the study after initial results indicated that its value was a function of the startup load and thus could not be related to configuration parameters in a meaningful way. The analysis of overhangs and daylighting resulted in correction factors to the solar heat gain and lighting heat gain terms, respectively. The resulting regression expression for the perimeter zone was of the form:

$$b_1 U_o A_T + b_2 k_o A_g SC + b_3 k_d A_f L + b_4 A_f \qquad (1)$$

where

$b's$ = solved for regression coefficients
U_o = exterior envelope overall U-value (Btu/hr-ft^2°F)
A_T = exterior wall area (ft^2)
A_g = window area (ft^2)
SC = shading coefficient
k_o = correction factor due to overhangs
A_f = floor area (ft^2)
L = lighting wattage (W/ft^2)
k_d = correction factor due to daylighting.

This form of the equation was used for each orientation for all three energy quantities studied. Its compact form and conveniently segregated terms permit a qualitative as well as quantitative analysis of individual components contributing to perimeter zone energy use. Tables 6.1 through 6.9 in the appendix present the regression coefficients and certain relevant statistical variables to indicate the reliability of the fit. Generally, the r^2 (square of the correlation between the predicted value and actual value) values are on the order of 0.97 and above (an r^2 value of 1.0 represents a perfect correlation), with the exception of the heating energy in the perimeter zones, which is usually below this value. However, when heating approaches the magnitude of cooling (this can be seen by observing the mean value of the data), the r^2 increases correspondingly. The skylight or rooftop envelope portion of the analysis yielded a regression expression similar to Eq. (1); the only difference being the lack of an overhang correction factor and an orientation variation. Tables 6.10 and 6.11 present the regression coefficients for configurations A and B, respectively.

The overhang correction factors to the solar radiation heat gain term were derived from a regression using overhang height/window height as the independent variable. Table 6.12 lists the regression coefficients for configuration A for the following equation:

$$k_o = 1. - b_5 R - b_6 R^2 \qquad (2)$$

where

k_o = correction factor
$b's$ = regression coefficients
R = overhang width/window height ratio.

Figures 3.2 to 3.4 present the overhang correction factors for the five base climates. Except for the cooling peak curves, each set of curves is somewhat climate-independent, indicating a useful approximation. The values indicate that an asymptote is approached at an overhang width/window height ratio value of $R = 0.6$ for all climates and orientations of south, east, and west. The amount of solar radiation reduced is on the order of 50% for heating and cooling at the limit of $R = 0.6$. For north-facing fenestration, the correction factor is monotonically decreasing in all cases, with a typical reduction of 25% solar occurring at $R = 0.6$. Selecting the heating curves from Madison as representative of the complete set (heating, cooling, cooling peak) would yield conservative (with respect to cooling peak) estimates.

The daylighting correction to the lighting term of the basic equation was obtained as a function of effective aperture. The effective aperture, which is a dimensionless parameter, is defined as the product of window/wall ratio and visible transmittance. For windows this quantity is multiplied by the overhang correction factor. For skylights, it is multiplied by the skylight well factor. The following expression was derived:

$$k_d = 1. - b_7 (E_a) - b_8 (E_a)^2 \qquad (3)$$

where

k_d = correction factor to the lighting wattage due to daylighting
$b's$ = regression coefficients
E_a = effective aperture.

This equation can be used for all three energy quantities analyzed. The coefficients are presented in Tables 6.13 and 6.14. Figures 3.5 and 3.6 present the daylighting correction factor for the five base climates. For perimeter zones, the regression for each climate differed less than 12% between locations. Thus one set of curves would be an acceptable approximation. These curves are shown on Fig. 3.6. For all perimeter zone orientations, an asymptote is approached which yields a 65% reduction in lighting at an effective aperture of 0.20.

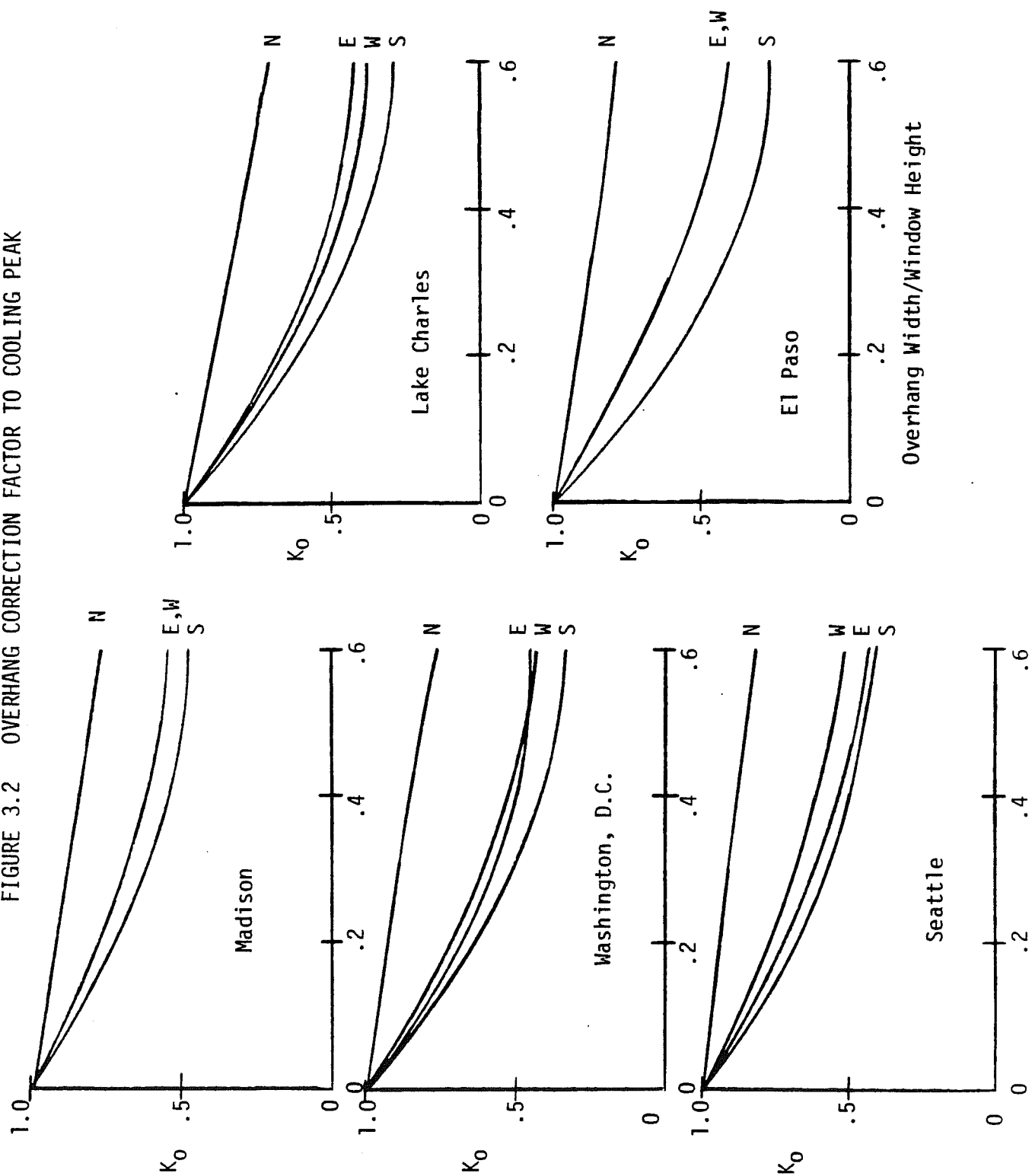FIGURE 3.2 OVERHANG CORRECTION FACTOR TO COOLING PEAK

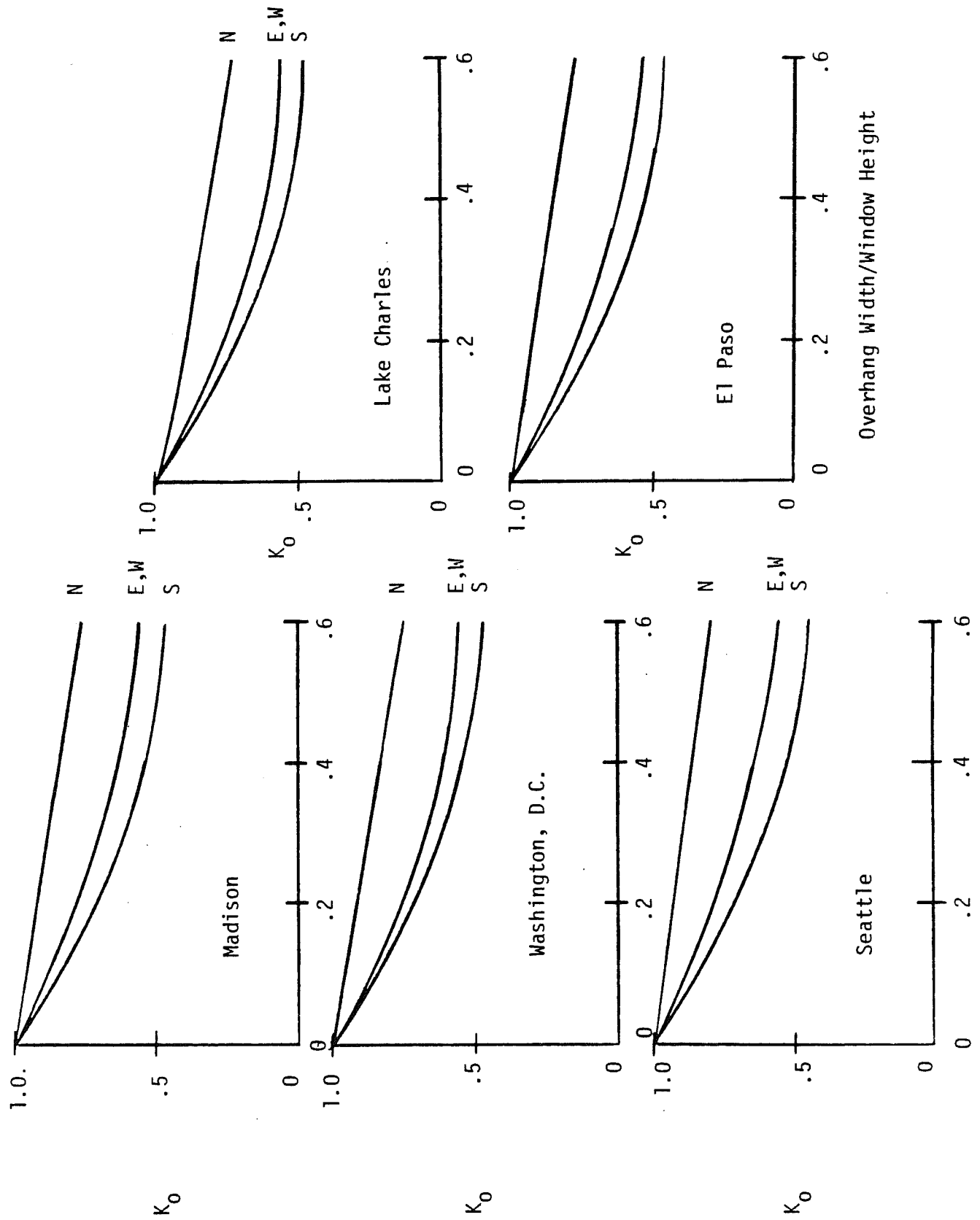FIGURE 3.3 OVERHANG CORRECTION FACTOR TO COOLING ENERGY

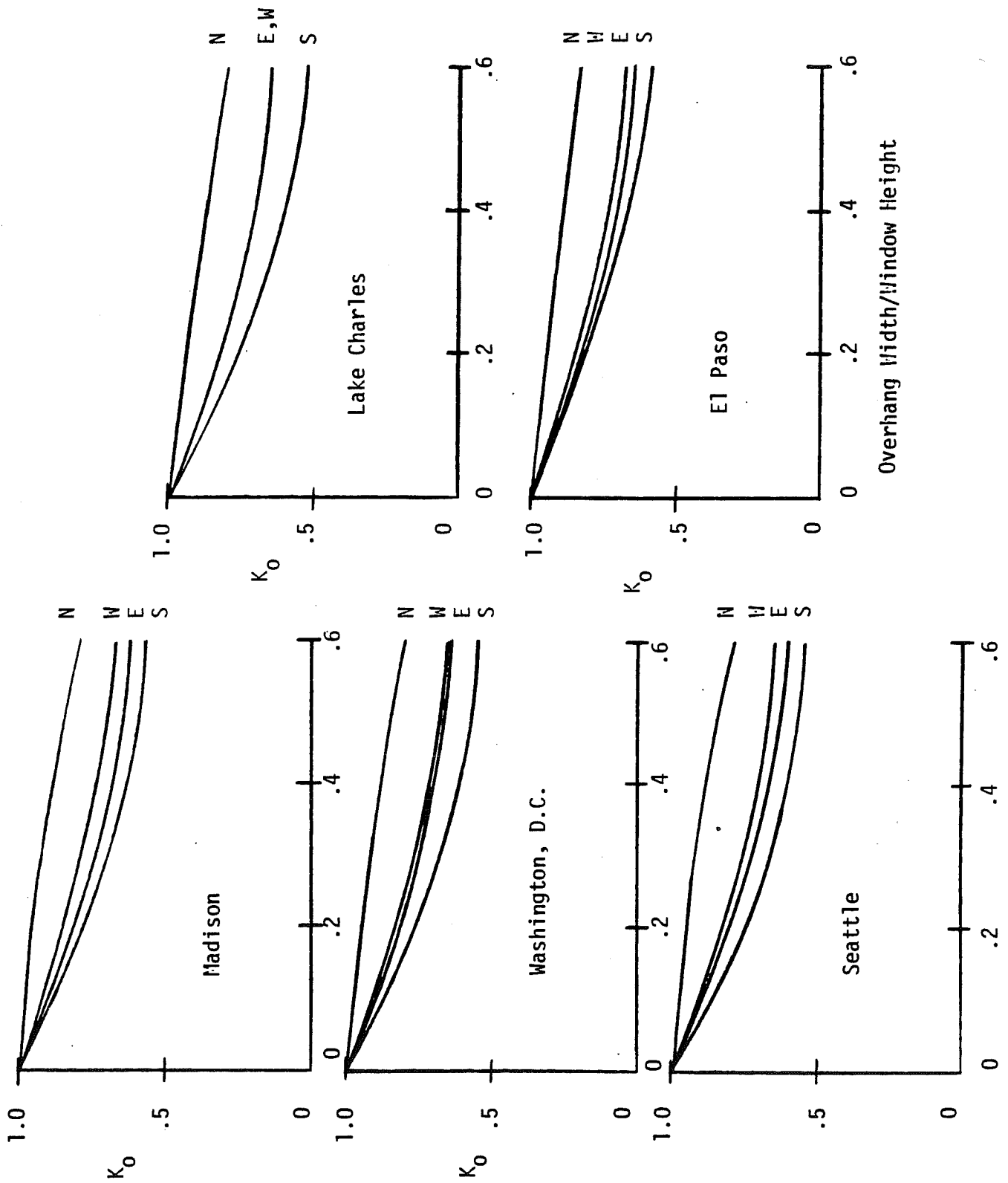FIGURE 3.4 OVERHANG CORRECTION FACTOR TO HEATING ENERGY

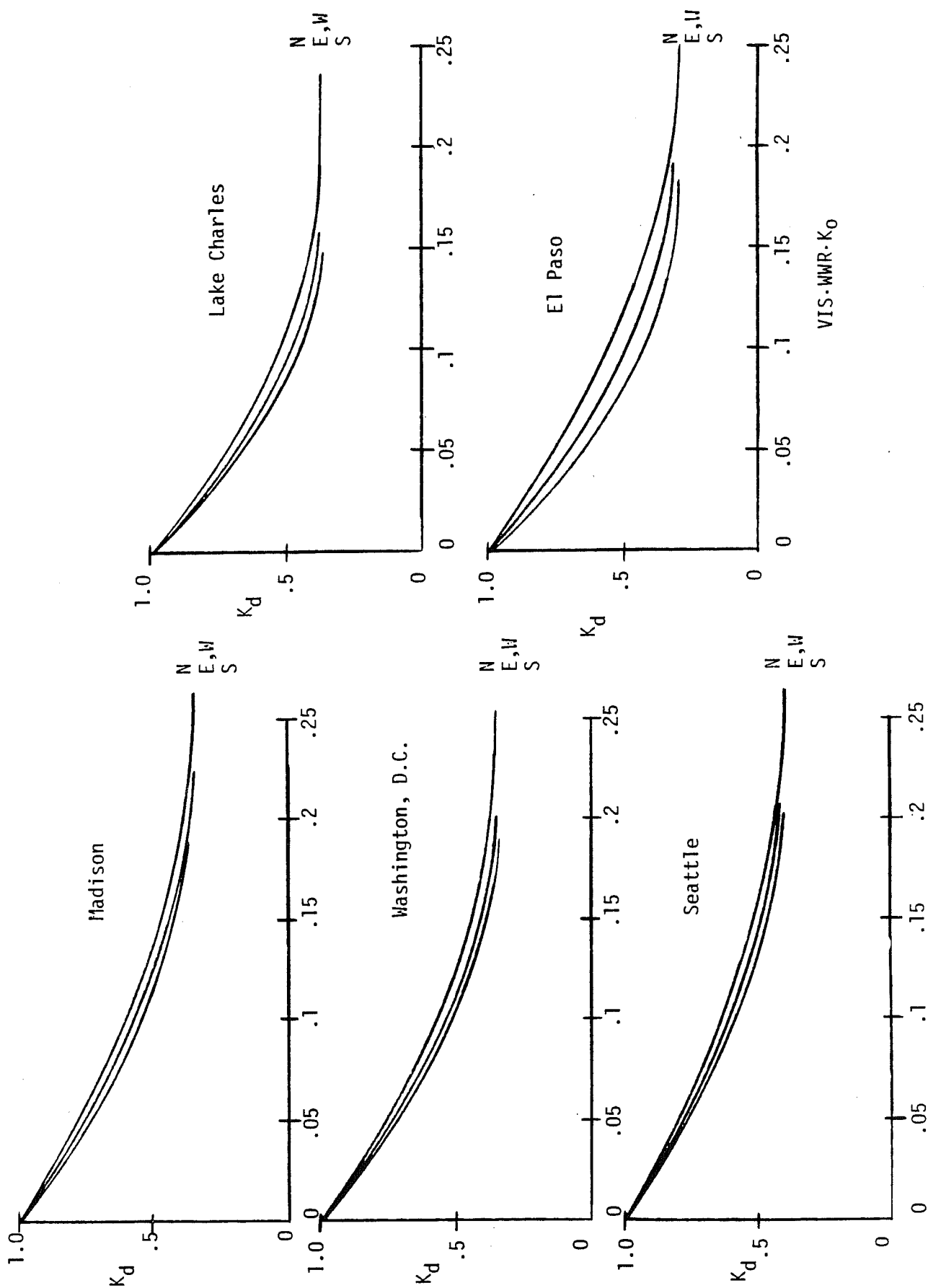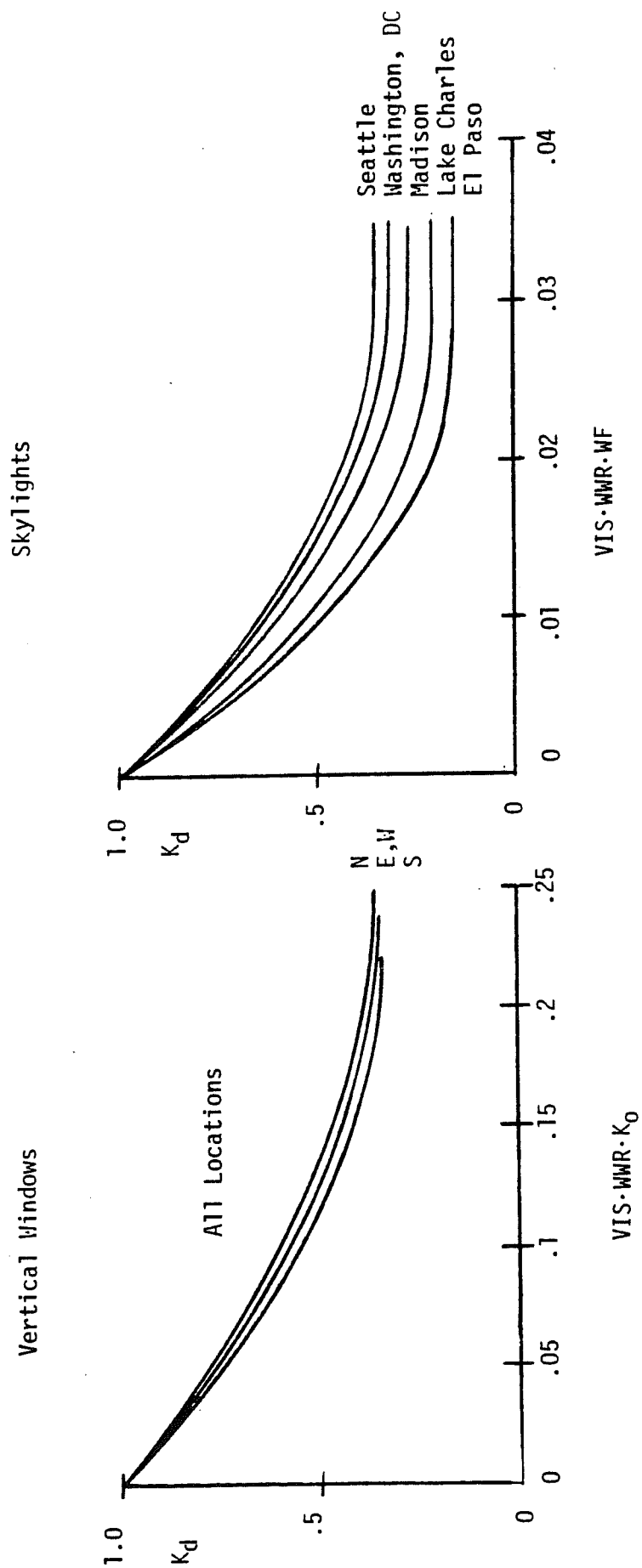FIGURE 3.5 DAYLIGHTING CORRECTION FACTOR TO LIGHTING LOAD – VERTICAL WINDOWS

FIGURE 3.6 DAYLIGHTING CORRECTION FACTOR FOR LIGHTING LOAD

Later in this report, one will observe that this figure can result in a cooling energy savings for perimeter zones on the order of 15% depending on the configuration being studied. Heating energy increases due to reduced electric lighting also approach or exceed this value. However, the base heating required for all locations is much smaller than the corresponding cooling required. The skylight reduces electric lighting from 65% in Seattle to 84% in El Paso, as seen in Fig. 3.6. This variation is different than that observed with the vertical windows due to the lack of shading management for the skylight model. The trend reflects the influence of sky cover and latitude.

Regression of the core zone data, although not required for Standard 90, was nevertheless accomplished. The core zone equation is much simpler than Eq. (1). This is due to the nature of the heat gain/loss components, i.e., there are no solar inputs and only small-zone-to-zone transmission effects. Each load component is a function of the inherent internal heat gains and the external infiltration/ventilation. The regression expression therefore consists of two terms as follows:

$$b_3 A_f L + b_4 A_f \qquad (4)$$

where b_3 and b_4 are the regression coefficients for interior lighting and remaining internal load and ventilation/infiltration quantities, respectively. Tables 6.15 to 6.17 present b values for the three use patterns studied. The difference between the predicted values and the actual values (residual) is very small for both the cooling peak and cooling energy ($r^2 = 0.99$). The heating residuals tend to be large at low energy levels. However, this fact is relatively unimportant because the heating requirements are quite small.

3.3.7 Climate Generalization

The objective of the complete study was to define energy use as a function of both configuration and climatic variables. However, initially the data base contained results from only five geographic locations. To enable a satisfactory climate/configuration interface, nine additional locations using configuration A were simulated. The additional climates analyzed were Albuquerque NM, Boise ID, Dallas TX, Las Vegas NV, Los Angeles CA, Medford OR, Nashville TN, Omaha NE and New York NY. Revisions were applied to the DOE-2.1B weather processing program so that a data base could be constructed to contain both configuration and climate variables. After numerous trial-and-error regression runs, feasible parameters and expressions were selected for the building envelope criteria. This is not to say that the results represent the best fit. Various other solutions yielded more satisfactory predictions but did not lend themselves to presentation suitable for use in Standard 90. Equation 1 was the final form of the expression selected for predicting the desired energy usage quantity (cooling peak, cooling, heating). Climate generalizations for the other configurations were obtained by

relating the regression coefficients for the five basic climates and assuming that the correlation would also be valid for the other geographic locations. Figures 6.1 through 6.12 in the appendix present these relationships for the perimeter zone for configurations B and C and Figs. 6.13 through 6.18 for the rooftop zone for configuration B. Configuration C was not used in the skylight model. Climate was not generalized for the core zone. The purpose of the climate correlation was to make each of the b regression coefficients a function of particular climatic parameters.

For cooling peak, the design dry bulb temperature at the 5% level was selected as the independent variable. A linear relationship was used for each orientation of the perimeter zone and the rooftop zone for each component (conduction, solar, lighting, other). Rewriting Eq.(1) using P instead of b for peak yields:

$$\text{Cooling peak (Btu/hr)}(i^{th} \text{ orientation}) =$$
$$P_{1i}U_{o}A_{T} + P_{2i}k_{o}A_{g}SC + P_{3}k_{d}A_{f}L + P_{4}A_{f} \qquad (5)$$

where

$$P_{1i} = P_{11i}DT + P_{12i}$$
$$P_{2i} = P_{21i}DT + P_{22i} \qquad (6)$$
$$P_{3} = P_{31}DT + P_{32}$$
$$P_{4} = P_{41}DT + P_{42}$$

where

$$p's = \text{solved for regression coefficients}$$
$$DT = \text{design dry bulb temperature at } 5\%.$$

Results for orientations of south, east, and west were forced into yielding the same solution both for simplicity and because the statistical parameters used for measuring goodness of fit indicated such a procedure was valid. A separate solution was also obtained for the north orientation. Tables 6.18 and 6.19 present the values of the above p coefficients.

The cooling energy coefficients are also presented in the above tables. They relate to the following expressions [(where C has replaced b in Eq.(1))]:

$$\text{Cooling energy (kBtu) }(i^{th} \text{orientation}) =$$
$$C_{1i}U_{o}A_{T} + C_{2i}k_{o}A_{g}SC + C_{3}k_{d}A_{f}L + C_{4}A_{f} \qquad (7)$$

where

$$C_{1i} = c_{111}CDD^2 + c_{121}CDD + c_{131}$$
$$C_{2i} = c_{211}LAT + c_{221}$$
$$C_3 = c_{31}LAT + c_{32}$$
$$C_4 = c_{41}LAT + c_{42}$$

(8)

where

$c's$ = the solved for regression coefficients
CDD = annual cooling degree hours (at 80°F)/24
LAT = latitude in degrees.

The regression for the rooftop zone indicated that the squared degree days term was not necessary. This fact was also true of the heating energy equation, which in its final form was expressed as:

Heating energy (kBtu)(i^{th}orientation) =
$$H_{1i}U_oA_T + H_{2i}k_oA_gSC + H_{3i}k_dA_fL + H_4A_f$$

(9)

where

$$H_{1i} = h_{111}HDD^2 + h_{121}HDD + h_{131}$$
$$H_{2i} = h_{211}HDD^2 + h_{221}HDD + h_{231}$$
$$H_{3i} = h_{311}HDD^2 + h_{321}HDD + h_{331}$$
$$H_4 = h_{41}HDD + h_{42}$$

(10)

where

$h's$ = solved for regression coefficients
HDD = heating degree hours (at 55°F)/24.

4.0 Discussion and Summary of Results

The statistical correlations presented in the appendix for the various multiple regressions indicate that good predictions of DOE-2 results are obtained by using an equation of the form of Eq. 1 in Section 3.3.6, with regression coefficients calculated independently for each climate. Actually, the form could be made more accurate by considering quadratic and cross-coupled independent variables of the input heat gain/loss components. Generally, the more detailed the regression model, the better the predictive quality of the final equation. Although large numbers of independent variables may be more accurate in a mathematical sense, their use is limited in a practical sense by the Standard 90 building envelope criteria. Architects and engineers, who in their day-to-day operations will be using Standard 90, require a technique or tool that is easily understood, efficient, and accurate. The basic Eq. (1) with the climate generalizations expressed in Eqs. (5) through (10) fulfill these requirements. It should be kept in mind, however, that the results of this study are valid only within the range of variables parameterized. One should use care in attempting to define a building's energy use from these results. More importantly, however, is the validity of performing a qualitative analysis using these results. This

discussion will proceed with an analysis of results of the five base climates for configuration A, after which the climate generalization will be treated.

4.1 Individual Climate Analysis

The regression coefficients presented in Tables 6.1 through 6.17 can be used in conjunction with Eqs. (1) to (4) in examining the effects of various configuration parameters on energy use. The values give some indication of the importance of each energy usage quantity. For example, the solar radiation heat gain dominates the cooling peak and cooling energy values, followed by infiltration/ventilation, internal heat gains, and envelope conductance. Heating energy, however, is somewhat more complicated because of the presence of negative as well as positive influences. Generally, the solar and internal gains are offset by a portion of the conductance and infiltration/ventilation losses. However, there is a net loss resulting from the fact that most of the conductance and infiltration effects occur during the hours when there are no solar or internal gains. The above statements, of course, could change if the areas involved (wall, glazing, floor) differ significantly. This is easily seen by observing the relative size of the perimeter and rooftop zone solar radiation coefficients. For all climates, the rooftop zone values are much larger; however, the effective apertures are generally smaller than the perimeter zone values, which yields a lower net solar component for the rooftop zones.

Quantitatively, the conductance contribution to the cooling peak and cooling energy is not as consistent as the other coefficients. In the case of cooling peak, this is due to the variation in the particular hour's cooling peak calculation for each configuration. Small component contributions to the cooling peak, especially for those that are temperature-dependent, will tend to appear somewhat random. For the cooling energy coefficients, the conductance contribution is very small, with the possibility of both positive and negative coefficient values. Such a situation is indicative of actual occurrences. For some northerly locations, a conductance loss occurs during some of the hours associated with cooling.

Coefficient values for the conductance portion of the heating energy are more easily examined. North orientations for all configurations and locations yield larger coefficients and thus higher energy use levels. East and west orientation quantities are approximately the same at intermediate values between north and south. It appears that an eventual climatic temperature-dependence might be extracted from the heating energy results. However, it is uncertain at present what form the cooling-related coefficient dependence will have. The rooftop zone values tend to vary in a manner similar to north perimeter zone values.

The regression coefficients of the solar radiation terms for determining cooling peak are more consistent by orientation than by geographic location. First appearances indicate no substantial variation between geographic locations. However, upon closer examination, anomalies exists in both Lake Charles LA and Seattle WA. Generally, the magnitude variation follows a north, east, south, and west pattern from low to high. This variation seems unrelated to the observed weather data for maximum incident solar radiation. Thus, there may be some difficulty in correlating the coefficients to specific solar variables. An additional complication with respect to the solar term involves the management of window shading. In the methodology section of this paper, it was noted that interior shading was implemented at a transmitted direct solar radiation value exceeding 20 Btu/ft^2. The regression model has no method of indicating whether management was employed during the particular hour that the cooling peak was defined. Thus, some irregularities are to be expected between configurations. This fact also complicates the correlation of the perimeter and rooftop zone values because management was not used for the skylights. Generally, the cooling peak rooftop solar values are two to three times as large as the south perimeter zone values. Seattle's values, however, are more than three times as large.

The solar portion of the perimeter zone cooling energy follows a similar north, east, south, and west variation with increasing magnitude. However, there also seems to be a definite climatic variation with latitude, i.e., increasing coefficients with decreasing latitude. Seattle stands out possibly because of a larger amount of cloud cover. Heating energy solar coefficients follow a similar pattern (increasing coefficient implies less negative). The rooftop zone solar coefficients for cooling and heating energy are all larger than the corresponding perimeter zone values, but follow the same climatic variation.

The small incremental changes in the electric lighting coefficients for all configurations and locations for each perimeter zone orientation indicate that a valid approximation would be to lump all four orientations into one coefficient as is the case with the other internal loads and infiltration/ventilation term (b_4). For cooling peak, the variation among orientations almost equals the variation among climates. The cooling and heating energy coefficients, however, vary in a manner similar to the solar term, i.e., proportional to a latitude or temperature difference. This latter statement is also true of the b_4 coefficients. A discernible trend is not apparent with the cooling peak values.

Core zone coefficients follow a pattern similar to the b_3 and b_4 terms of the other zones. The only difference occurs with the heating energy values because there is little or no heating required (see Tab. 6.15). It is interesting to note that the cooling energy coefficients for the perimeter, rooftop, and core zones are of about the same magnitude. This is related to the fact that cooling for these zones is occurring at

the same instant for similar space temperatures; whereas heating requirements for the zones does not necessarily occur simultaneously, i.e., the perimeter zones will experience more heating during the late afternoon hours than the core zone.

4.1.1 Discussion of Example

The usefulness of the regression expressions can be ascertained by calculating thermal load values for a specific example. Figures 4.1 to 4.3 present component breakdowns per square foot of floor area (conductance, solar, lighting, other) for the cooling peak, and the cooling and heating energies in Madison WI. All perimeter zones were assumed to be 15ft in depth and the exterior wall 12 ft in height. Rooftop zone floor-to-ceiling height was 11.5 ft. Parameter values used in the example were:

Perimeter	Rooftop
U_o = 0.211 Btu/ft^2°F	U_o = 0.049 Btu/ft^2°F
WWR = 0.4	WWR = 0.05
SC = 0.8	SC = 0.06
VIS = 0.48	VIS = 0.86
E_a = 0.192	WF = 0.7
L = 1.67 W/ft^2	E_a = 0.03
k_d = 1.0	L = 1.67 W/ft^2
k_o = 1.0	k_d = 1.0

Regardless of the perimeter and rooftop zone floor size (length), the percent contribution of the heat gain/loss components to each zone's respective energy is the same. This fact results from defining the problem through overall U-value, glazing size, and shading coefficient in conjunction with the fixed values of perimeter depth and wall and ceiling height. A linear variation of energy with floor area exists for each zone. This can be seen by rewriting Eq. (1) using the relationships between floor area, exterior wall, and glass area as follows:

Perimeter
$$E/A_f = 0.799 \, b_1 U_o + 0.799 \, b_2 k_o SC \, WWR + b_3 k_d L + b_4$$
Rooftop
$$E/A_f = b_1 U_o + b_2 SC \, WWR + b_3 k_d L + b_4.$$

After substituting the configuration variables, a further reduction is obtained:

Perimeter
$$E/A_f = 0.169 \, b_1 + 0.256 \, b_2 k_o + 1.67 \, b_3 + b_4$$
Rooftop
$$E/A_f = 0.049 \, b_1 + 0.030 \, b_2 + 1.67 \, b_3 + b_4.$$

FIGURE 4.1 COOLING PEAK/FLOOR AREA
MADISON – CONFIGURATION A

LEGEND:
C – Conductance
S – Solar
L – Lighting
O – Other
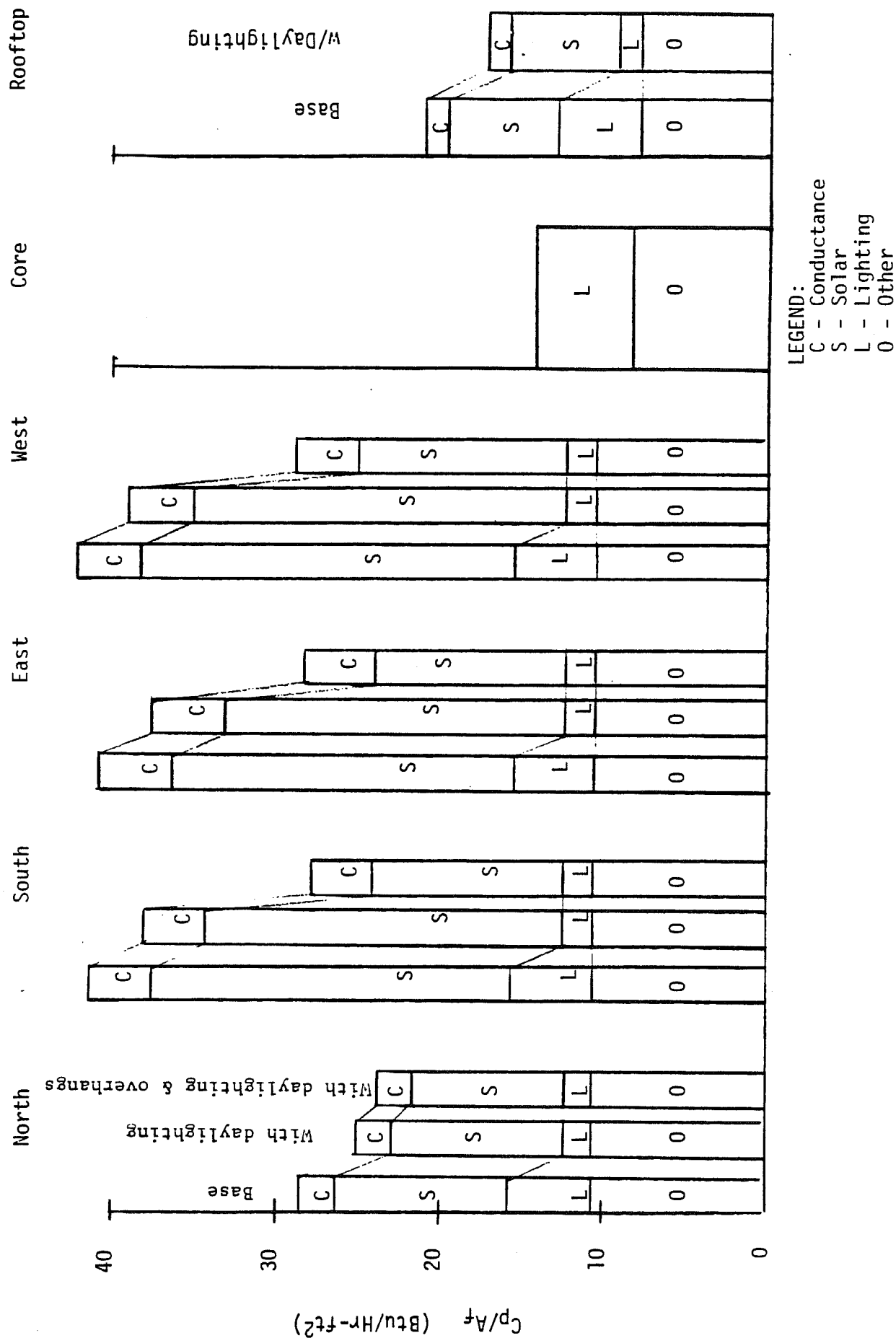
FIGURE 4.2   COOLING ENERGY/FLOOR AREA
MADISON - CONFIGURATION A

Legend: C   Conductance
          S   Solar
          L   Lighting
          0   Other

C_e/A_f (KBtu/ft^2)
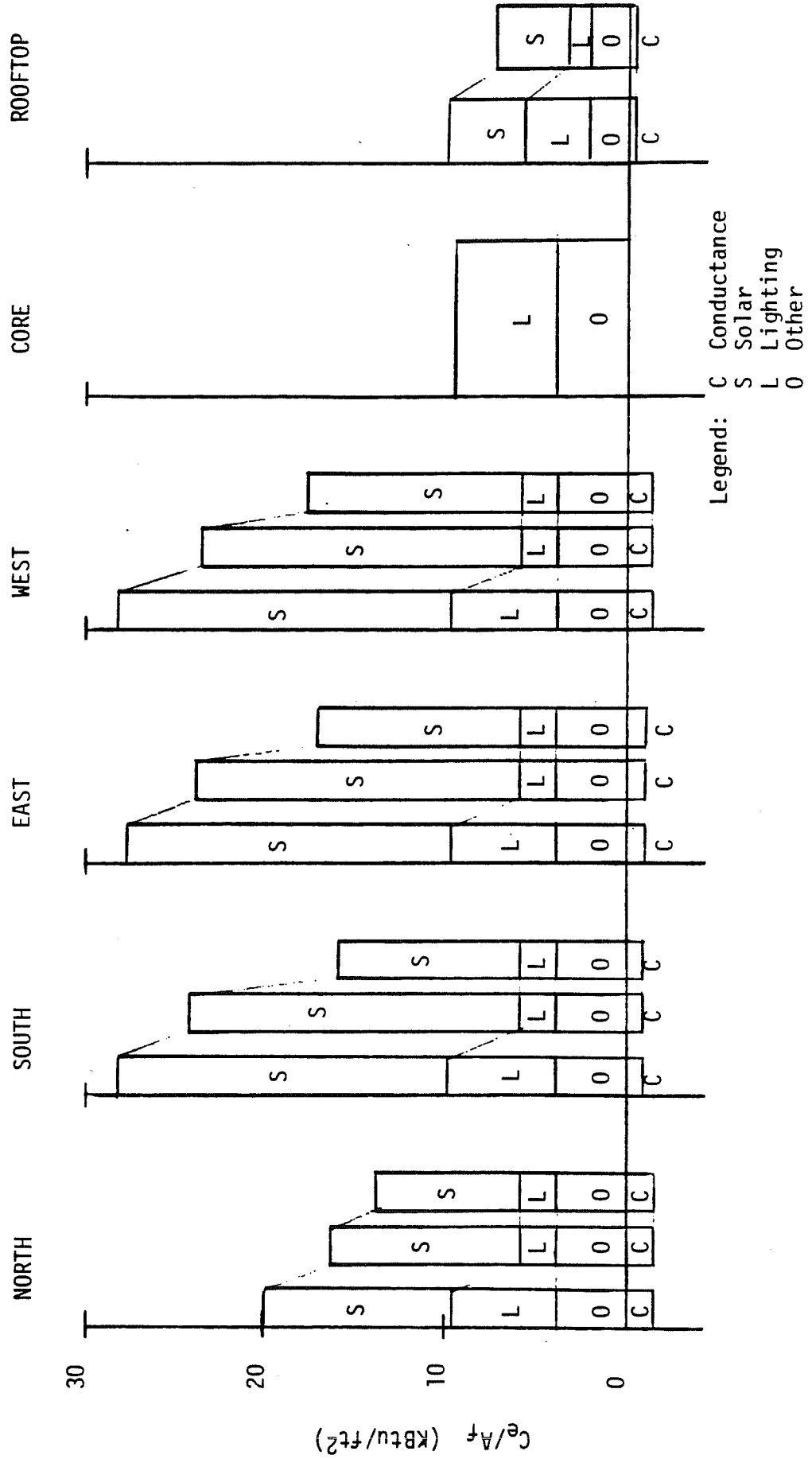
FIGURE 4.3   HEATING ENERGY/FLOOR AREA
MADISON - CONFIGURATION A

Legend

C   Conductance
S   Solar
L   Lighting
0   Other

H_e/A_f (KBtu/ft^2)
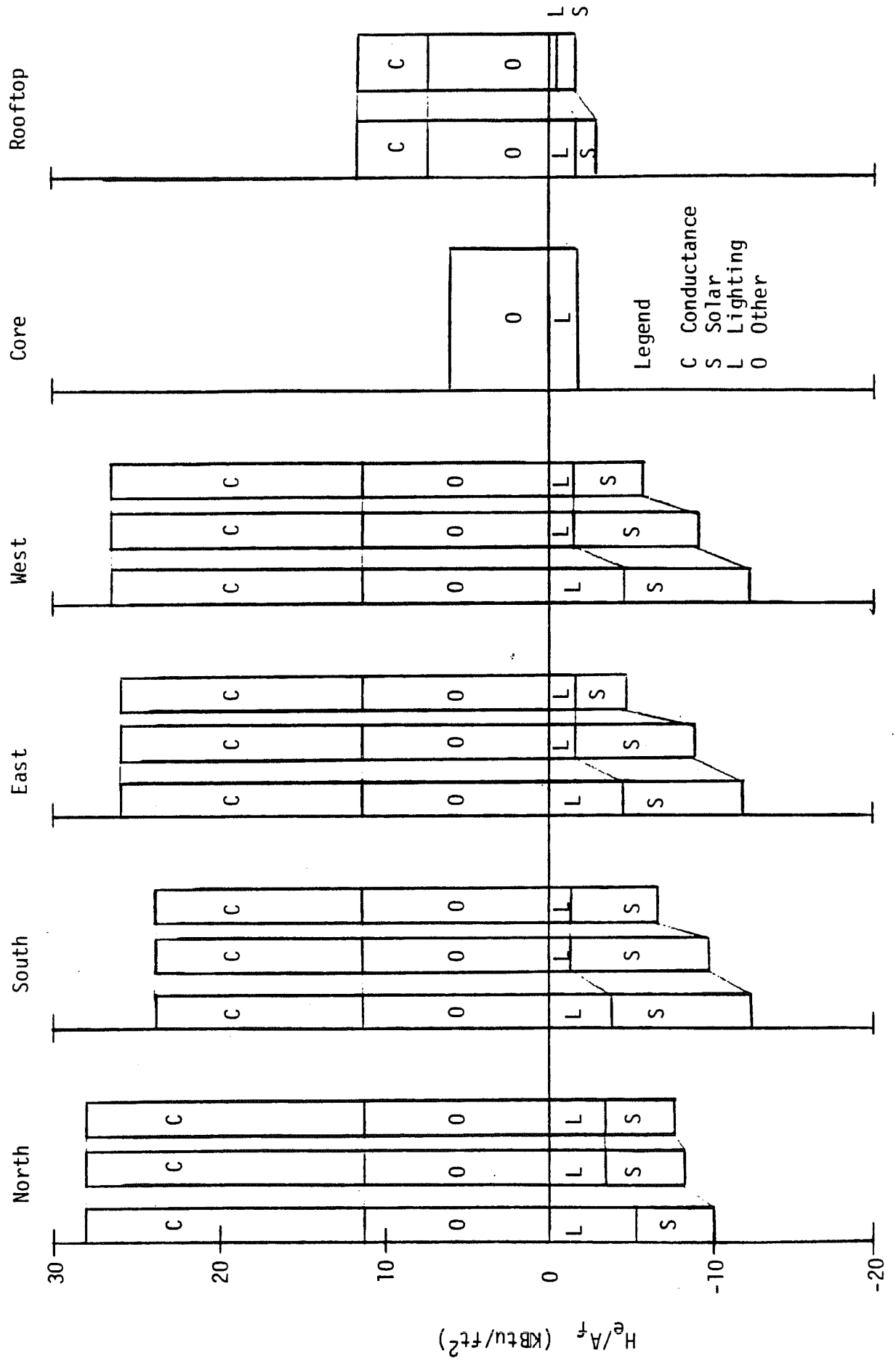
The core zone results, at a fixed lighting wattage, reduce to a similar form:

$$E/A_f = 1.67 \, b_5 + b_6.$$

Figures 4.1 to 4.3 represent plots of these equations in addition to showing incremental effects to the total load due to overhangs (R = 0.4) and daylighting using a k_d = 0.35 at an effective aperture of 0.192 for windows and a k_d = 0.27 at an effective aperture of 0.03 for skylights.

After defining 0.03 these base curves, one can begin studying the effect of changes in configuration variables. For example, it is immediately apparent that perimeter zone conductance has little effect on cooling peak and almost no effect on cooling energy. This fact was stated previously in the discussion of the complete set of regression coefficients, and is quite obvious from this example. For heating, however, the overall U-value is the primary contributor to the eventual heating load. Decreasing the U-value by half would reduce heating requirements approximately by half also.

Perimeter zone solar radiation influences cooling and heating in a significantly. For cooling peak (Fig. 4.1), the solar is approximately 37% for north and 50% for south, east, and west; whereas about 56% to 67% of the cooling energy is determined by the solar component. The effective aperture used in the example was quite high (E_a = 0.192), thus some reduction of this parameter seems feasible, especially in decreasing the visible transmittance value. For a VIS = 0.24, the solar contribution is reduced by 50%, which translates into a maximum 25% to 34% reduction in cooling peak and cooling energy, respectively.

Other major reductions in cooling are obtained by considering daylighting and overhangs. Although the correction factor for daylighting is used in the electric lighting term, its magnitude is a function of effective aperture (see Fig. 3.5). Daylighting, in this example, decreases total cooling energy from 15% for south, east, and west perimeter zones to 20% for north. Use of the R = 0.4 overhangs gives an additional reduction of 30% for south and 8% for north. Cooling peak changes are about half the above except for the south zone, where total savings are 37%.

These design features, while beneficial for cooling, tend to increase the required heating energy. The solar term itself varies from approximately 28% of the conductance load for a north orientation to 67% for south. Although the percent increase in heating is large when using daylighting and overhangs (about 50% for a south orientation), the increase is half the cooling energy reduction.

Effects of electric lighting on the cooling peak in the perimeter zones are similar to those of conductance — small. It accounts for about 18% of the total for the north zone and 12% for the south zone. Contributions to the cooling energy vary from 31% for north to 22% for the other orientations. This represents about one-half to one-third of the solar component. In the case of heating energy, the lighting term is about the same as the solar term for the north zone. For the other zones, this figure drops to half. The implication here is that lighting influences heating energy but not as strongly as cooling energy. Daylighting, as discussed previously, is responsible for a maximum 65% decrease in lighting requirements.

The other internal loads and infiltration/ventilation loads exert a major effect on all energy levels. Occupant and equipment heat gain inputs can be approximated by using the lighting wattage regression coefficient. Schedules for each are about the same. For example, Eq. (1) can be rewritten as:

$$b_1 U_o A_T + b_2 k_o A_g SC + b_3 (k_d L + 0 + E) A_f + b_4' A_f$$

where 0 and E are the occupant and equipment heat gains, respectively. The b_4' coefficient that contains the infiltration/ventilation effect can be calculated using the input values for 0 and E above, i.e. $0 = 0.675$ W/ft^2 and $E = 0.50$ W/ft^2, therefore:

$$b_4' = b_4 - 1.175 b_3.$$

From this expression, it can be seen that in this example the occupant and equipment heat gain is about 66% of the lighting input (1.67 W/ft^2).

Core zone results for cooling are similar to the perimeter zone data, as stated previously in the discussion on the regression coefficients. Heating energy per square foot for the core is about half that required for the perimeter for internal gains and infiltration/ventilation.

The rooftop zone data follow expected patterns when compared with perimeter zone results for the examples described previously. For all energy quantities, both the conductance and solar radiation contributions per square foot of floor area are much lower (about 60%) than the corresponding perimeter zone values. This fact reflects the use of a lower surface U-value (0.049) and reduced skylight size (5%). Internal load and infiltration/ventilation cooling peak and cooling energy levels are about the same as for the perimeter and core zones. However, these quantities account for more than 60% of the total. Because of this large percentage, daylighting reduces the cooling peak 18% and cooling energy 28%.

4.2 Climate Generalization

Tables 6.18 and 6.19 present the regression coefficients for the generalized climate results for configuration A. A more convenient way of interpreting the results is shown in Figs. 6.19 through 6.30 for perimeter zones and Figs. 6.31 through 6.42 for rooftop zones. These figures are composite plots that take into account all the variables associated with the final equations. Also, the relationships between configurations established on Figs. 6.1 to 6.18 were used so that all three configurations are represented. An attempt has been made to insure that the weather and configuration variables presented cover the range of expected values so that one can estimate each component's relative influence. Climatic effects are seen by observing the slope of the curves in the upper right-hand quadrant; usage pattern effects are in the upper left-hand quadrant, and configuration effects in the lower-left hand quadrant. The slope of each curve indicates the significance of a particular quantity on the resultant energy use parameter.

5.0 Conclusions and Recommendations

This report has described the derivation and use of simple algebraic expressions for analyzing various aspects of building energy performance. The purpose of the study was to provide a basis for establishing criteria for defining building envelope thermal and daylighting characteristics as part of upgrading ASHRAE/IES Standard 90. Building modules representative of perimeter, core, and rooftop zones, in addition to three distinct usage patterns, were defined and numerous DOE-2.1B energy analysis simulations performed that generated a data base that was subsequently used in conjunction with multiple regression procedures to relate energy use to specific configuration variables. The final equations included effects arising from building envelope conduction, solar radiation, internal heat gains and infiltration/ventilation as well as correction factors for overhangs and daylighting. Climate effects included geographic location (latitude), configuration, design, dry bulb temperature, and heating and cooling degree day levels.

Although the work described is complete in itself, certain qualifications must be attached to the use and interpretation of the results. Of particular importance is the fact that single-zone, constant-volume variable temperature HVAC systems were used for the whole study. The primary reason for this selection stems from the nature of the overall program objective, that of defining design criteria (and a procedure to test for compliance with the criteria) as a function of specific building envelope parameters. It was not the intent of the work to develop a model to predict energy use, but rather to generate accurate relative performance indices for different building configurations on an orientation basis. Thus, the responsive single-zone, constant-volume, variable temperature system was selected for use.

-34-

Another factor of importance to the study was the use of the simplified regression expressions, especially those describing the climate/building configuration interface. These equations provide a surprisingly good fit to the original data given their simplicity. More complicated expressions could have been generated which would have improved predictability. For example, in the heating energy regression results (Tab. 6.18), the standard deviation of 3.759 could have been reduced by half with the use of additional climate variables such as wind speed, incident solar radiation, cloud cover, and air temperature. The same is true of Eq. (1). Inclusion of quadratic terms in fenestration parameters would have improved the data fit even further. However, it would be impossible to present such equations in a simplified form suitable for Standard 90.

Future additions to this work to make it more generally applicable include the following:

1. Location: The climate generalized regression coefficients were obtained by analyzing results from 14 locations having wide climate diversity. The full 14 climate data base was used in the analysis of Configuration A and then extended to Configurations B and C. These extensions based on correlations developed in the original five climate data base were assumed to be reliable approximations. These assumptions could be validated by completing the data set with Configurations B and C runs in the additional nine climates.

Further refinements may also be attainable by increasing the number of weather parameters used in the regression models.

2. Internal Loads: Installed electric lighting power, as a primary concern in this study, is explicitly expressed in the correlation expressions. Internal loads generated by equipment and occupants are accommodated by schedule selection and the effects are implicit in the fourth term of the general equation. A parametric analysis of equipment and occupant loads would allow their explicit inclusion as independent variables in the equations for greater flexibility in use.

3. Infiltration/Ventilation: This study has indicated that these quantities form a large part of the resultant energy usage values. Therefore, it is recommended that additional simulations be run covering a sufficient range of infiltration and ventilation levels to enable their use as an independent variable in the regressions.

4. HVAC System Types: This proposed variation may be the most important for predicting energy use. Two alternatives to the single-zone, constant-volume system are suggested: using a variable-volume system serving the four perimeter zones with a constant volume for the core, or using a variable-volume system for all five zones. A major difficulty of these approaches is the

modularization of the model so that a generalized scheme can be developed such as the one(s) presented in this report. It would also be interesting to compare total building energy consumption (instead of coil loads) for each HVAC system modeled.

References

1) DOE-2 Reference Manual, Version 2.1, Lawrence Berkeley Laboratory and Los Alamos Scientific Laboratory, 1982, LBL 8706 Rev. 1.

2) DOE-2 Supplement, Version 2.1B, Lawrence Berkeley Laboratory, Berkeley, 1983. LBL-8706 Rev. 3 Suppl.

3) F.C. Winkelmann, Daylighting Calculations in DOE-2, Lawrence Berkeley Laboratory, 1983, LBL-11353.

4) William L. Carroll, Thomas L. Webster, Atila Mertol, and Ronald C. Kammerud, The Effect of Envelope Thermal Mass on Building Heating and Cooling Loads, Report submitted to Battelle Pacific Northwest Laboratories, August 1983, Lawrence Berkeley Laboratory Report LBL-16358 (in press).

5) Richard Johnson, Stephen Selkowitz, Frederick Winkelmann, and Michael Zenter, Glazing Optimization Study for Energy Efficiency in Commercial Office Buildings, Presented at Third International Symposium as Energy Conservation in the Built Environment, Dublin, 1982. Lawrence Berkeley Laboratory, Berkeley, 1981, LBL-12764.

6) Recommendation for the Standard Evaluation Technique (SET) of the Building Energy Performance Standards (BEPS), W. S. Fleming Associates, Inc., Landover, Maryland, 1981.

7) Norman H. Nie et al., Statistical Package for the Social Sciences, Second Edition, McGraw-Hill Book Company, New York NY (1975).

8) Applied Science Division, Building Envelope Thermal and Daylighting Analysis in Support of Recommendations to Upgrade ASHRAE/IES Standard 90, Vol. II Data Base Definition and Procedural Guidelines, Lawrence Berkeley Laboratory, Berkeley CA (1983).

A P P E N D I C E S

Appendix 1:
Tables 6.1 - 6.19

Appendix 2:
Figures 6.1 - 6.42

TABLE 6.1 - Perimeter Zone Regression Coefficients: Cooling Peak,
Configuration $\underline{A}$

		Madison	Wash., DC	LChas	Seattle	El Paso
$U_o A_t$	n	12.206	21.536	21.998	2.263	24.755
	s	22.645	34.399	40.155	19.326	48.666
	e	27.184	34.490	51.412	38.889	60.684
	w	23.467	42.685	42.368	36.868	68.723
$A_g SC$	n	41.337	42.091	45.166	38.658	41.036
	s	86.620	81.941	70.435	86.278	83.474
	e	82.174	73.165	70.177	81.469	88.033
	w	89.995	81.698	76.533	93.553	93.335
$A_f L$	n	3.173	2.734	2.528	3.299	2.731
	s	3.084	2.55	2.466	2.996	2.152
	e	2.942	2.482	2.143	2.620	2.414
	w	3.0	2.356	2.412	2.513	2.319
A_f		10.814	11.551	13.699	6.820	9.623
Mean		44.984	48.146	54.037	39.676	52.396
r^2		0.981	0.973	0.970	0.979	0.959
σ		2.034	2.296	2.408	2.271	3.528

NOTE: For TABLES 6.1 through 6.11 and 6.15 through 6.17, the following units are used:

Cooling Peak:	Btu/Hr
Cooling/Heating Energy:	KBtu
U_o:	$Btu/Hr\text{-}ft^2\text{-}°F$
A_t, A_f, A_g:	ft^2
L:	W/ft^2
Mean (Cooling Peak):	KBtu/Hr
Mean (Cooling/Heating Energy):	MBtu

TABLE 6.2 - Perimeter Zone Regression Coefficients: Cooling Peak,
Configuration $\underline{B}$

		Madison	Wash., DC	LChas	Seattle	El Paso
$U_o A_t$	n	5.689	18.970	22.180	9.208	28.969
	s	27.289	23.732	27.878	23.081	48.680
	e	9.434	16.580	34.350	29.411	55.894
	w	20.136	42.997	34.349	38.988	64.720
$A_g SC$	n	45.110	45.588	60.010	37.513	44.768
	s	92.55	79.87	88.681	85.939	75.037
	e	74.537	71.803	93.305	76.109	82.352
	w	87.196	90.937	90.358	98.116	98.78
$A_f L$	n	3.846	3.160	2.874	3.303	3.269
	s	3.249	3.168	3.200	3.281	2.916
	e	3.510	3.197	2.919	2.425	2.459
	w	3.709	2.793	3.223	2.728	2.794
A_f		21.655	24.627	23.589	10.761	13.305
Mean		61.289	67.552	71.278	45.858	58.470
r^2		0.992	0.984	0.992	0.980	0.961
σ		1.302	1.838	1.435	2.216	3.273

TABLE 6.3 - Perimeter Zone Regression Coefficients: Cooling Peak,
Configuration $\underline{C}$

		Madison	Wash., DC	LChas	Seattle	El Paso
$U_o A_t$	n	14.983	19.205	24.085	11.955	30.203
	s	33.799	24.141	33.646	20.096	47.639
	e	16.953	23.548	42.170	36.915	61.775
	w	25.808	45.666	35.115	36.410	63.133
$A_g SC$	n	42.363	49.835	62.833	28.538	38.843
	s	96.403	89.514	89.686	84.062	80.108
	e	93.9	75.011	93.323	73.464	81.439
	w	96.627	90.112	92.219	96.163	105.389
$A_f L$	n	1.287	1.438	1.678	2.203	2.058
	s	1.413	1.240	1.010	1.343	0.727
	e	1.297	1.219	1.606	1.172	1.111
	w	1.276	1.236	1.497	1.867	1.661
A_f		9.917	11.519	12.667	4.031	4.893
Mean		41.096	44.906	52.474	31.941	42.703
r^2		0.992	0.989	0.990	0.978	0.966
σ		1.403	1.532	1.604	2.222	3.155

TABLE 6.4 - Perimeter Zone Regression Coefficients: Cooling Energy, Configuration $\underline{A}$

		Madison	Wash., DC	LChas	Seattle	El Paso
$U_o A_t$	n	-9.000	-1.203	2.613	-5.470	6.306
	s	-5.829	7.239	16.384	-3.174	25.134
	e	-6.641	4.816	20.143	-4.742	30.429
	w	-8.167	4.157	14.006	-4.862	28.081
$A_g SC$	n	41.566	56.689	89.879	25.548	77.443
	s	72.183	93.592	135.242	49.781	134.540
	e	70.707	90.180	132.791	43.389	143.557
	w	73.399	94.098	130.028	50.552	148.360
$A_f L$	n	3.478	4.691	7.323	2.256	6.283
	s	3.622	4.823	7.495	2.344	6.412
	e	3.583	4.783	7.331	2.284	6.385
	w	3.575	4.838	7.455	2.292	6.454
A_f		3.932	5.67	10.408	1.575	6.230
Mean		26.486	40.056	65.583	16.192	59.847
r^2		0.986	0.988	0.990	0.986	0.984
σ		1.512	1.830	2.399	1.017	3.193

TABLE 6.5 - Perimeter Zone Regression Coefficents: Cooling Energy, Configuration $\underline{B}$

		Madison	Wash.,DC	LChas	Seattle	El Paso
U_oA_t	n	-20.080	-5.777	-0.0454	-14.653	7.851
	s	-6.531	12.417	23.699	-3.840	40.339
	e	-8.619	8.142	23.326	-6.463	43.940
	w	-8.305	10.593	19.711	-3.454	45.021
A_gSC	n	61.508	81.949	122.957	36.918	103.110
	s	94.541	120.091	176.862	65.599	166.298
	e	91.481	115.002	171.007	56.662	174.103
	w	98.229	123.263	170.377	69.453	186.935
A_fL	n	5.290	7.120	11.015	3.323	8.945
	s	5.282	7.057	10.929	3.384	8.860
	e	5.236	7.079	10.872	3.253	5.684
	w	5.221	7.060	10.905	3.284	8.811
A_f		11.702	18.051	33.813	5.427	20.263
Mean		47.517	70.912	119.294	27.380	97.552
r^2		0.997	0.996	0.996	0.994	0.991
σ		0.974	1.405	1.991	0.904	3.110

TABLE 6.6 - Perimeter Zone Regression Coefficients: Cooling Energy, Configuration $\underline{C}$

		Madison	Wash., DC	LChas	Seattle	El Paso
$U_o A_t$	n	3.206	11.125	20.903	−5.842	25.654
	s	6.162	22.484	48.846	1.134	53.832
	e	4.317	18.496	51.920	−1.769	60.393
	w	5.280	21.095	41.436	0.778	60.109
$A_g SC$	n	53.598	80.184	130.447	31.438	100.638
	s	92.375	127.571	192.964	61.345	168.965
	e	90.456	121.034	191.051	54.141	188.434
	w	99.816	136.374	187.622	67.814	208.593
$A_f L$	n	2.879	4.683	7.704	1.748	5.953
	s	3.047	4.711	7.397	1.743	5.545
	e	3.030	4.808	7.272	1.688	5.494
	w	3.009	4.711	7.549	1.747	5.765
A_f		3.567	6.982	14.583	1.052	8.780
Mean		32.348	42.954	95.543	17.380	79.541
r^2		0.986	0.988	0.992	0.987	0.985
σ		1.875	2.362	2.937	1.168	0.984

TABLE 6.7 Perimeter Zone Regression Coefficients: Heating Energy,
Configuration $\underline{A}$

		Madison	Wash., DC	LChas	Seattle	El Paso
U_oA_t	n	100.470	50.892	14.902	57.208	24.879
	s	76.013	35.293	9.332	43.317	12.446
	e	88.051	42.528	10.039	45.449	14.110
	w	91.260	43.461	11.810	48.238	16.233
A_gSC	n	-19.040	-14.313	-5.806	-12.503	-8.162
	s	-33.732	-21.143	-6.849	-19.298	-9.888
	e	-29.196	-19.272	-6.166	-17.156	-8.888
	w	-30.279	-19.732	-6.664	-18.646	-9.650
A_fL	n	-3.242	-2.212	-0.767	-2.541	-1.078
	s	-2.369	-1.526	-0.503	-1.823	-0.571
	e	-2.739	-1.810	-0.526	-1.979	-0.627
	w	-2.758	-1.828	-0.607	-2.035	-0.709
A_f		11.471	6.282	1.704	5.487	2.217
Mean		22.955	12.476	3.497	10.674	4.473
r^2		0.975	0.963	0.955	0.944	0.958
σ		1.417	1.089	0.399	1.337	0.554

TABLE 6.8 Perimeter Zone Regression Coefficients: Heating Energy,
Configuration B_

		Madison	Wash., DC	LChas	Seattle	El Paso
U_oA_t	n	127.777	56.777	14.459	58.138	23.661
	s	90.417	36.365	8.657	40.412	12.287
	e	108.383	45.405	9.651	44.521	13.101
	w	108.894	45.578	11.154	46.042	15.653
A_gSC	n	−24.922	−15.766	−4.722	− 9.617	−6.822
	s	−37.469	−18.082	−4.173	−13.409	−6.232
	e	−33.838	−17.767	−4.115	−12.425	−5.724
	w	−35.218	−18.153	−4.585	−13.847	−6.823
A_gL	n	− 4.585	− 2.684	−0.630	− 2.482	−0.866
	s	− 3.278	− 1.685	−0.343	− 1.552	−0.375
	e	− 3.867	− 2.143	−0.401	− 1.802	−0.432
	w	− 3.772	− 2.088	−0.458	− 1.792	−0.504
A_f		8.123	3.372	0	1.487	0.540
Mean		18.330	8.476	2.058	5.908	2.851
r^2		0.962	0.932	0.922	0.891	0.932
σ		2.152	1.559	0.441	1.716	0.576

TABLE 6.9 - Perimeter Zone Regression Coefficients: Heating Energy,
Configuration $\underline{C}$

		Madison	Wash., DC	LChas	Seattle	El Paso
U_oA_t	n	167.667	103.078	41.270	140.444	62.028
	s	147.571	81.685	25.938	115.936	34.568
	e	163.985	95.445	26.276	125.003	38.520
	w	163.193	93.982	31.336	124.182	38.898
A_gSC	n	-34.426	-31.374	-17.574	-29.368	-21.514
	s	-72.725	-53.839	-21.2	-55.445	-28.427
	e	-62.163	-46.935	-20.067	-52.203	-27.244
	w	-69.717	-54.165	-21.089	-59.170	-30.572
A_fL	n	- 4.829	- 4.102	- 2.137	- 5.763	- 2.652
	s	- 4.443	- 3.511	- 1.484	- 4.722	- 1.589
	e	- 4.636	- 3.862	- 1.513	- 4.882	- 1.697
	w	- 4.541	- 3.698	- 1.684	- 4.807	- 1.720
A_f		29.389	18.88	6.471	18.423	7.401
Mean		53.505	34.170	11.462	34.090	13.319
r^2		0.992	0.989	0.974	0.982	0.970
σ		1.507	1.338	0.891	1.987	1.267

TABLE 6.10 - Rooftop Zone Regression Coefficients: Configuration A

	Madison	Wash., DC	LChas	Seattle	El Paso
			COOLING PEAK		
$U_o A_t$	27.584	51.421	61.515	26.296	84.980
$A_f SC$	227.775	209.993	208.251	249.63	262.462
$A_f L_p$	3.23	3.099	3.054	3.160	3.015
$A_f P$	8.188	8.275	8.267	4.948	5.431
Mean	193.014	222.399	237.680	171.962	260.391
r^2	0.999	0.998	0.997	0.997	0.998
σ	1.341	1.93	2.483	2.368	2.116
			COOLING ENERGY		
$U_o A_t$	-4.628	6.964	15.401	-0.194	35.874
$A_f SC$	169.211	214.889	314.393	116.881	420.310
$A_f L_p$	3.158	4.234	6.745	1.968	5.866
$A_f P$	3.832	5.965	10.503	1.823	5.533
Mean	118.872	176.027	291.401	71.957	296.446
r^2	0.999	0.999	0.999	0.999	0.998
σ	1.233	1.496	1.988	0.838	2.876
			HEATING ENERGY		
$U_o A_t$	99.829	50.838	17.194	59.389	23.323
$A_f SC$	-41.691	-34.570	-17.002	-28.513	-33.766
$A_f LP$	- 1.515	- 1.117	- 0.414	- 1.27	- 0.554
A_f	8.191	4.419	1.247	3.387	1.950
Mean	108.095	68.811	21.093	63.907	26.591
r^2	0.982	0.977	0.981	0.966	0.974
σ	3.095	2.822	0.989	3.82	1.543

TABLE 6.11 - Rooftop Zone Regression Coefficients: Configuration B

	Madison	Wash., DC	LChas	Seattle	El Paso
COOLING PEAK					
$U_o A_t$	14.466	39.242	24.427	25.220	67.000
$A_o S_C^g$	249.422	231.976	244.752	251.406	290.596
$A_f^g L$	3.515	3.228	3.363	3.292	3.162
$A_f^f P$	18.819	19.992	21.359	9.572	11.231
Mean	300.186	333.731	340.060	219.721	288.164
r^2	0.999	0.999	0.999	0.998	0.993
σ	1.605	1.606	1.451	2.098	4.715
COOLING ENERGY					
$U_o A_t$	-14.799	4.440	12.771	-5.753	45.277
$A_o S_C^g$	244.496	298.379	437.677	164.717	529.117
$A_f^g L$	4.708	6.330	9.881	7.957	8.655
$A_f^f P$	10.819	16.637	30.111	5.425	18.204
Mean	222.239	330.536	558.631	127.774	459.720
r^2	0.999	0.999	0.999	0.999	0.999
σ	0.711	1.153	1.845	1.282	3.132
HEATING ENERGY					
$U_o A_t$	137.534	62.148	15.886	62.447	26.371
$A_o S_C^g$	-57.226	-41.745	-12.331	-24.995	-26.179
$A_f^g L$	- 2.660	- 1.563	- 0.303	- 1.261	- 0.433
$A_f^f P$	4.190	1.630	0.1156	- 0.0202	0.307
Mean	68.273	43.114	11.061	33.522	19.169
r^2	0.974	0.950	0.937	0.904	0.953
σ	5.621	5.796	1.562	6.862	2.199

TABLE 6.12 – Overhang Correction Factor Regression Coefficients:
Configuration A

		Madison	Wash., DC	LChas	Seattle	El Paso
				COOLING PEAK		
R	n	0.194	0.204	0.514	0.236	0.448
	s	2.003	2.120	2.335	1.892	2.410
	e	1.654	1.847	1.832	1.564	1.673
	w	1.453	1.580	2.089	1.315	1.703
R^2	n	0.242	0.282	-0.0578	0.139	-0.158
	s	-1.672	-1.684	-1.927	-1.502	-2.0
	e	-1.122	-1.570	-1.479	-1.014	-1.087
	w	-0.935	-1.057	-1.803	-0.840	-1.176
				COOLING ENERGY		
R	n	0.366	0.389	0.510	0.295	0.442
	s	1.713	1.664	1.712	1.787	1.721
	e	1.295	1.393	1.334	1.266	1.348
	w	1.333	1.324	1.349	1.318	1.359
R^2	n	0.045	0.042	-0.0993	0.106	-0.132
	s	-1.406	-1.313	-1.432	-1.449	-1.386
	e	-0.944	-1.089	-0.995	-0.903	-0.988
	w	-1.0	-0.990	-0.758	-0.963	-1.027
				HEATING ENERGY		
R	n	0.173	0.154	0.267	0.162	0.246
	s	1.362	1.389	1.440	1.507	1.095
	e	1.082	1.056	1.029	1.098	0.961
	w	0.832	0.924	1.042	0.960	0.874
R^2	n	0.266	0.271	0.105	0.288	0.059
	s	-1.091	-1.067	-1.080	-1.245	-0.673
	e	-0.764	-0.775	-0.721	-0.735	-0.615
	w	-0.489	-0.585	-0.758	-0.641	-0.560

TABLE 6.13 - Perimeter Zone Daylighting Correction Factor Regression
           Coefficients: Configuration A

		Madison	Wash., DC	LChas	Seattle	El Paso
VIS·WWR	n	4.805	5.327	6.095	4.301	5.011
	s	5.843	6.400	7.814	5.120	7.843
	e	5.301	5.871	7.108	4.735	6.568
	w	5.274	5.831	6.890	4.709	6.226
$(VIS·WWR)^2$	n	- 8.710	-11.005	-14.934	- 7.611	- 7.872
	s	-13.033	-15.591	-23.871	-11.037	-21.850
	e	-10.780	-13.311	-20.263	- 9.447	-15.991
	w	-10.627	-13.109	-18.979	- 9.306	-14.241

TABLE 6.14 - Rooftop Zone Daylighting Correction Factor Regression
           Coefficients: Configuration A

	Madison	Wash., DC	LChas	Seattle	El Paso
VIS·WWR·WF	48.468	49.528	57.424	42.337	64.488
$(VIS·WWR·WF)^2$	-800.387	-844.46	-1037.164	-682.526	-1203.001

Table 6.15 - Core Zone Regression Coefficients: Configuration A

	Madison	Wash., DC	LChas	Seattle	El Paso
Cooling peak					
A_fL	3.554	3.537	3.607	3.539	3.573
A_f	8.625	9.114	10.819	5.722	8.402
Mean	146.662	151.274	169.502	117.375	144.769
r^2	0.995	0.998	0.991	0.998	0.993
σ	2.096	1.26	2.89	1.468	2.425
Cooling					
A_fL	3.376	4.522	7.064	2.147	5.710
A_f	4.051	6.531	11.271	1.881	8.856
Mean	97.909	142.176	232.804	55.303	185.626
r^2	0.987	0.992	0.994	0.989	0.993
	3.211	3.380	4.409	1.854	3.966
Heating					
A_fL	-1.105	-0.527	-0.1282	-0.5044	-0.141
A_f	6.129	2.559	0.4706	1.903	0.627
Mean	42.504	16.636	2.526	10.455	3.884
r^2	0.931	0.924	0.864	0.910	0.826
σ	2.52	1.267	0.424	1.329	0.538

TABLE 6.16 - Core Zone Regression Coefficients: Configuration B

	Madison	Wash., DC	LChas	Seattle	El Paso
Cooling peak					
A_fL	4.421	4.131	4.268	3.927	4.118
A_f	18.429	21.043	20.191	9.156	11.926
Mean	259.45	280.656	274.464	158.315	189.279
r^2	0.999	0.999	0.999	0.999	0.997
σ	0.651	0.462	0.746	0.953	1.83
Cooling					
A_fL	5.247	7.154	11.565	3.110	8.237
A_f	11.050	17.379	30.778	5.866	22.255
Mean	199.688	295.412	504.386	111.531	362.581
r^2	0.999	0.999	0.999	0.998	0.999
σ	1.624	1.851	2.939	1.146	2.333
Heating					
A_fL	-1.056	-0.139	0.0088	0.00356	0.0126
A_f	2.902	0.419	0.00919	0.0693	0.0243
Mean	11.064	1.829	0.242	0.753	0.458
r^2	0.884	0.795	0.606	0.045	0.5
σ	3.199	0.590	0.059	0.137	0.105

TABLE 6.17 - Core Zone Regression Coefficients: Configuration C

	Madison	Wash., DC	LChas	Seattle	El Paso
Cooling peak					
A_fL	1.783	2.689	2.349	1.914	1.987
A_f	7.788	8.006	9.670	4.239	6.931
Mean	108.186	125.766	136.637	74.930	103.094
r^2	0.981	0.999	0.980	0.999	0.999
σ	2.069	0.330	2.778	0.464	0.164
Cooling					
A_fL	2.901	4.637	7.510	1.659	5.432
A_f	5.298	9.741	17.178	2.282	14.851
Mean	102.287	176.242	299.457	51.018	240.862
r^2	0.999	0.999	0.999	0.999	0.999
σ	0.497	0.662	0.917	0.429	0.649
Heating					
A_fL	-2.913	-1.809	-0.444	-1.882	-0.360
A_f	15.114	7.917	1.605	6.654	1.486
Mean	101.629	48.416	8.491	34.544	8.740
r^2	0.991	0.981	0.966	0.965	0.964
σ	2.289	2.078	0.701	2.974	0.583

TABLE 6.18 – Perimeter Zone Regression Coefficients: All Climates, Configuration A

Cooling Peak

	N	S	E	W		
P_{11}	-0.033	0.182	0.182	0.182		
P_{12}	13.976	14.5	14.5	14.5		
P_{21}	1.499	1.067	1.067	1.067		
P_{22}	-76.303	7.14	7.14	7.14	Mean	51.56°
					r^2	0.873
P_{31}	-0.025	-0.025	-0.025	-0.025	σ	6.710
P_{32}	4.9	4.9	4.9	4.9		
P_{41}	0.29	0.29	0.29	0.29		
P_{42}	-13.44	-13.44	-13.44	-13.44		

Cooling

	N	S	E	W		
C_{11}	-0.2813^{-4}	0.1301^{-4}	0.1529^{-4}	-0.561^{-4}		
C_{12}	0.1025	0.0831	0.1198	0.1456		
C_{13}	-24.975	-13.598	-23.109	-25.149		
C_{21}	-2.955	-4.996	-4.574	-5.249	Mean	43.850
C_{22}	177.795	298.149	286.681	308.337	r^2	0.990
					σ	5.085
C_{31}	-0.181	-0.181	-0.181	-0.181		
C_{32}	12.051	12.051	12.051	12.051		
C_{41}	-0.477	-0.477	-0.477	-0.477		
C_{42}	25.09	25.09	25.09	25.09		

Heating

	N	S	E	W		
H_{11}	-0.2376^{-6}	0.6939^{-6}	0.9937^{-6}	0.4535^{-6}		
H_{12}	0.02192	0.01256	0.01292	0.01727		
H_{13}	-0.2302	-0.7092	-0.2265	-1.170		
H_{21}	0.7476^{-6}	0.3898^{-6}	0.5426^{-6}	0.4717^{-6}	Mean	9.80
H_{22}	-0.007178	-0.0083	-0.00834	-0.007902	r^2	0.921
H_{23}	-0.612	-0.3	-0.1255	-1.007	σ	3.759
H_{31}	0.9517^{-7}	0.5579^{-7}	0.5544^{-7}	0.7167^{-7}		
H_{32}	-0.001091	-0.000705	-0.000765	-0.000898		
H_{33}	0.1173	0.1032	0.1232	0.1547		
H_{41}	0.00181	0.00181	0.00181	0.00181		
H_{42}	0	0	0	0		

TABLE 6.19 – Rooftop Zone Regression Coefficients: All Climates, Configuration A

Cooling Peak

P_{11}	2.325		
P_{12}	-151.806		
P_{21}	0.853		
P_{22}	148.682	Mean	214.002
		r^2	0.946
P_{31}	-0.00658	σ	11.39
P_{32}	3.503		
P_{41}	0.0107		
P_{42}	6.426		

Cooling

C_{11}	0.0		
C_{12}	0.0988		
C_{13}	-11.769		
C_{21}	-14.376	Mean	185.55
C_{22}	805.241	r^2	0.977
		σ	12.8
C_{31}	-0.245		
C_{32}	13.765		
C_{41}	-0.244		
C_{42}	14.389		

Heating

H_{11}	0.0		
H_{12}	0.0168		
H_{13}	0.0		
H_{21}	0.0	Mean	58.243
H_{22}	-0.0122	r^2	0.933
H_{23}	0.0	σ	18.12
H_{31}	0.0		
H_{32}	-0.000416		
H_{33}	0.0		
H_{41}	0.0018		
H_{42}	0.0		

FIGURE 6.1   CLIMATE GENERALIZATION BETWEEN CONFIGURATIONS
PERIMETER ZONE - COOLING PEAK P_1 TERM
All Orientations
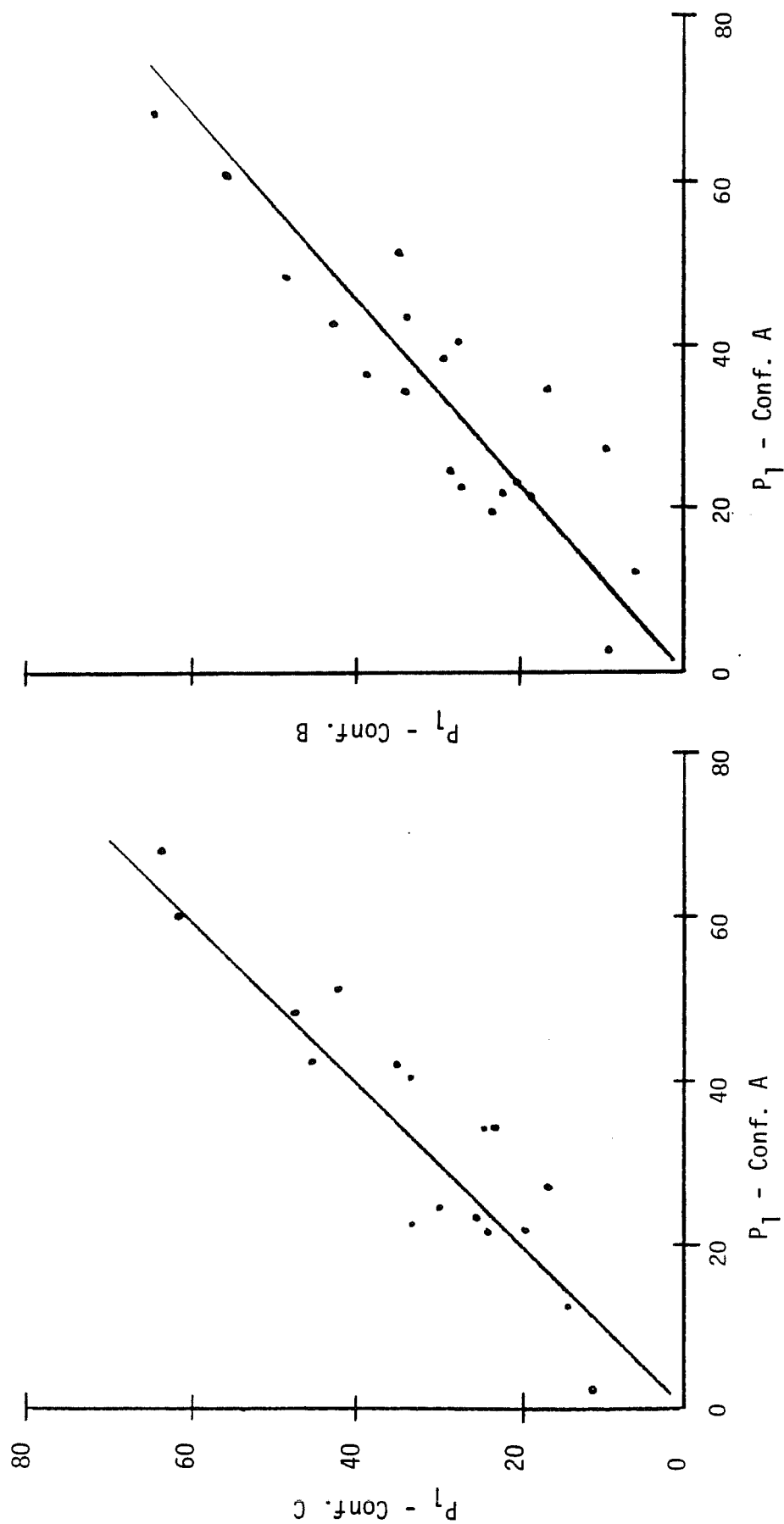
FIGURE 6.2   CLIMATE GENERALIZATION BETWEEN CONFIGURATIONS
PERIMETER ZONE - COOLING PEAK P_2 TERM
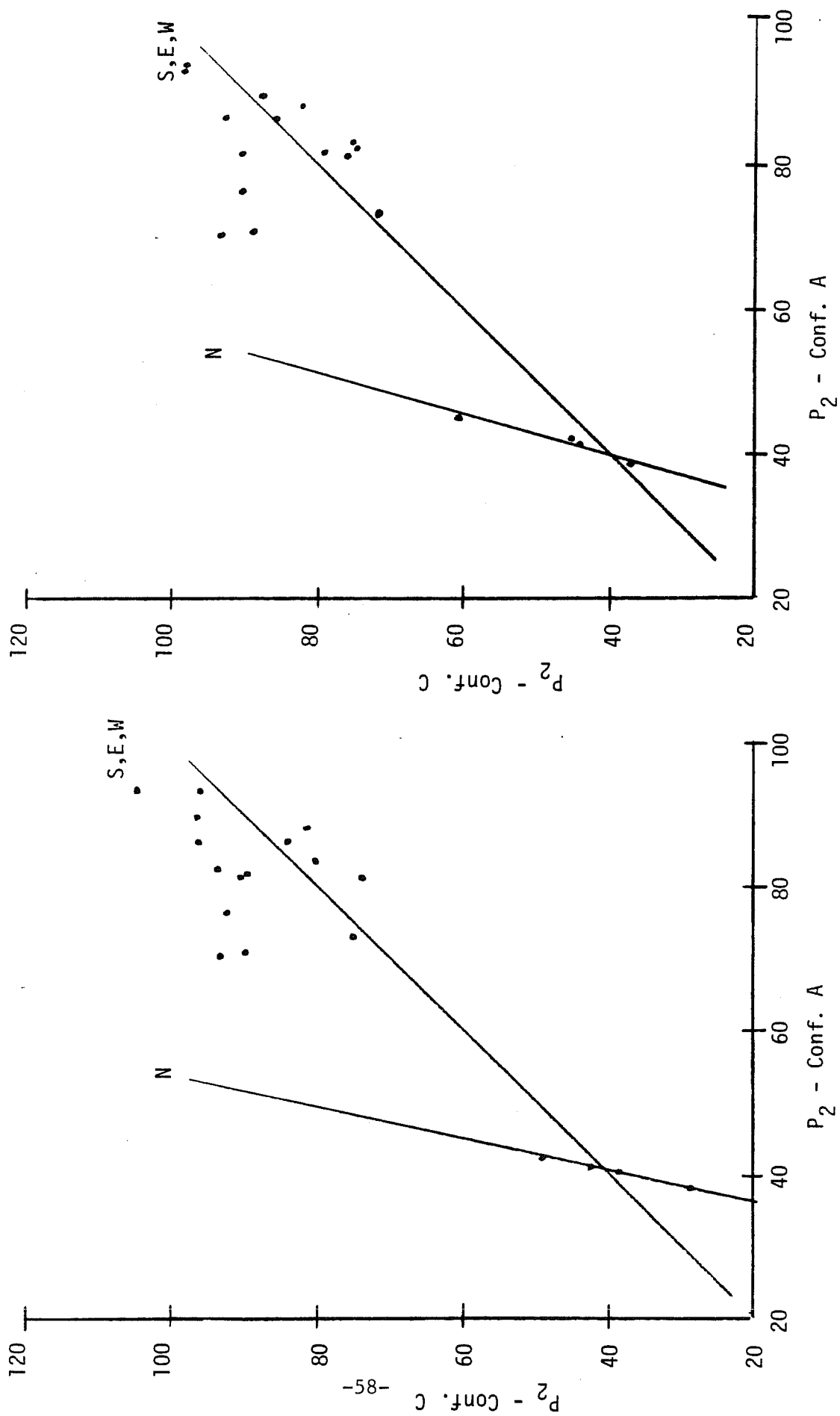
FIGURE 6.3   CLIMATE GENERALIZATION BETWEEN CONFIGURATIONS

PERIMETER ZONE - COOLING PEAK P_3 TERM

All Orientations
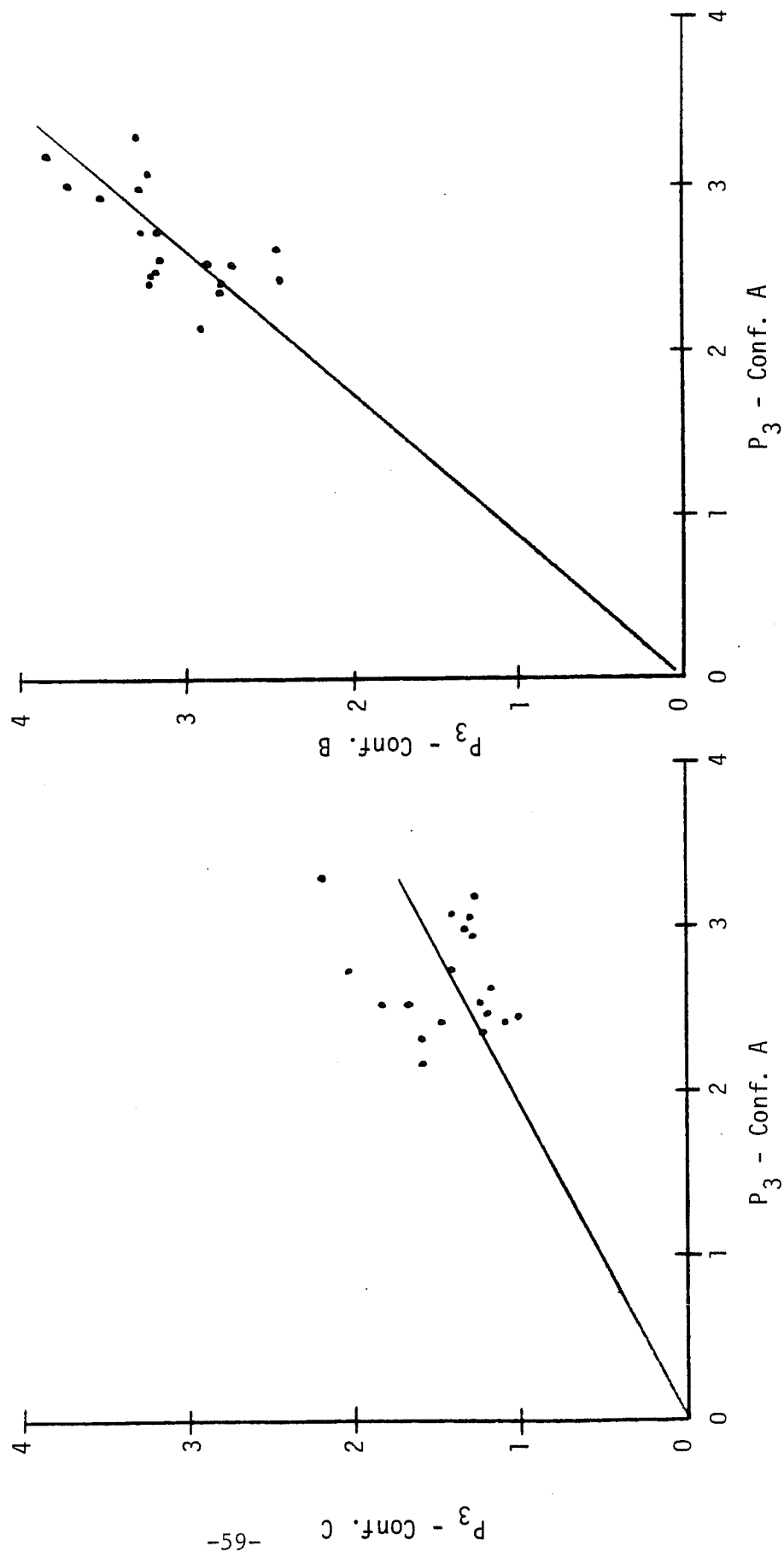
FIGURE 6.4 CLIMATE GENERALIZATION BETWEEN CONFIGURATIONS

PERIMETER ZONE - COOLING PEAK P_4 TERM

All Orientations
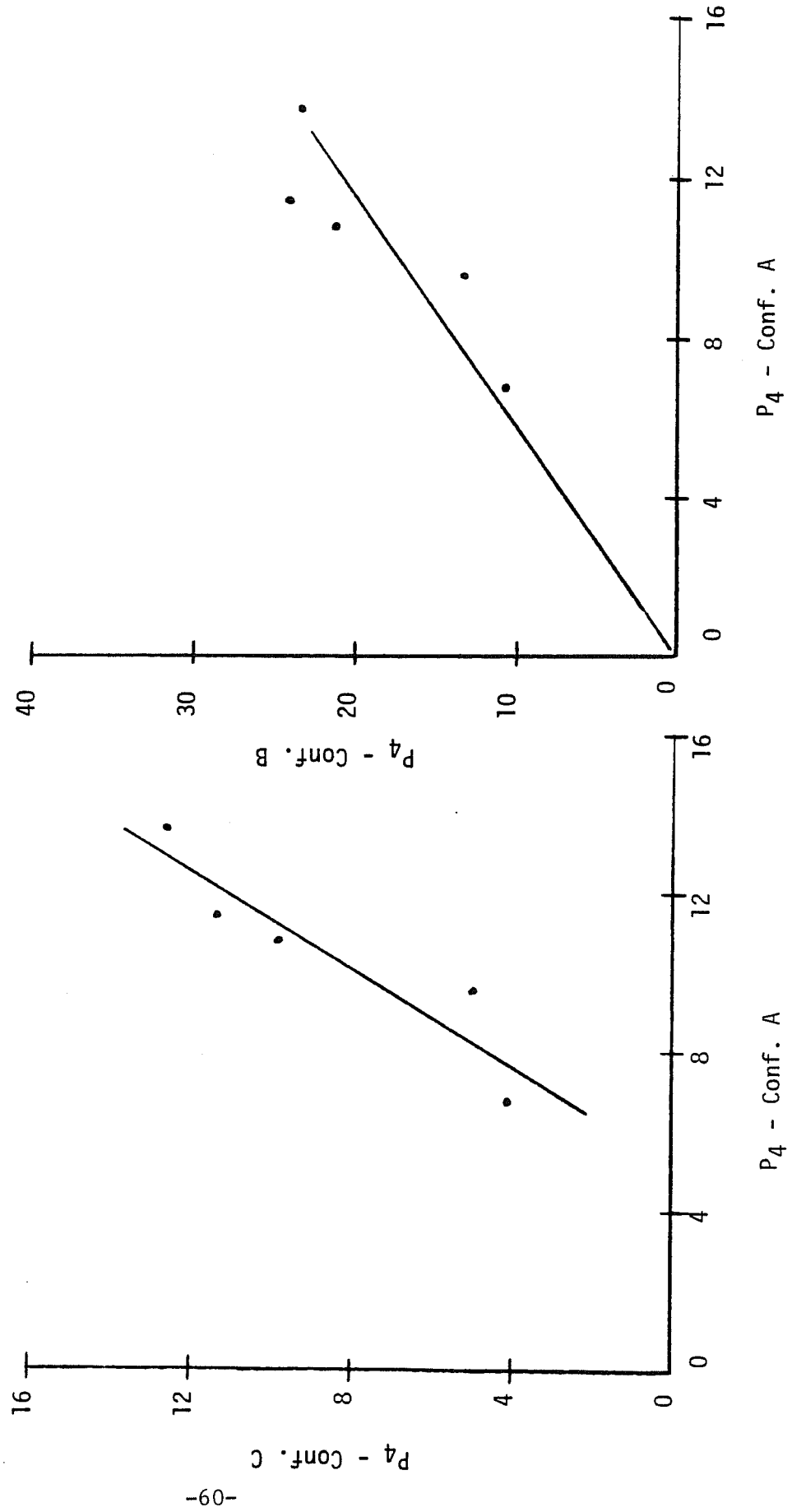
FIGURE 6.5 CLIMATE GENERALIZATION BETWEEN CONFIGURATIONS

PERIMETER ZONE - COOLING ENERGY C_1 TERM

All Orientations
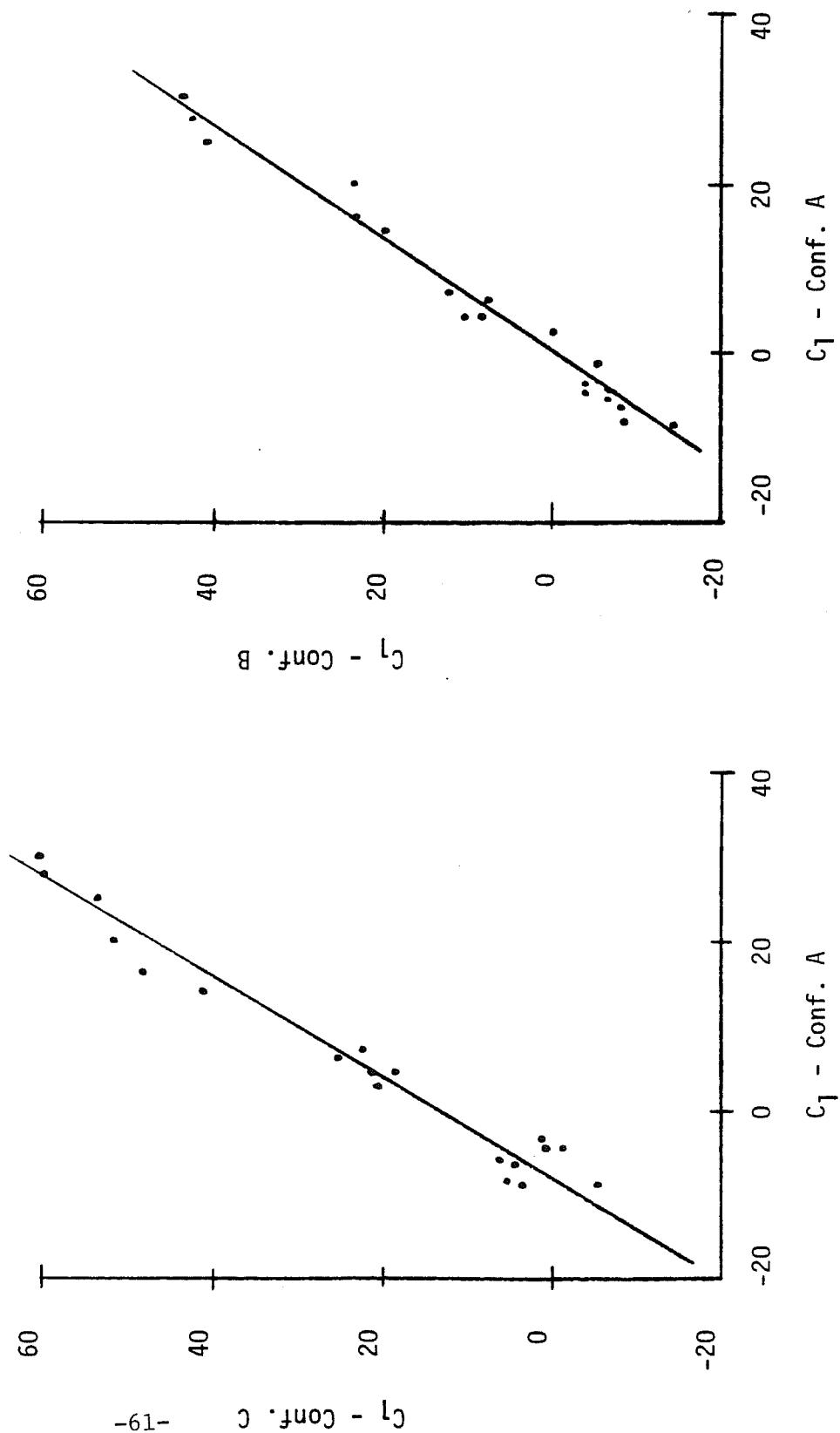
FIGURE 6.6   CLIMATE GENERALIZATION BETWEEN CONFIGURATIONS

PERIMETER ZONE - COOLING ENERGY C_2 TERM

All Orientations
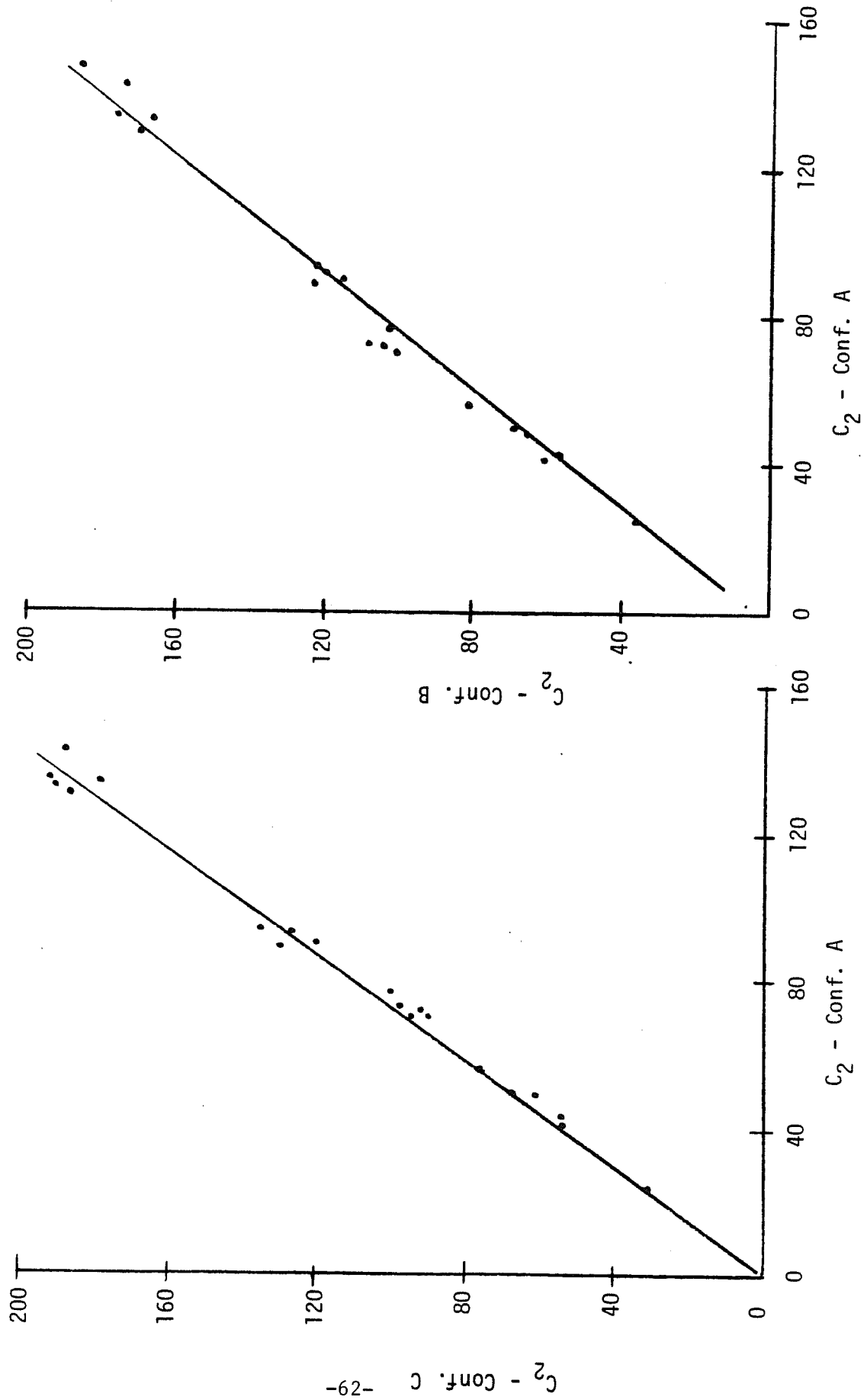
FIGURE 6.7   CLIMATE GENERALIZATION BETWEEN CONFIGURATIONS

PERIMETER ZONE – COOLING ENERGY C_3 TERM

All Orientations
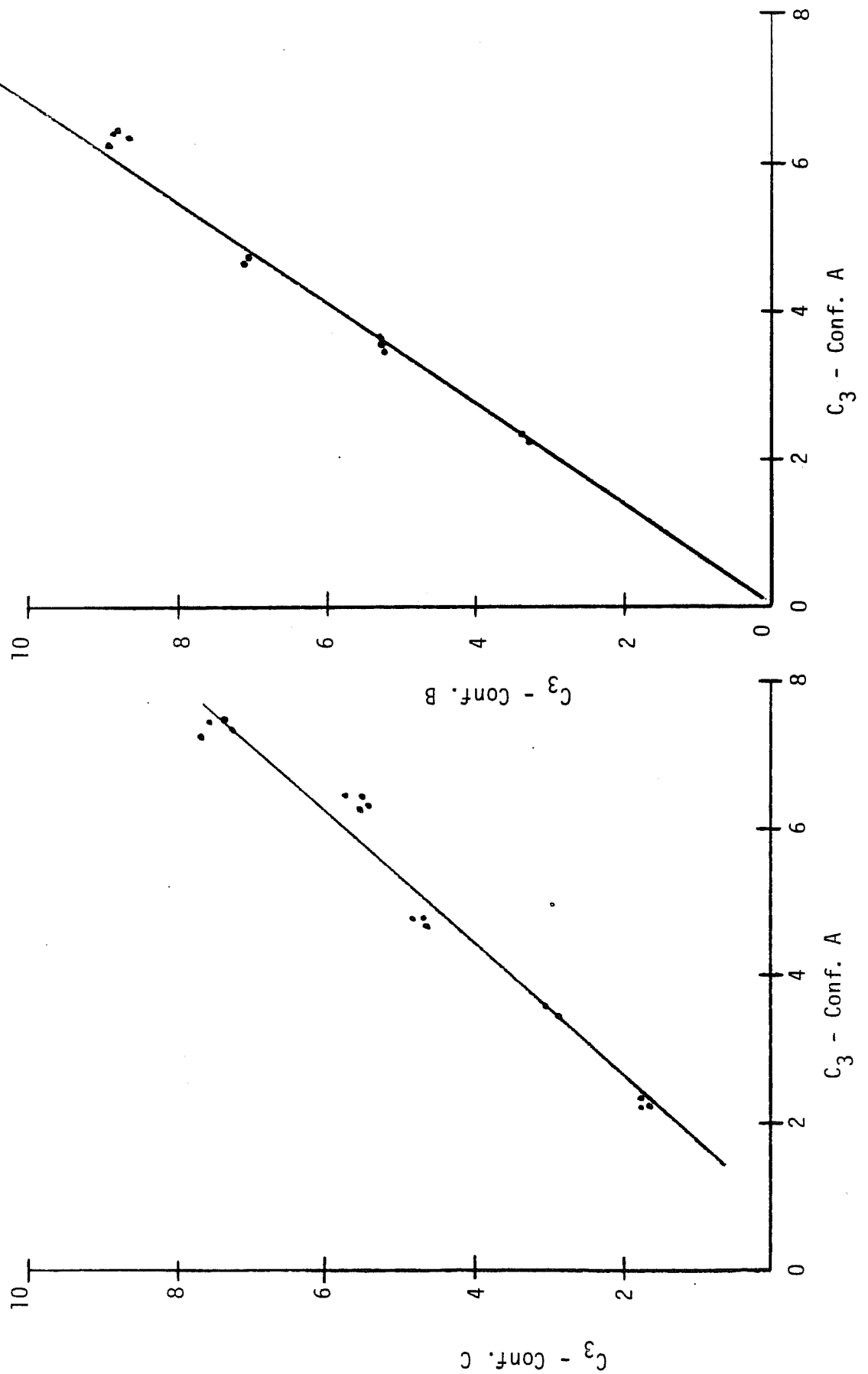
FIGURE 6.8   CLIMATE GENERALIZATION BETWEEN CONFIGURATIONS
PERIMETER ZONE - COOLING ENERGY C_4 TERM
All Orientations
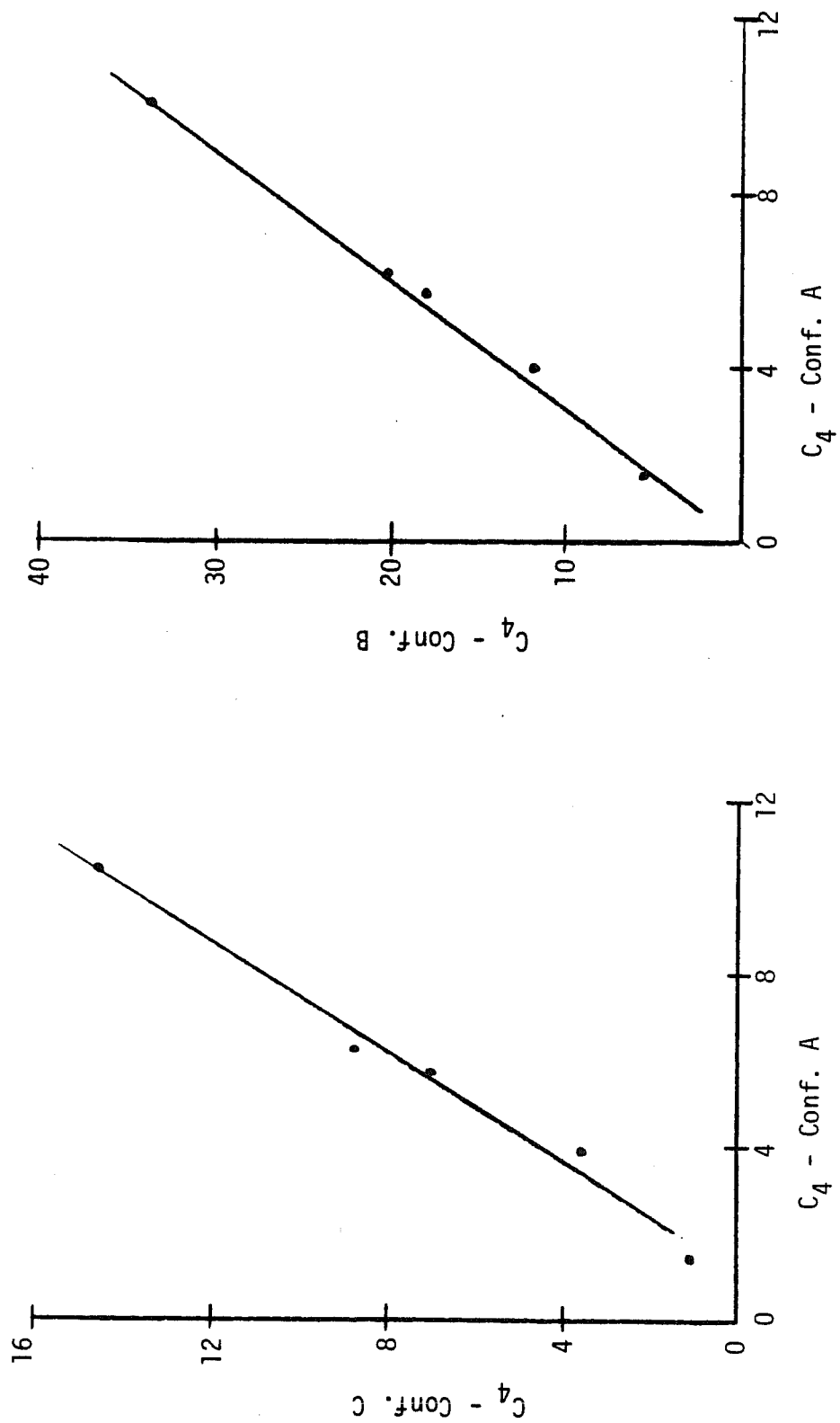
FIGURE 6.9   CLIMATE GENERALIZATION BETWEEN CONFIGURATIONS
PERIMETER ZONE - HEATING ENERGY H_1 TERM
All Orientations
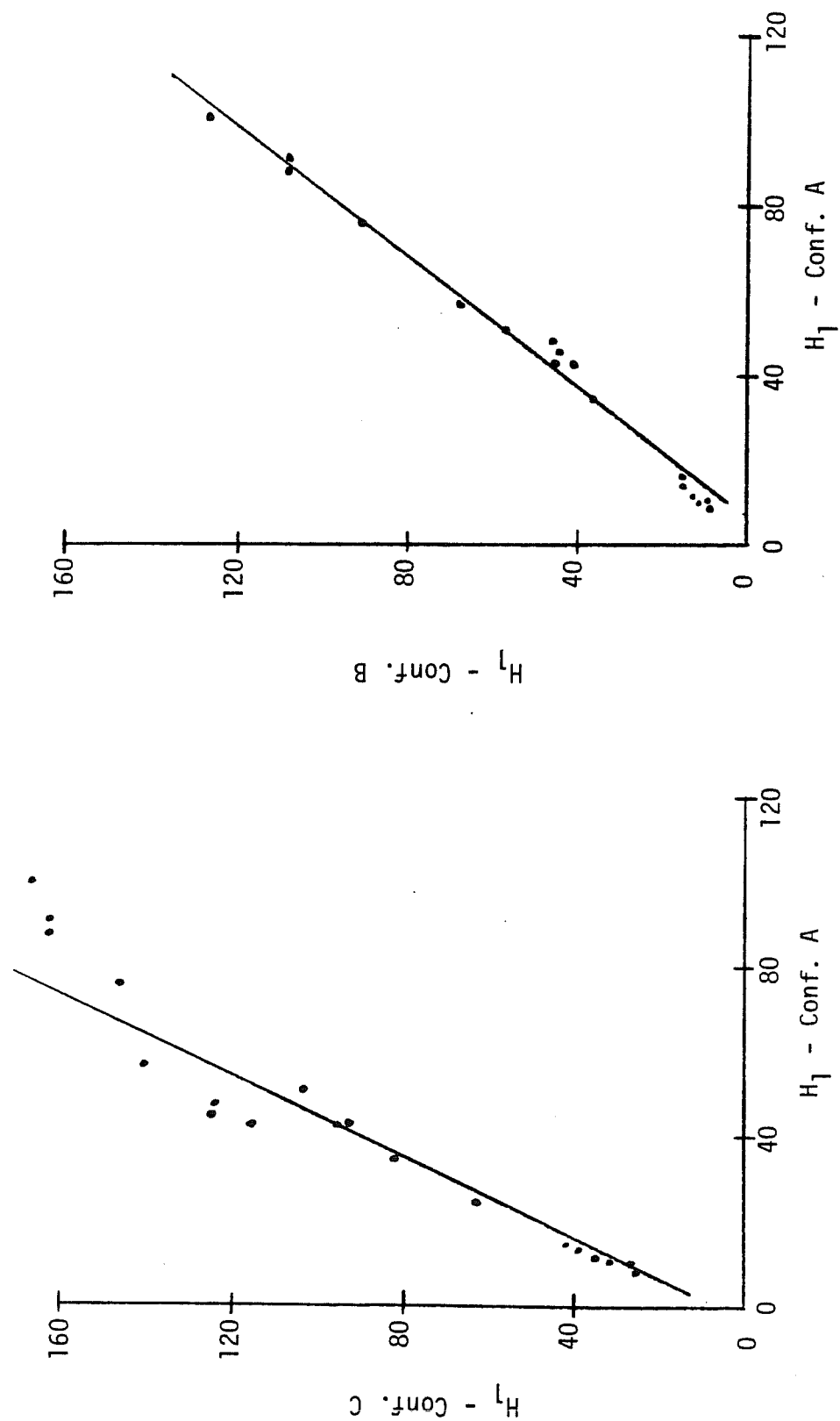
FIGURE 6.10   CLIMATE GENERALIZATION BETWEEN CONFIGURATIONS

PERIMETER ZONE - HEAITNG ENERGY H_2 TERM

All Orientations
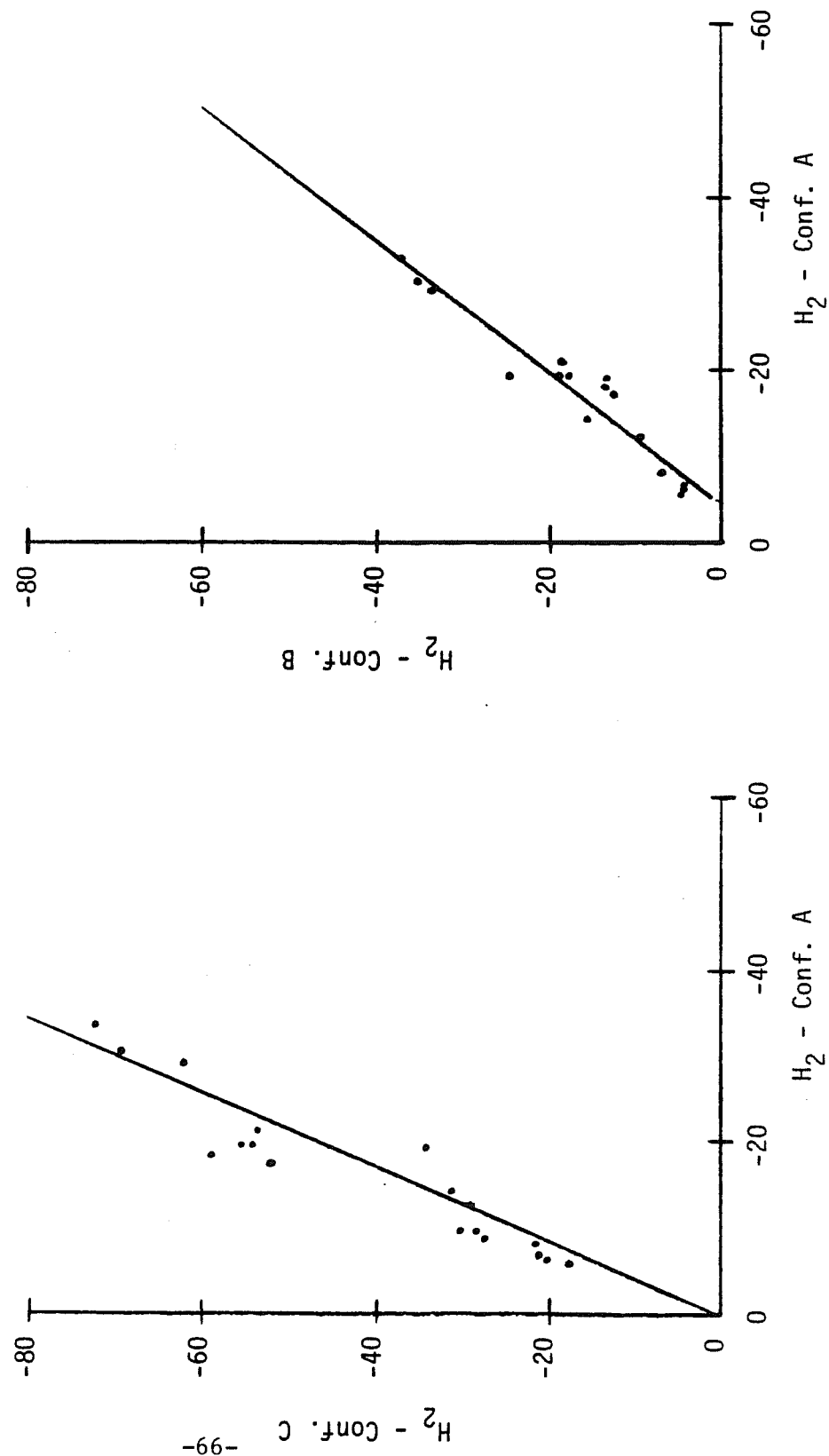
FIGURE 6.11   CLIMATE GENERALIZATION BETWEEN CONFIGURATIONS
PERIMETER ZONE - HEATING ENERGY H_3 TERM
All Orientations
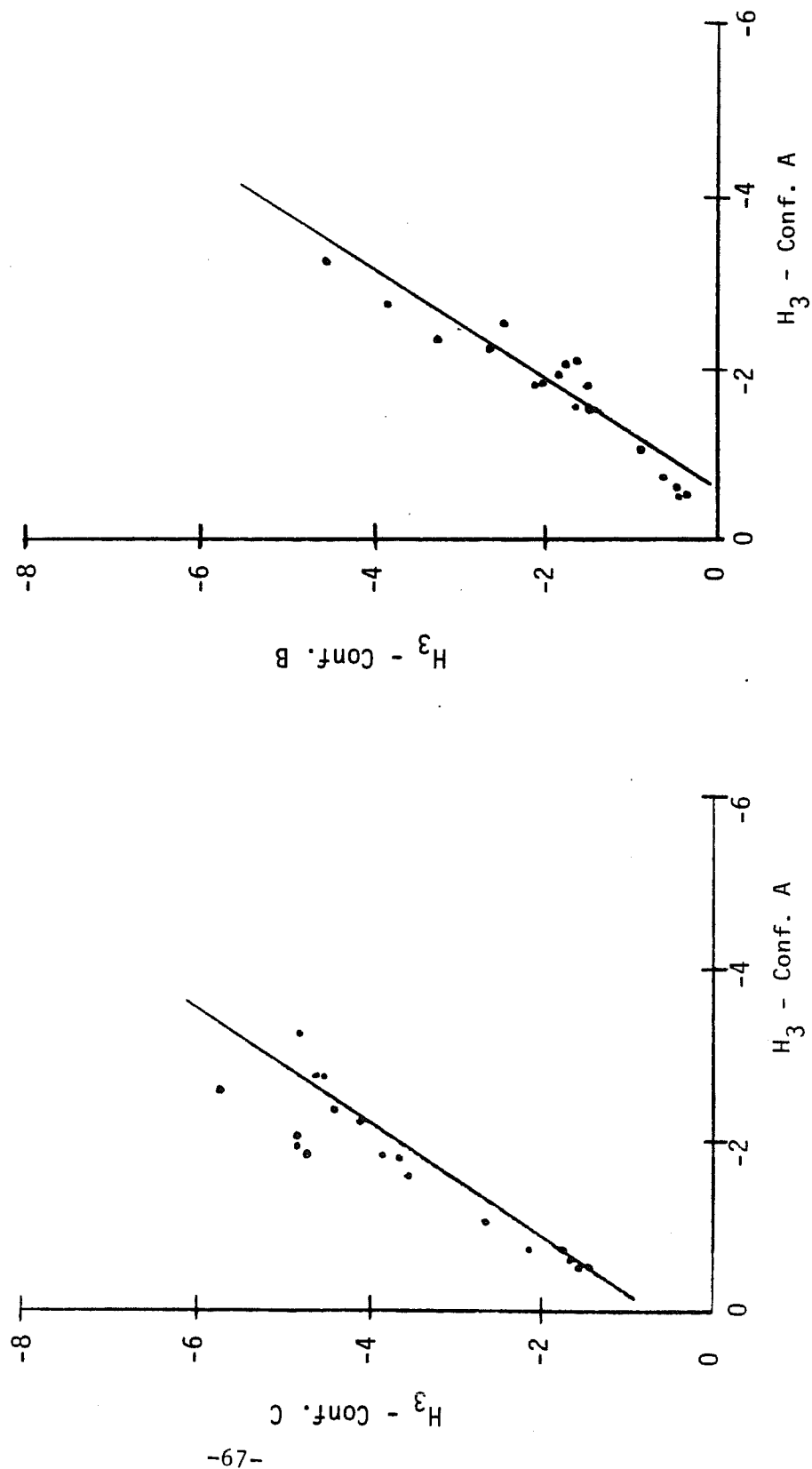
FIGURE 6.12 CLIMATE GENERALIZATION BETWEEN CONFIGURATIONS
PERIMETER ZONE – HEATING ENERGY H_4 TERM
All Orientations
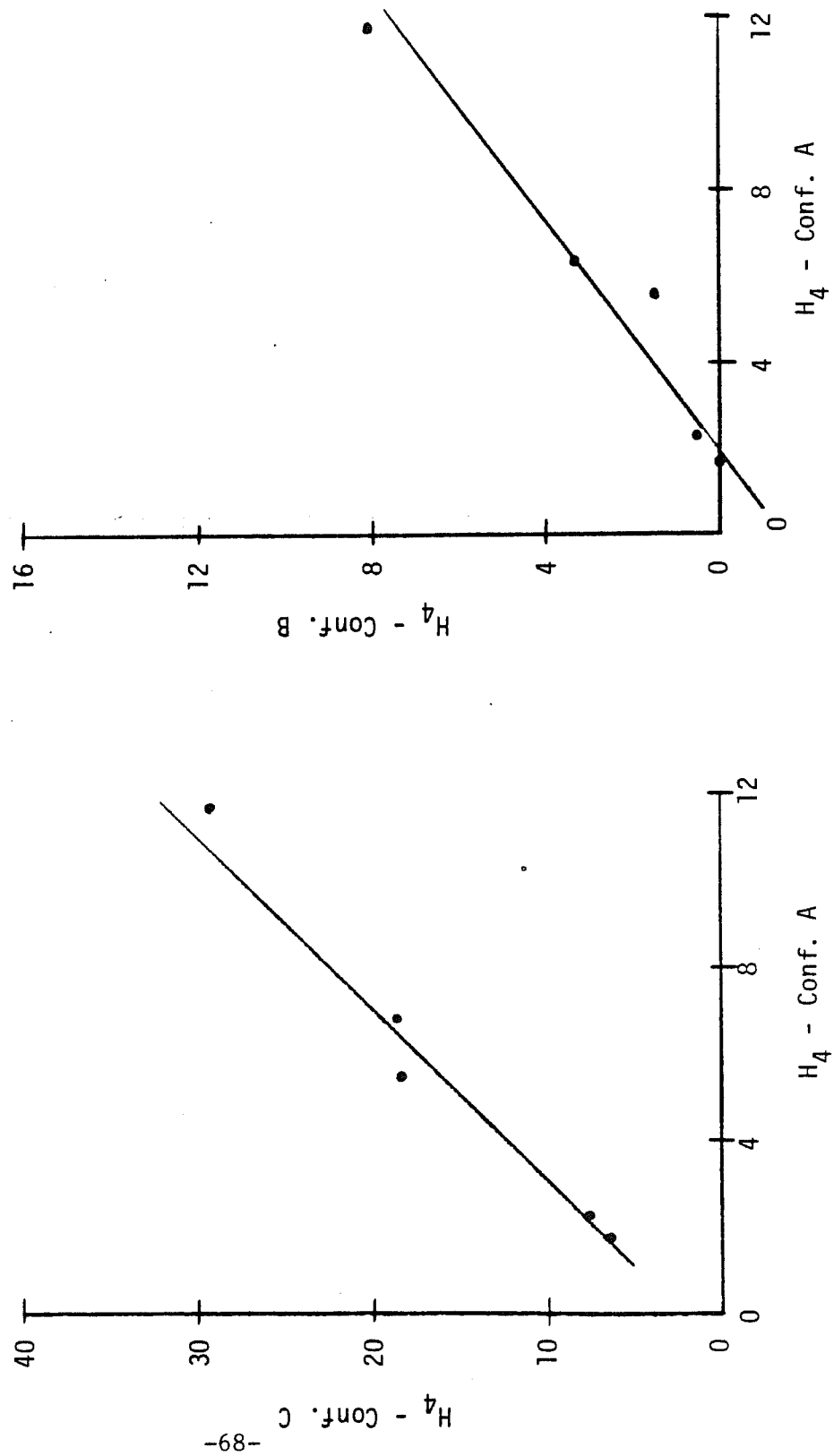
FIGURE 6.13   CLIMATE GENERALIZATION BETWEEN CONFIGURATIONS
ROOFTOP ZONE - COOLING PEAK P_1 AND P_2 TERMS
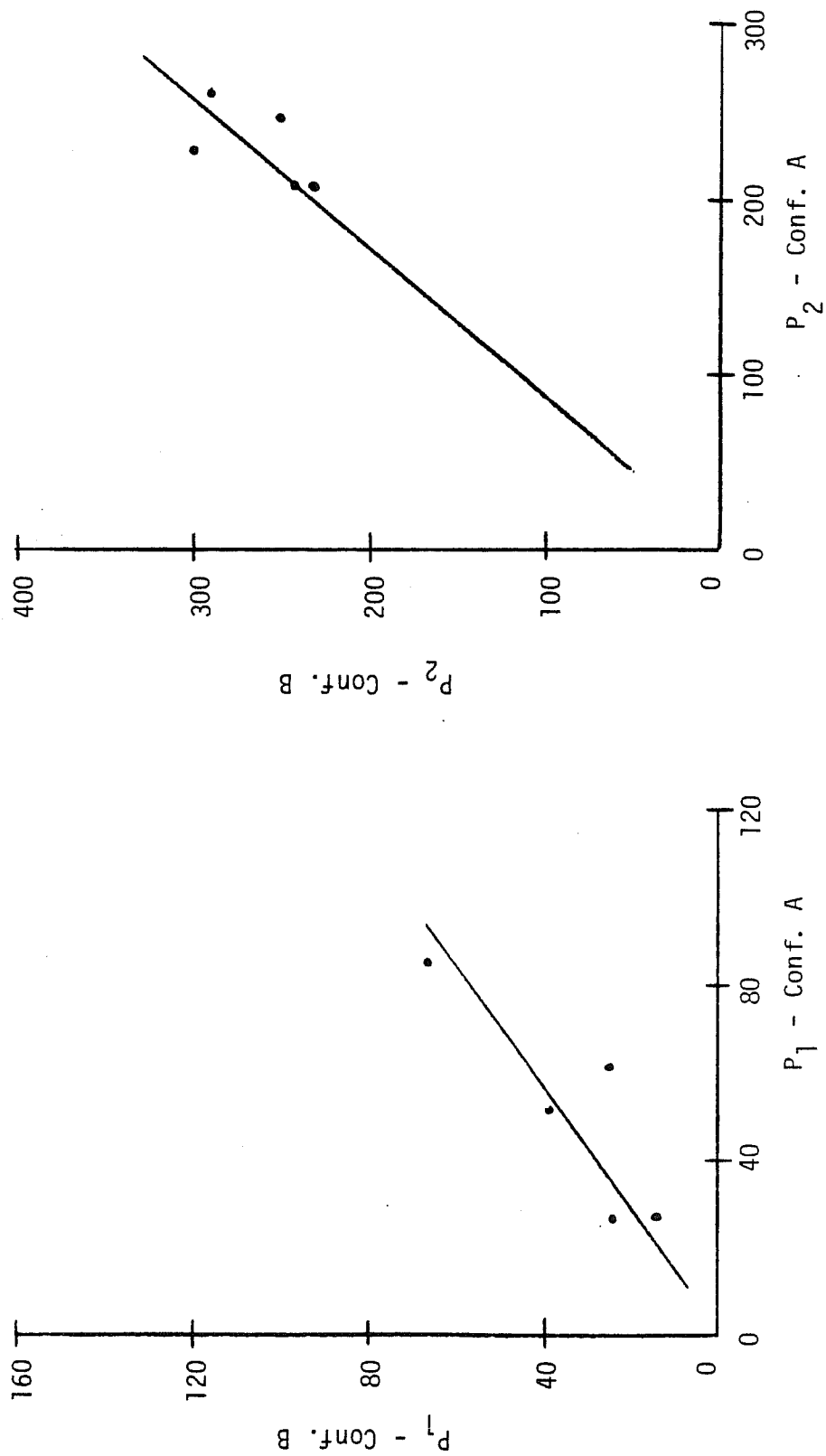
FIGURE 6.14   CLIMATE GENERALIZATION BETWEEN CONFIGURATIONS

ROOFTOP ZONE – COOLING PEAK P_3 AND P_4 TERMS
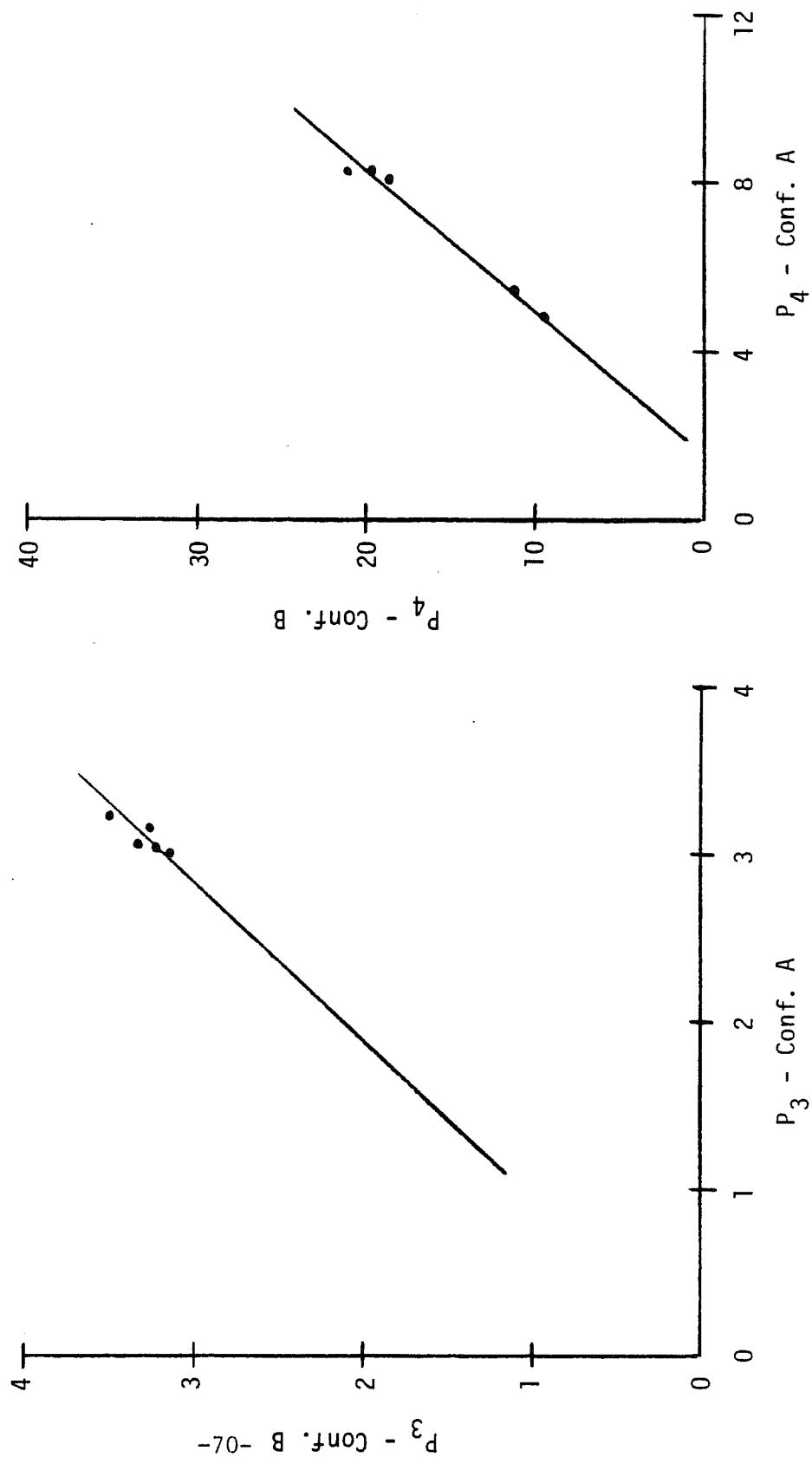
FIGURE 6.15   CLIMATE GENERALIZATION BETWEEN CONFIGURATIONS
ROOFTOP ZONE - COOLING ENERGY C_1 AND C_2 TERMS
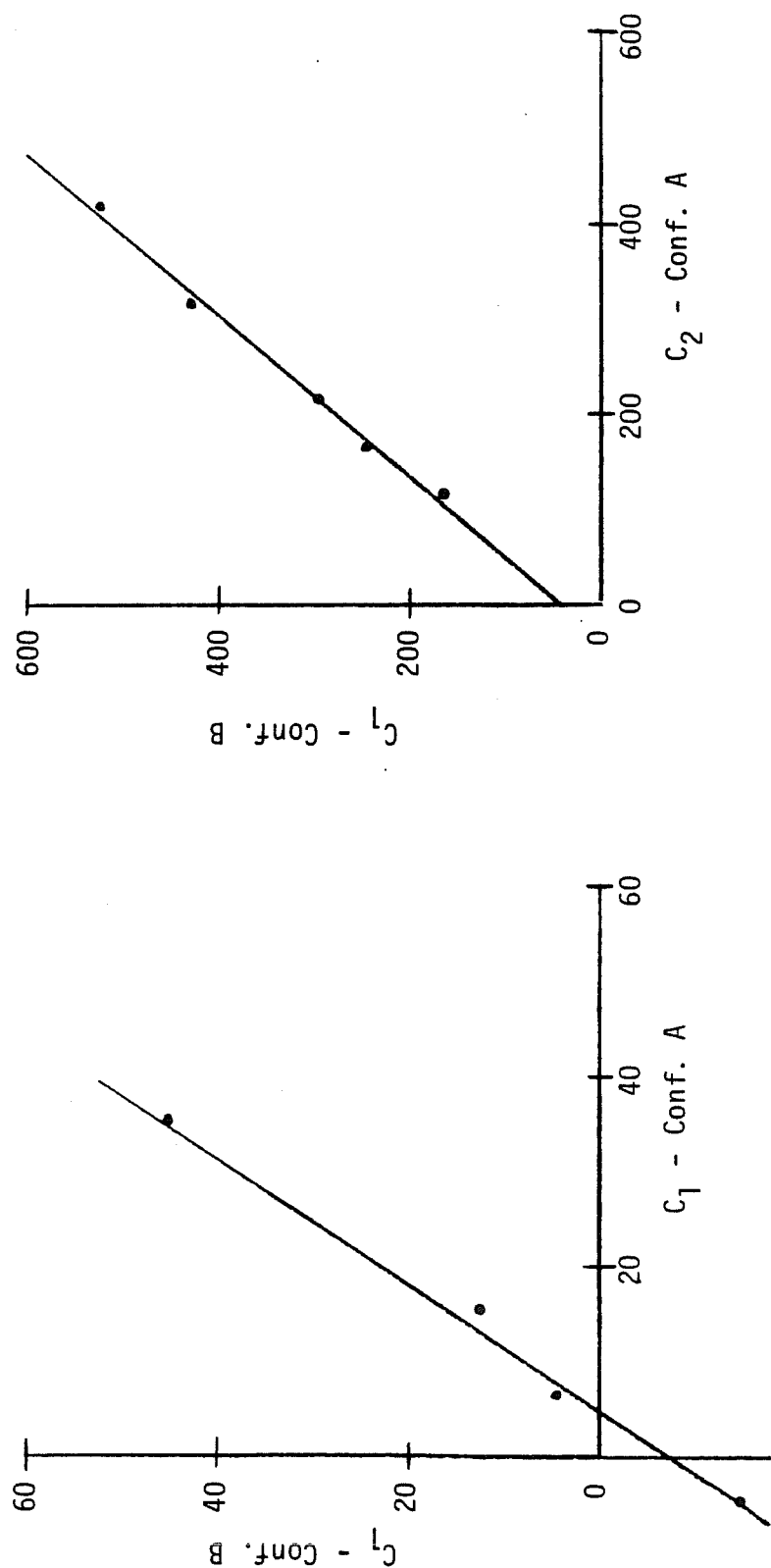
FIGURE 6.16   CLIMATE GENERALIZATION BETWEEN CONFIGURATIONS
ROOFTOP ZONE – COOLING ENERGY C_3 AND C_4 TERMS
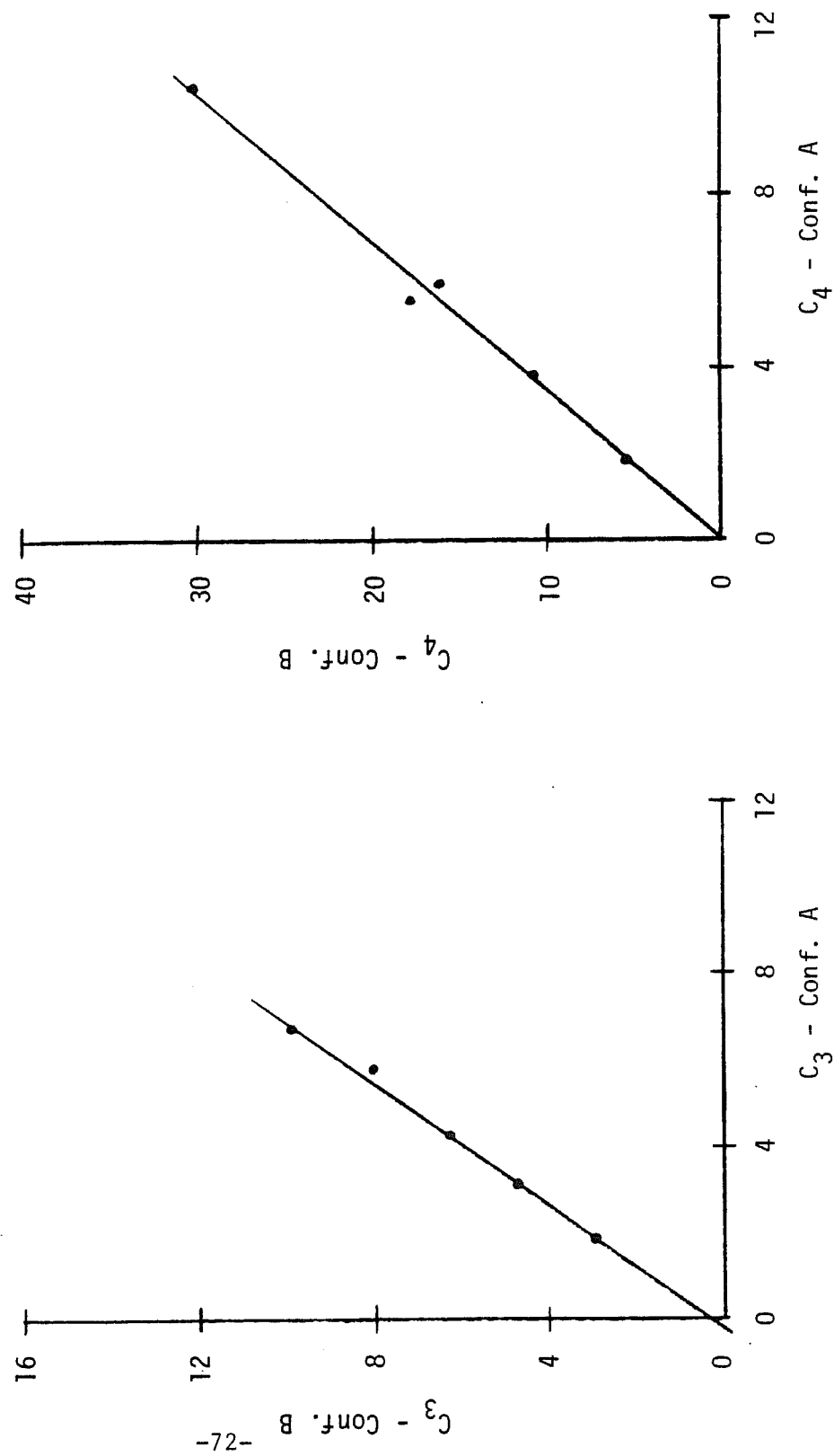
FIGURE 6.17   CLIMATE GENERALIZATION BETWEEN CONFIGURATIONS
ROOFTOP ZONE – HEATING ENERGY H_1 AND H_2 TERMS
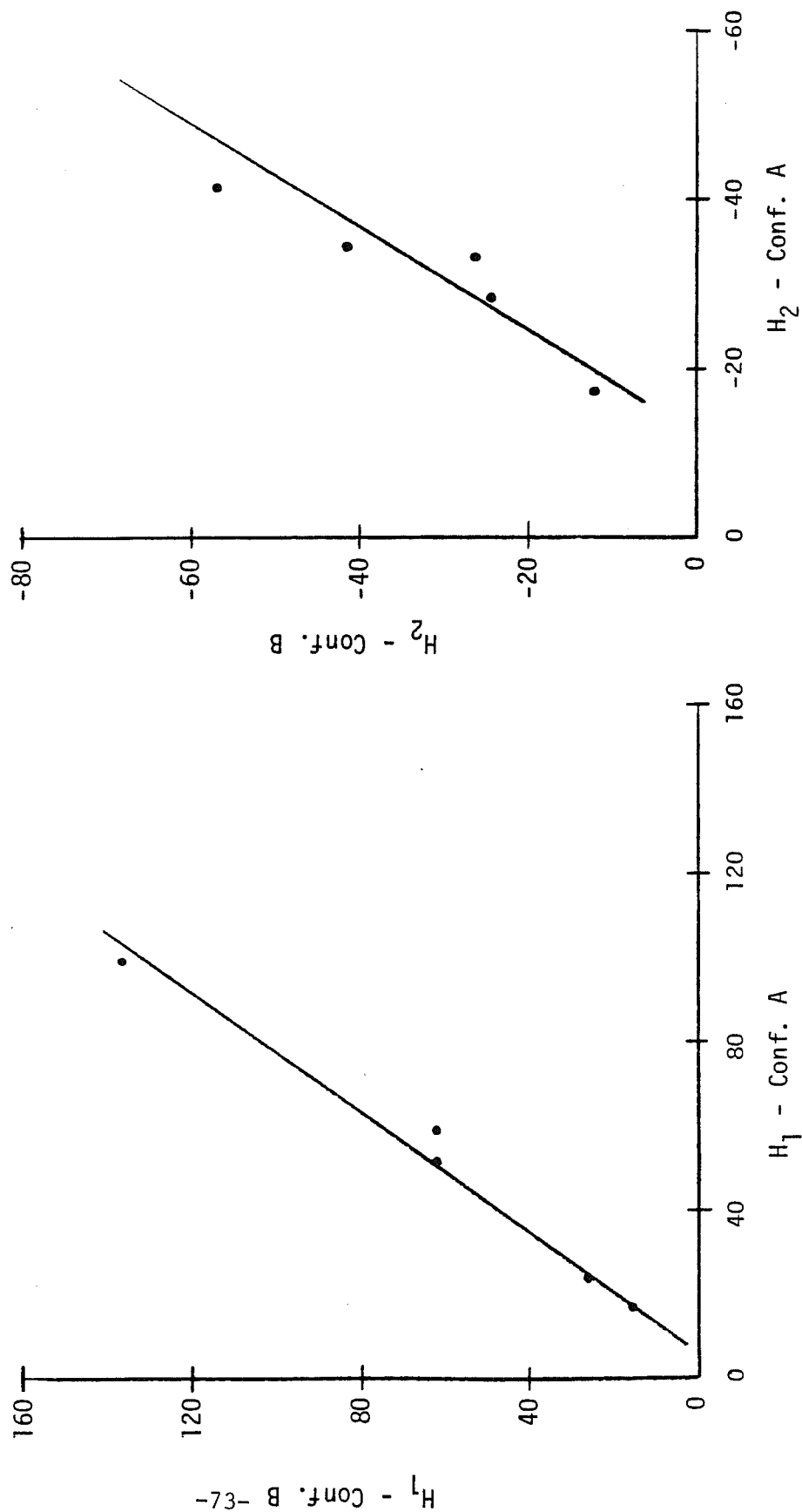
FIGURE 6.18   CLIMATE GENERALIZATION BETWEEN CONFIGURATIONS
ROOFTOP ZONE – HEATING ENERGY H_3 AND H_4 TERMS
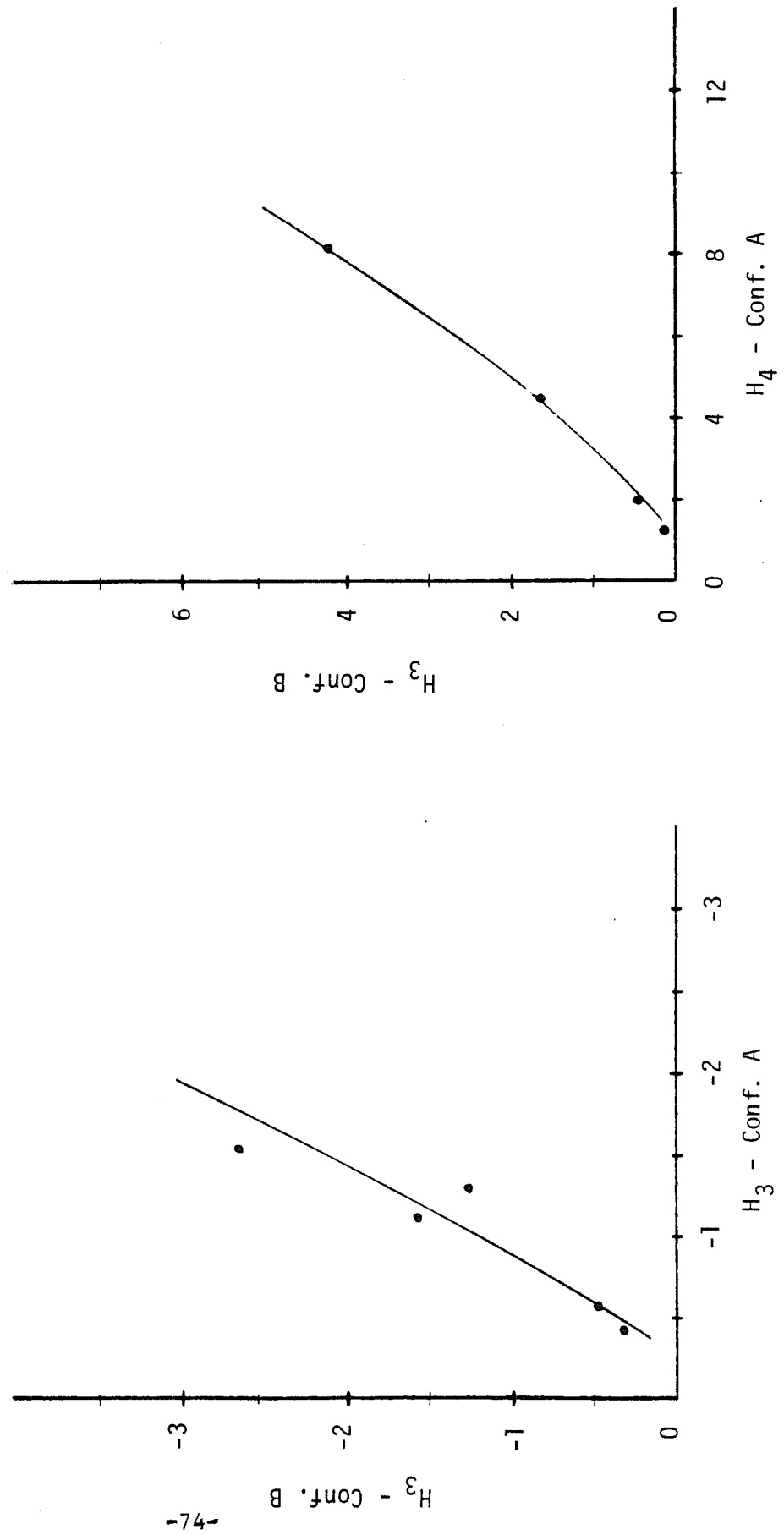
FIGURE 6.19   COOLING PEAK DUE TO CONDUCTION - PERIMETER
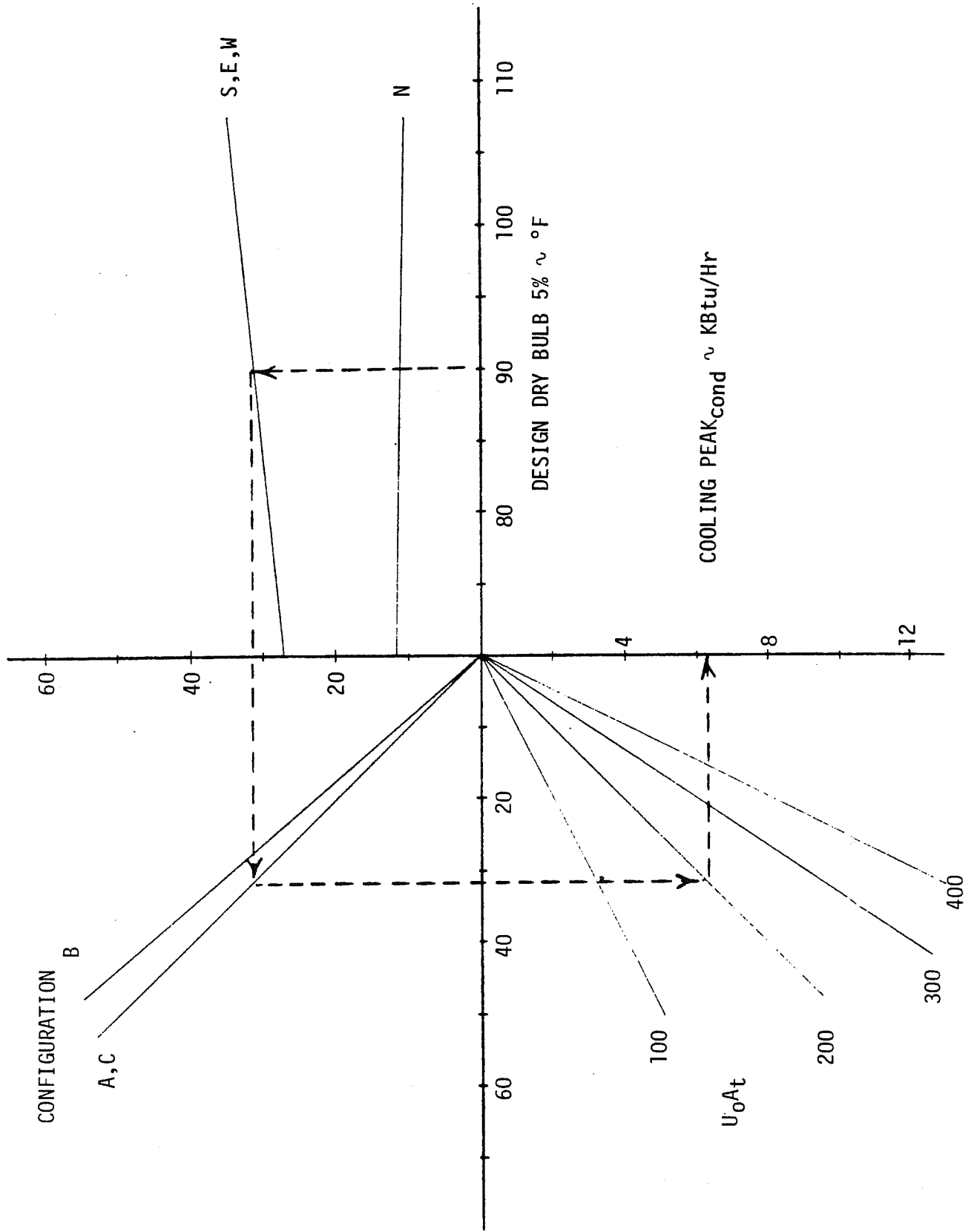
FIGURE 6.20   COOLING PEAK DUE TO SOLAR RADIATION - PERIMETER
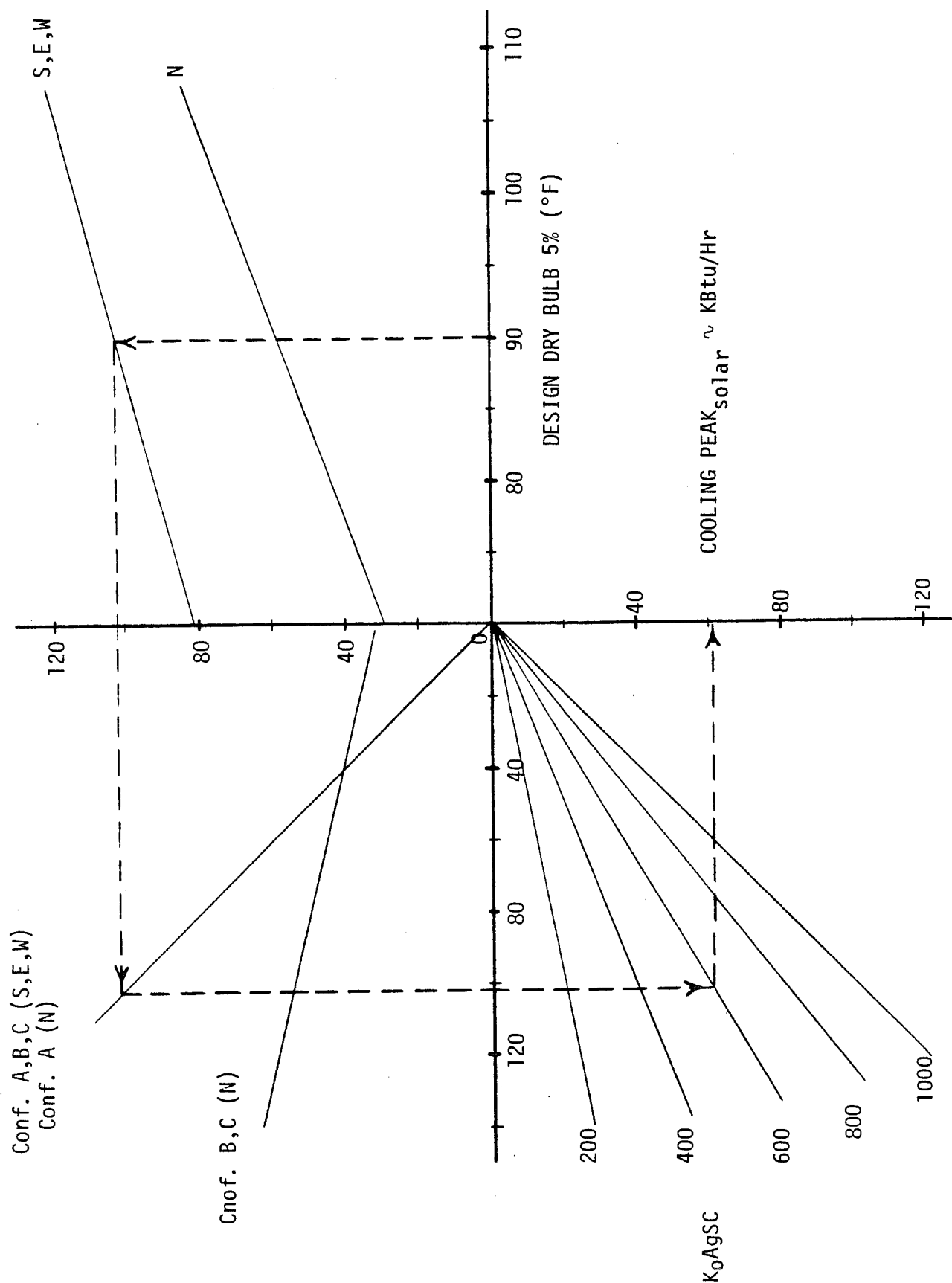
FIGURE 6.21 COOLING PEAK DUE TO LIGHTING - PERIMETER
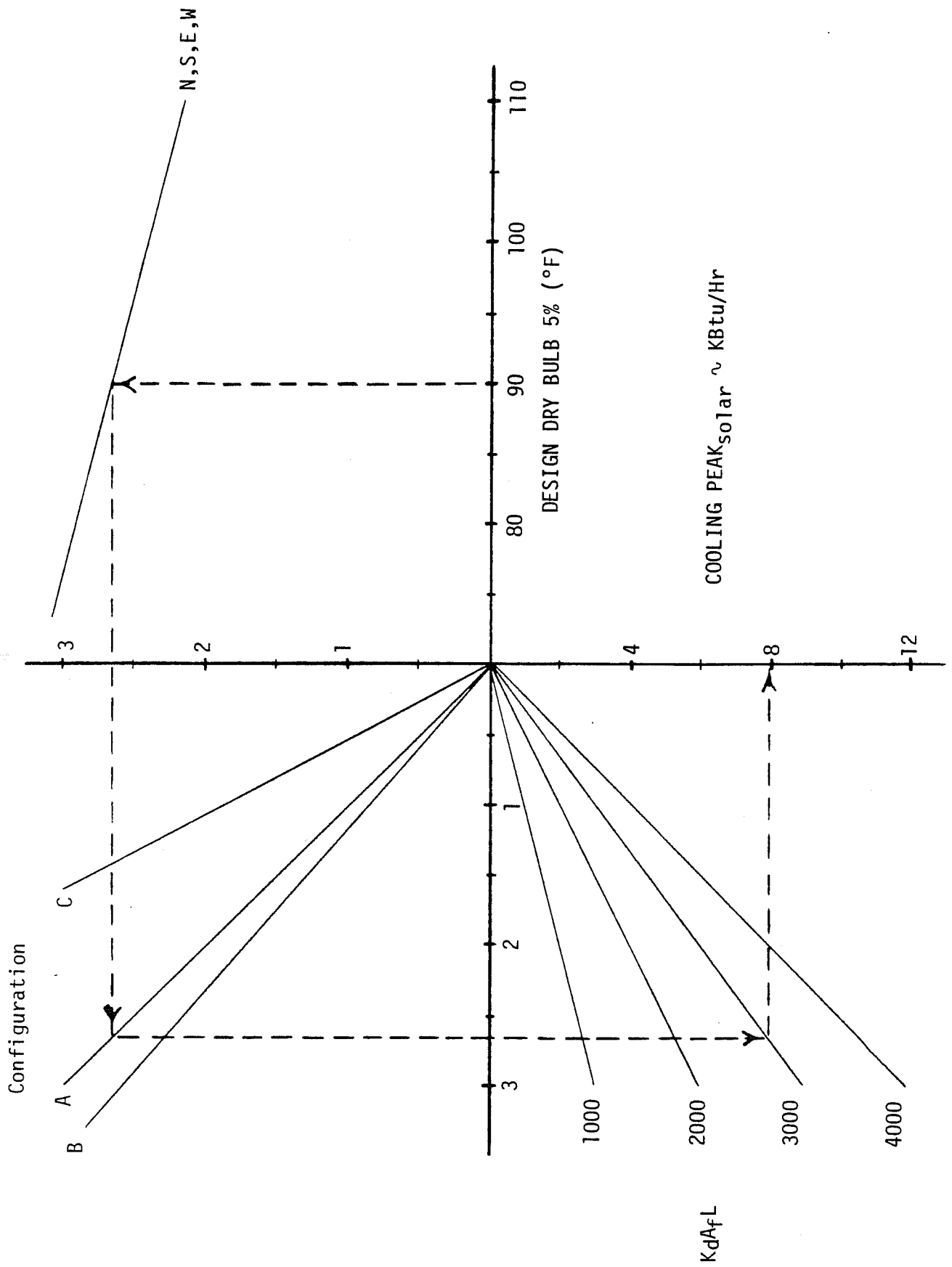
FIGURE 6.22   COOLING PEAK DUE TO OCCUPANTS, EQUIP, INF/VENT - PERIMETER
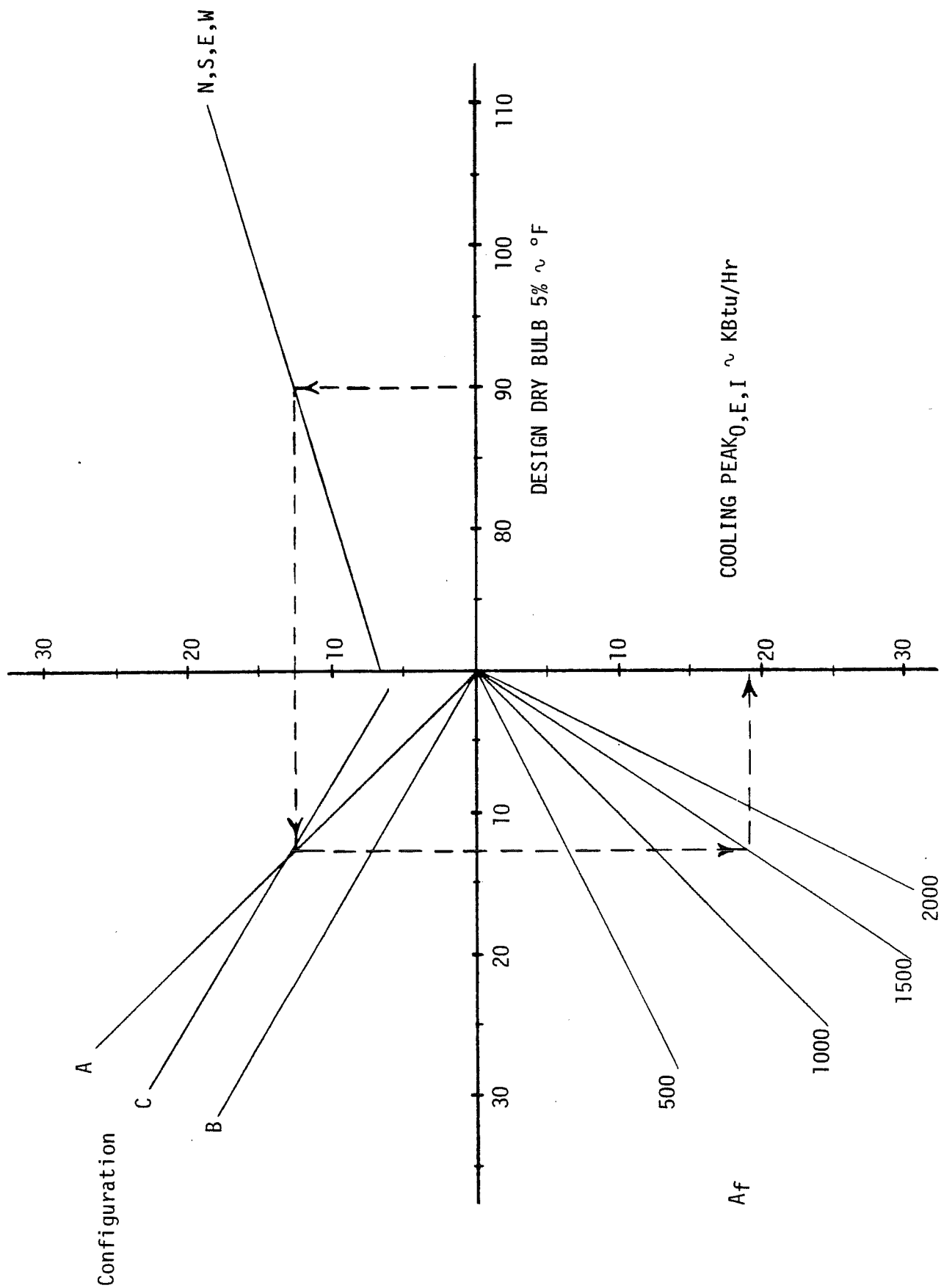
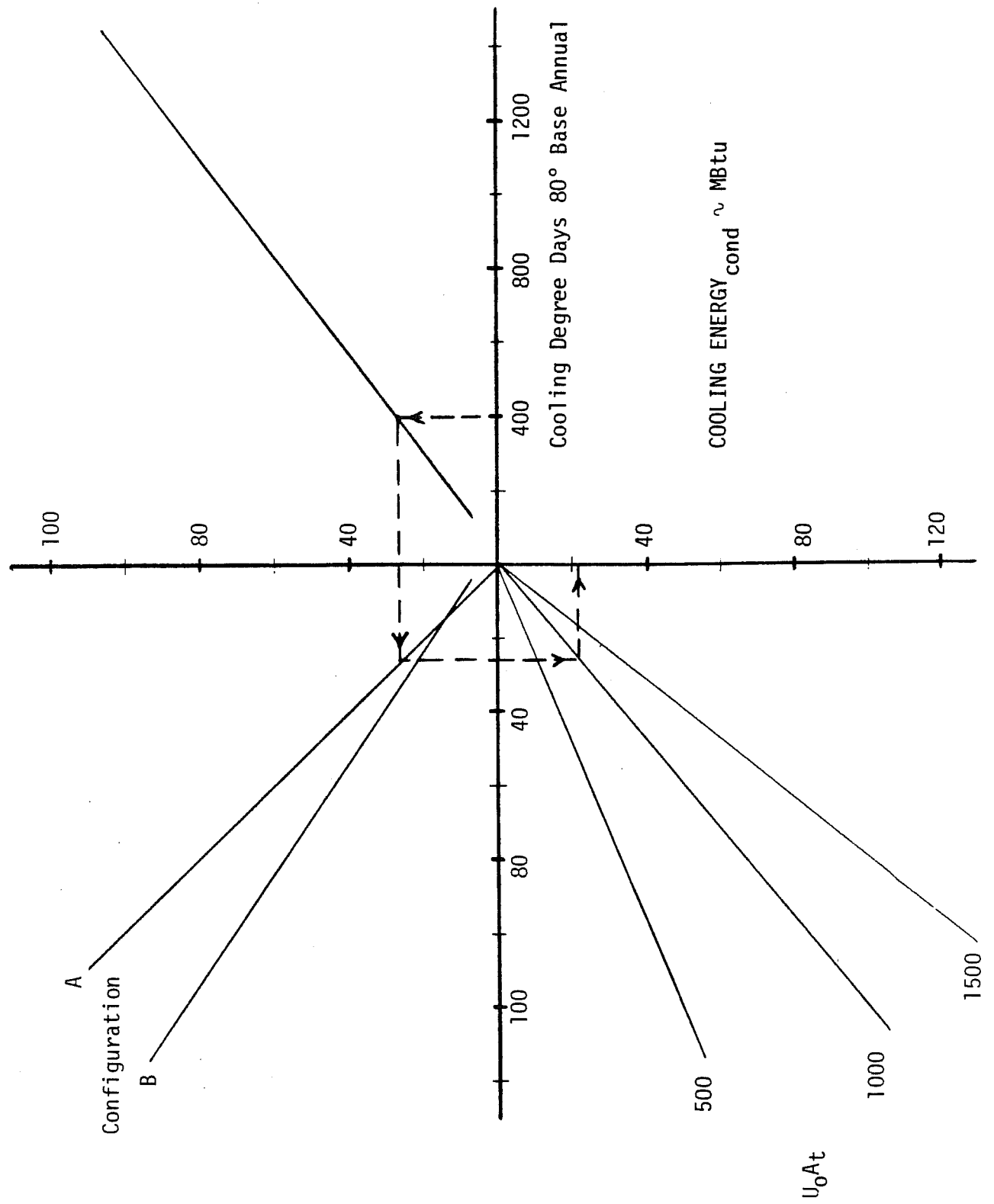FIGURE 6.23   COOLING ENERGY DUE TO CONDUCTION - PERIMETER
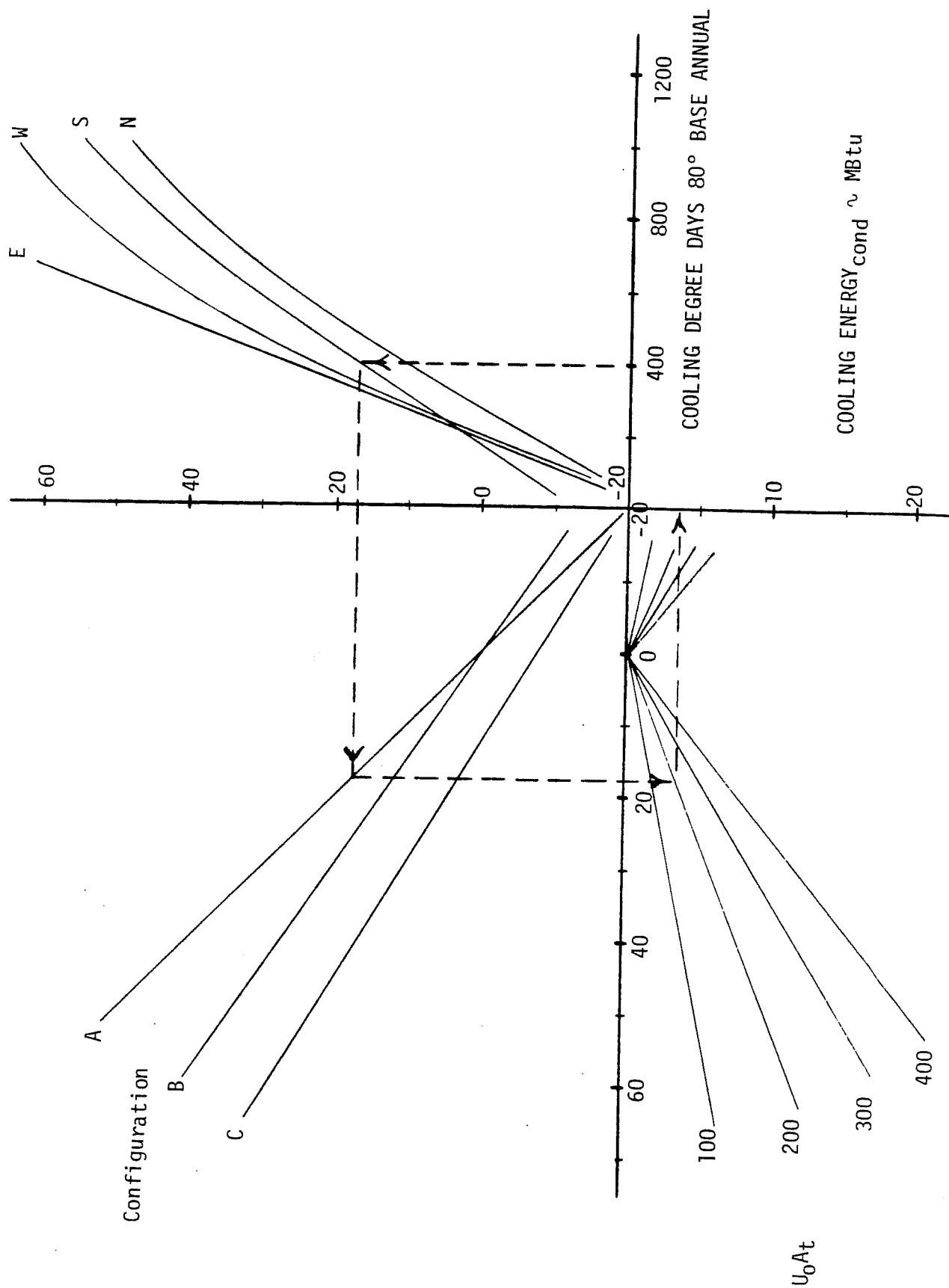
FIGURE 6.24   COOLING ENERGY DUE TO SOLAR RADIATION - PERIMETER
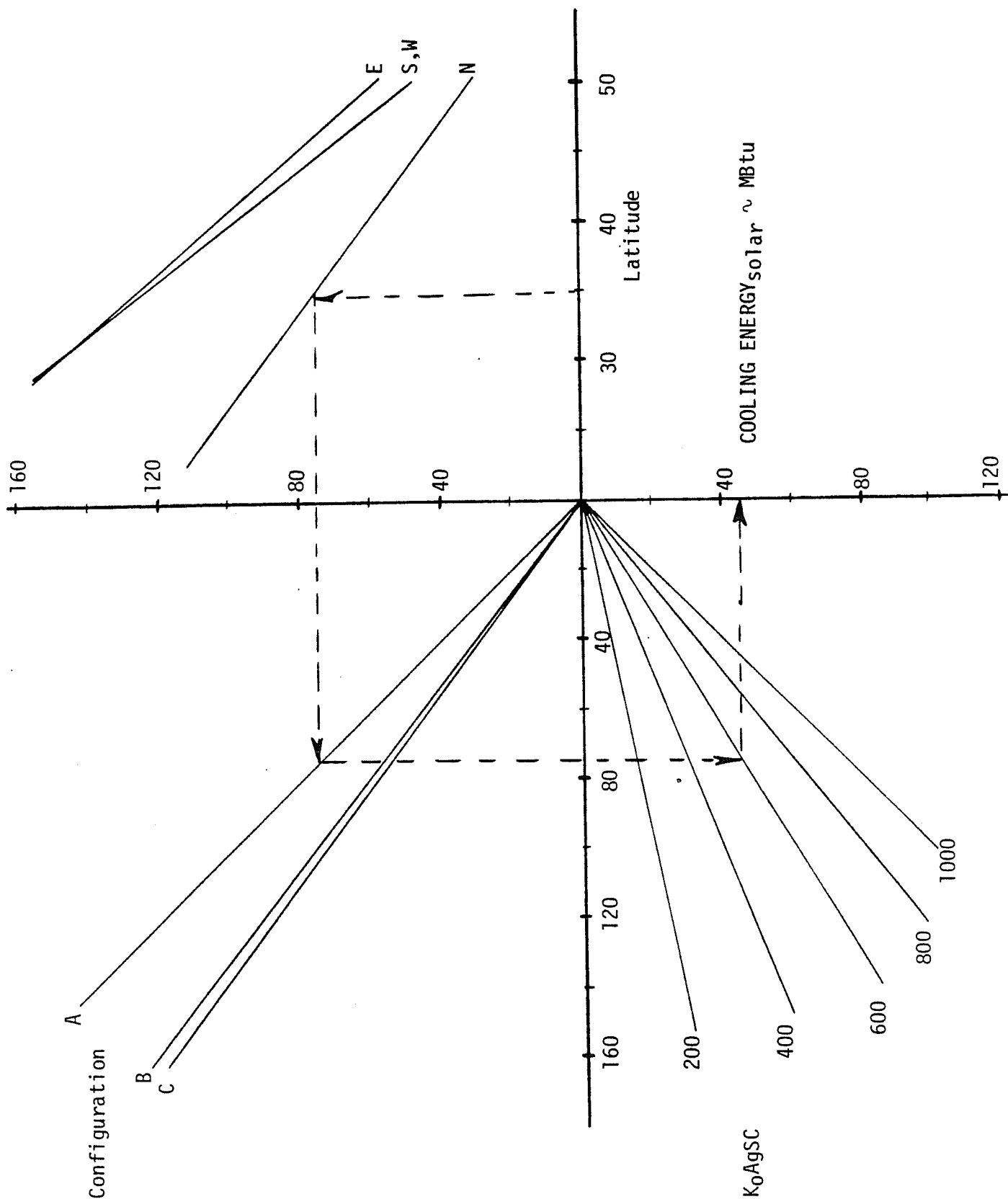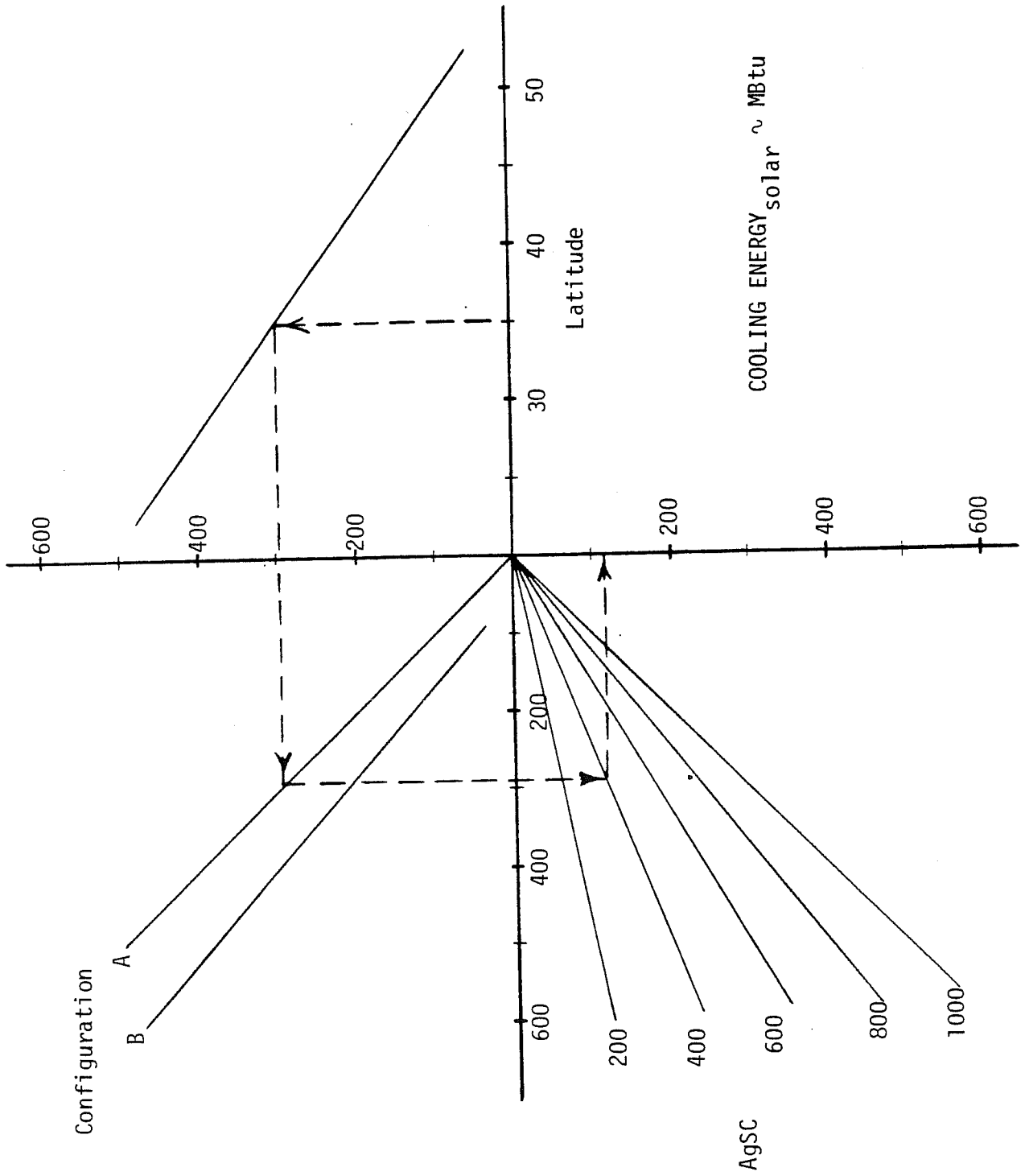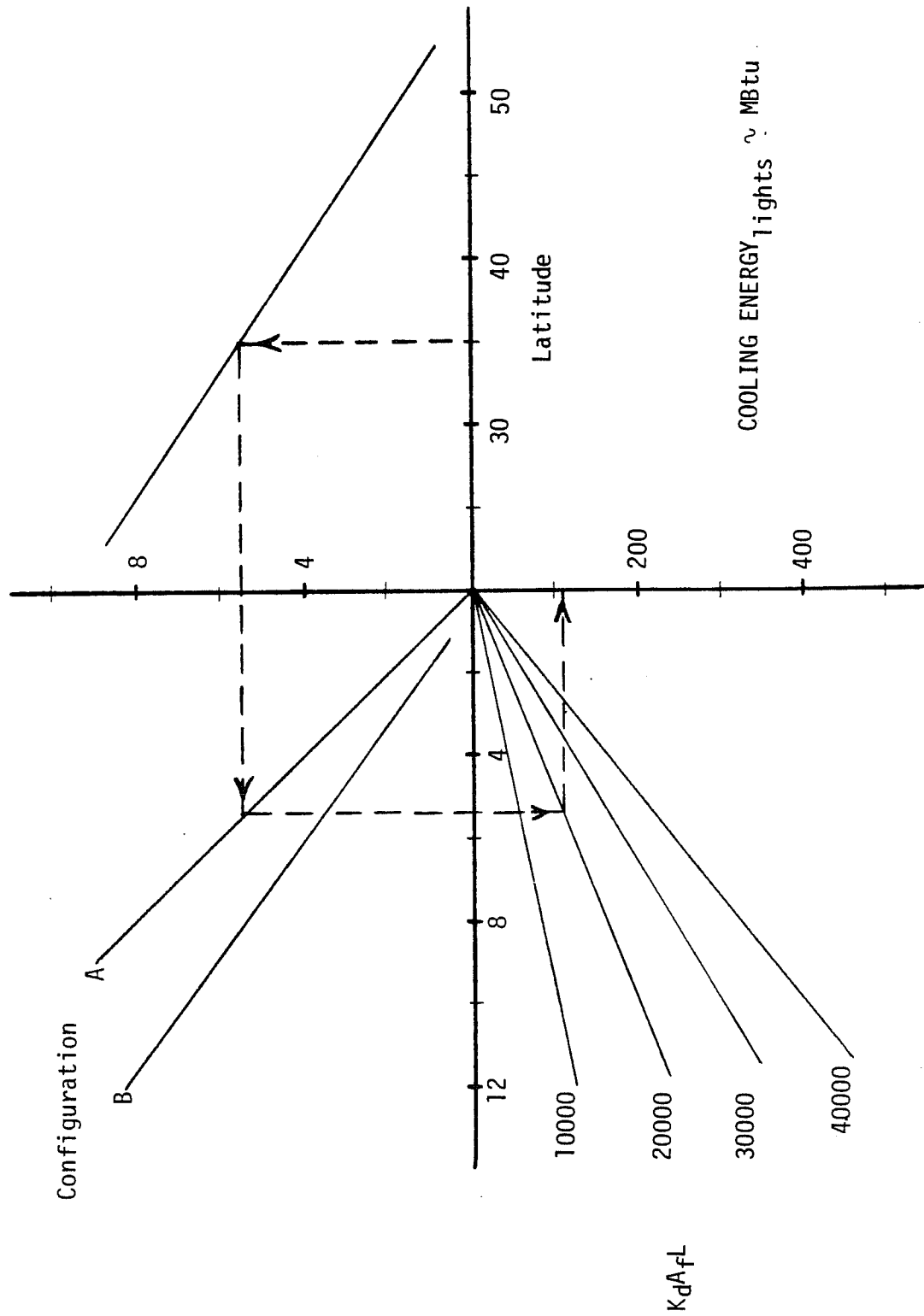
FIGURE 6.25   COOLING ENERGY DUE TO LIGHTING – PERIMETER
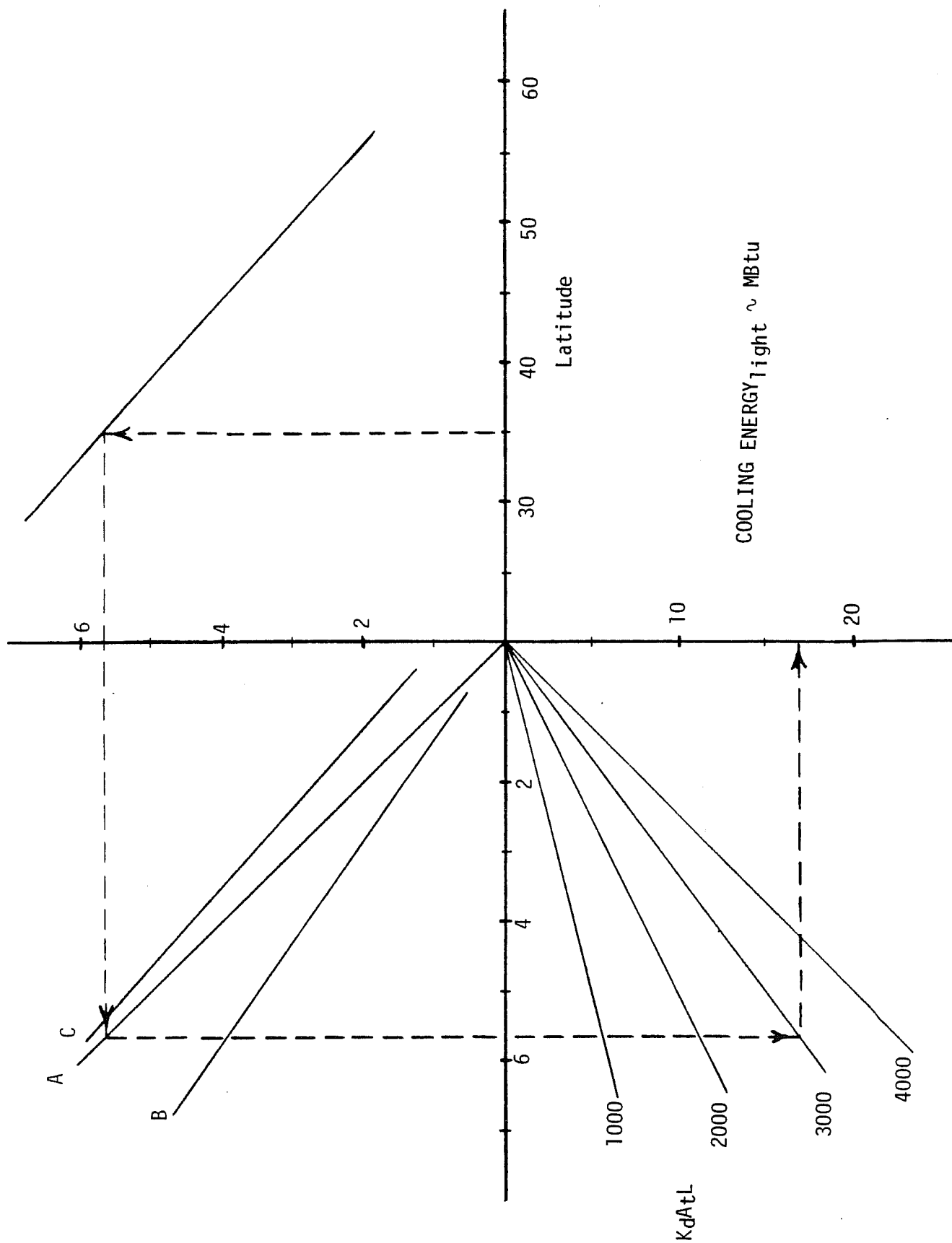
FIGURE 6.26   COOLING ENERGY DUE TO OCCUP, EQUIP, INF/VENT - PERIMETER
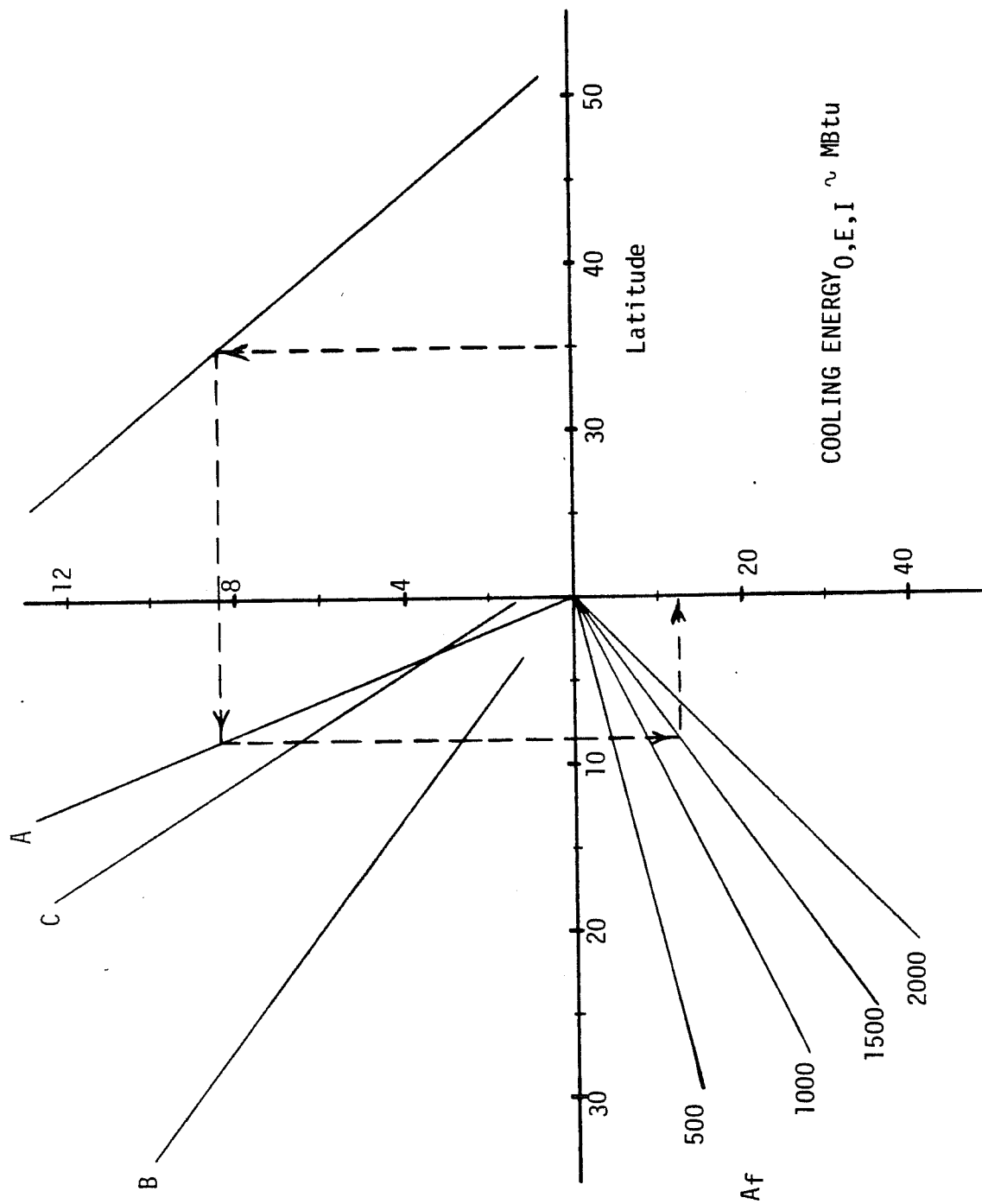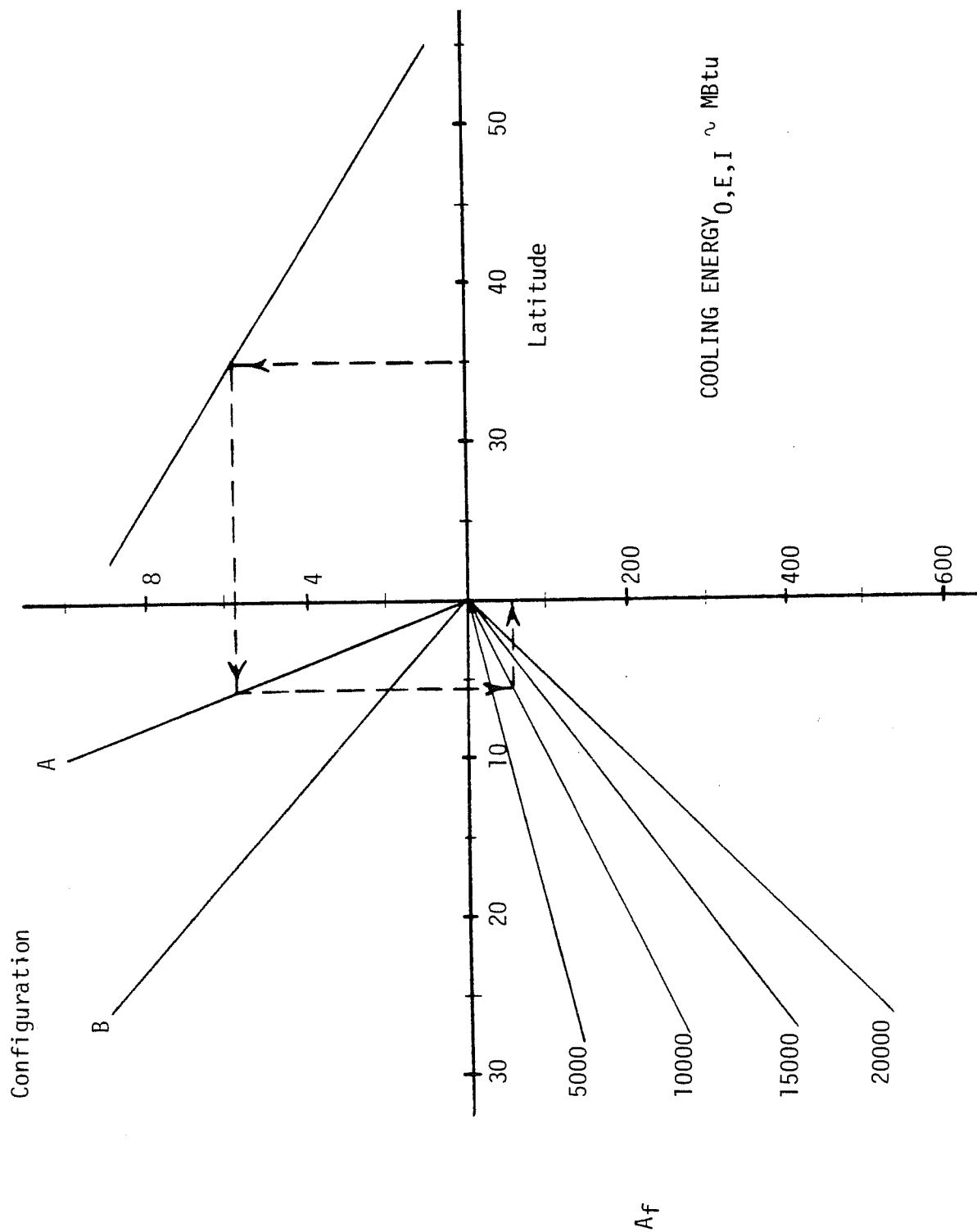
FIGURE 6.27   HEATING ENERGY DUE TO CONDUCTION – PERIMETER
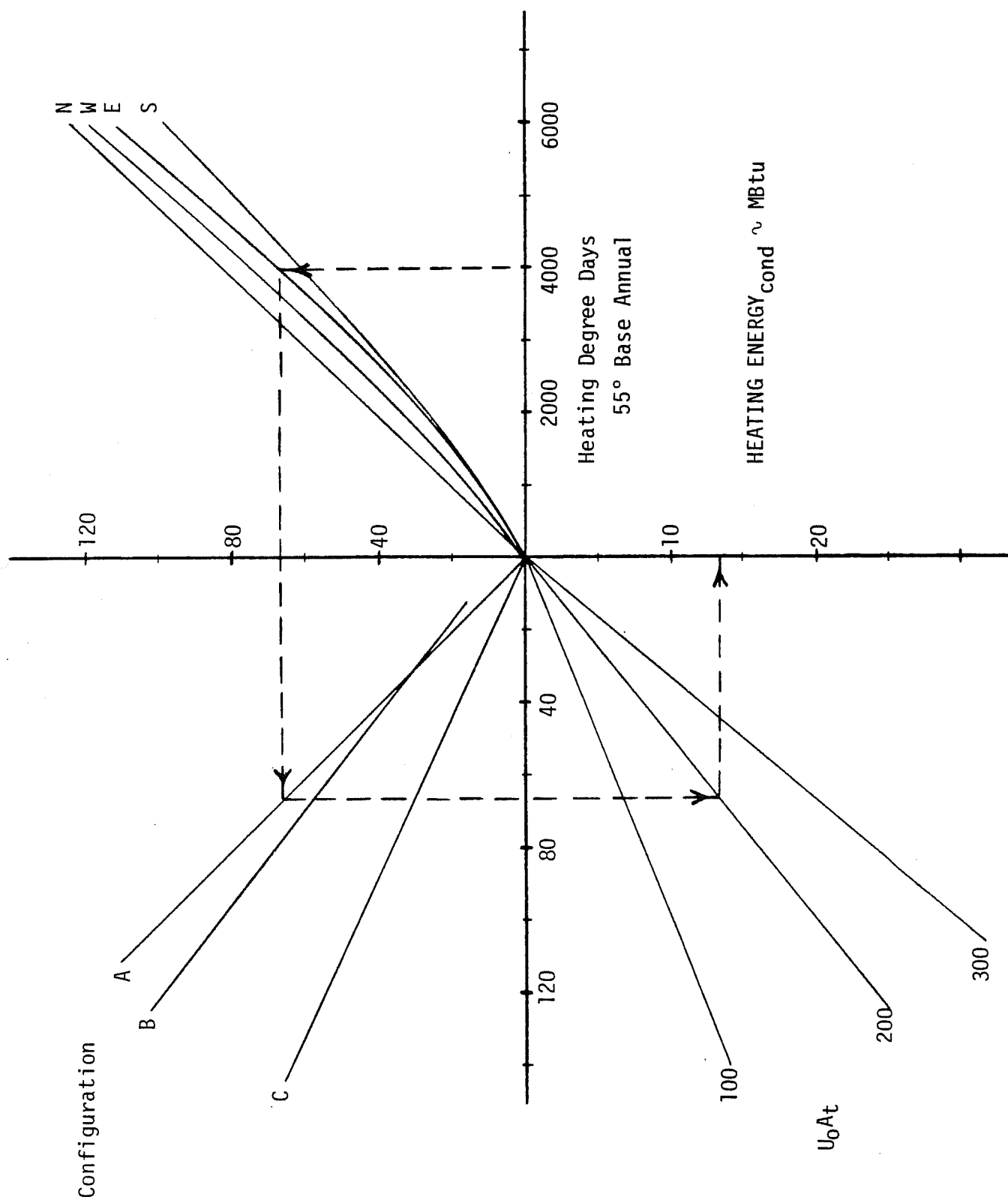
FIGURE 6.28   HEATING ENERGY DUE TO SOLAR RADIATION - PERIMETER
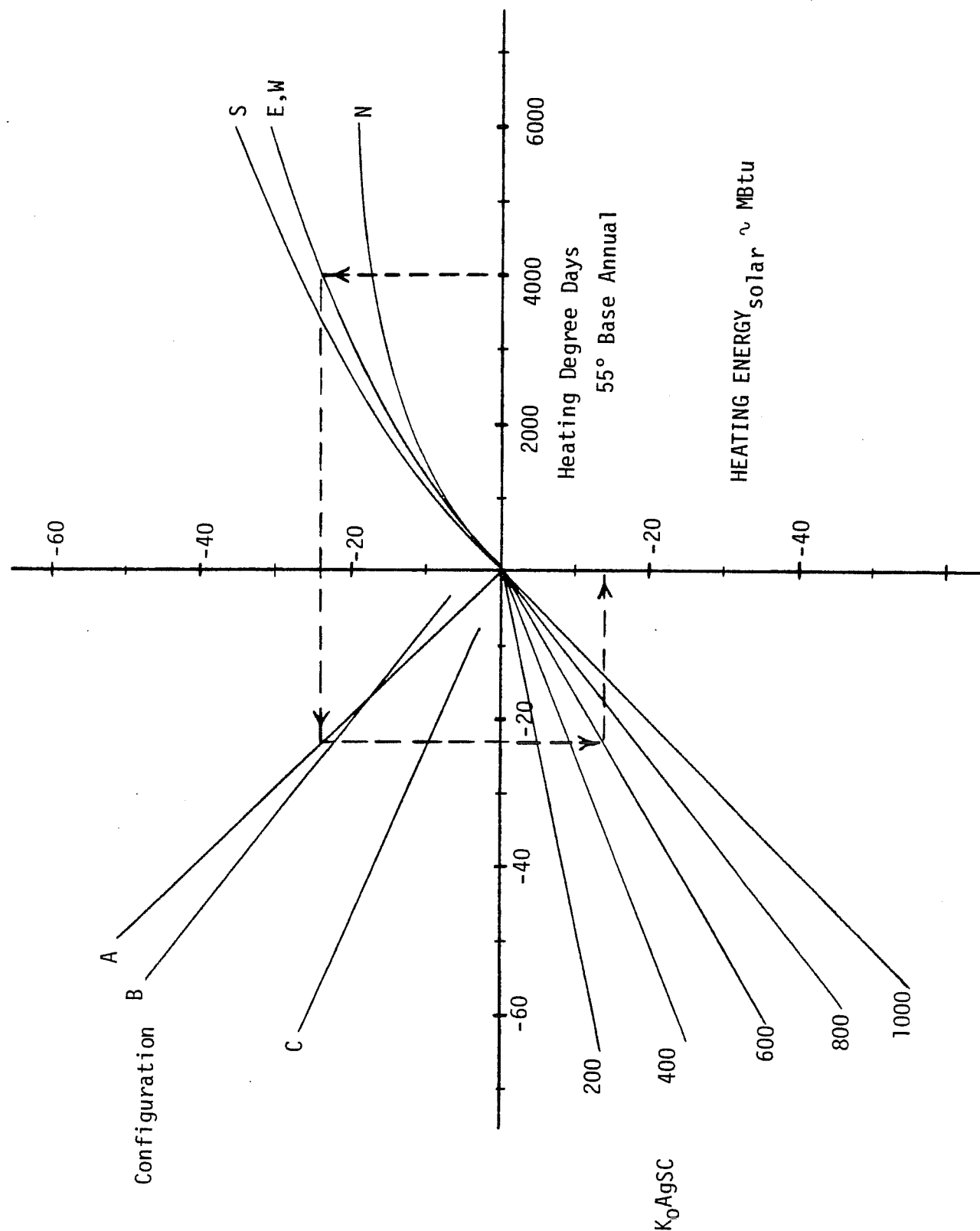
FIGURE 6.29   HEATING ENERGY DUE TO LIGHTING - PERIMETER
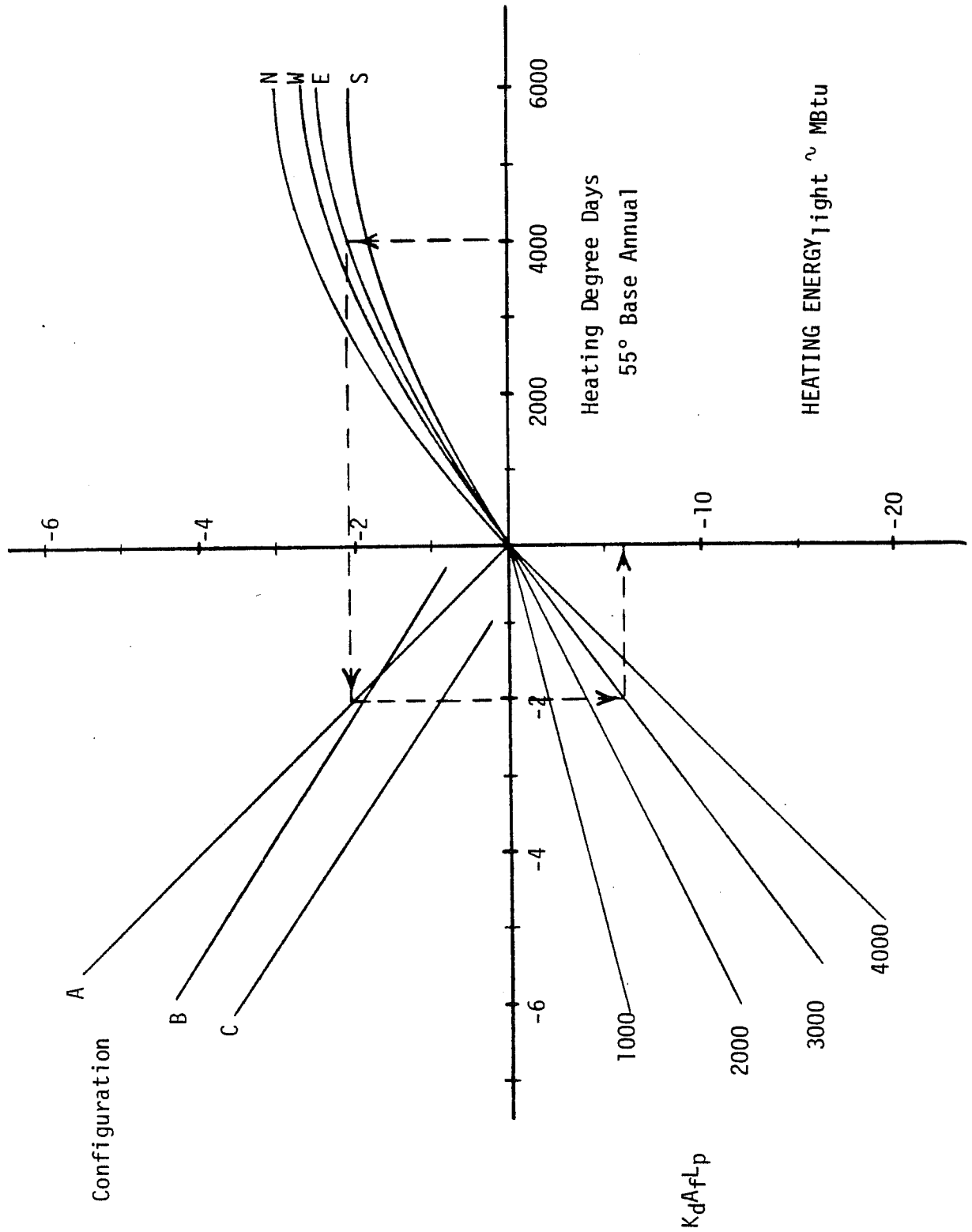
FIGURE 6.30   HEATING ENERGY DUE TO OCCUP, EQUIP, INF/VENT - PERIMETER
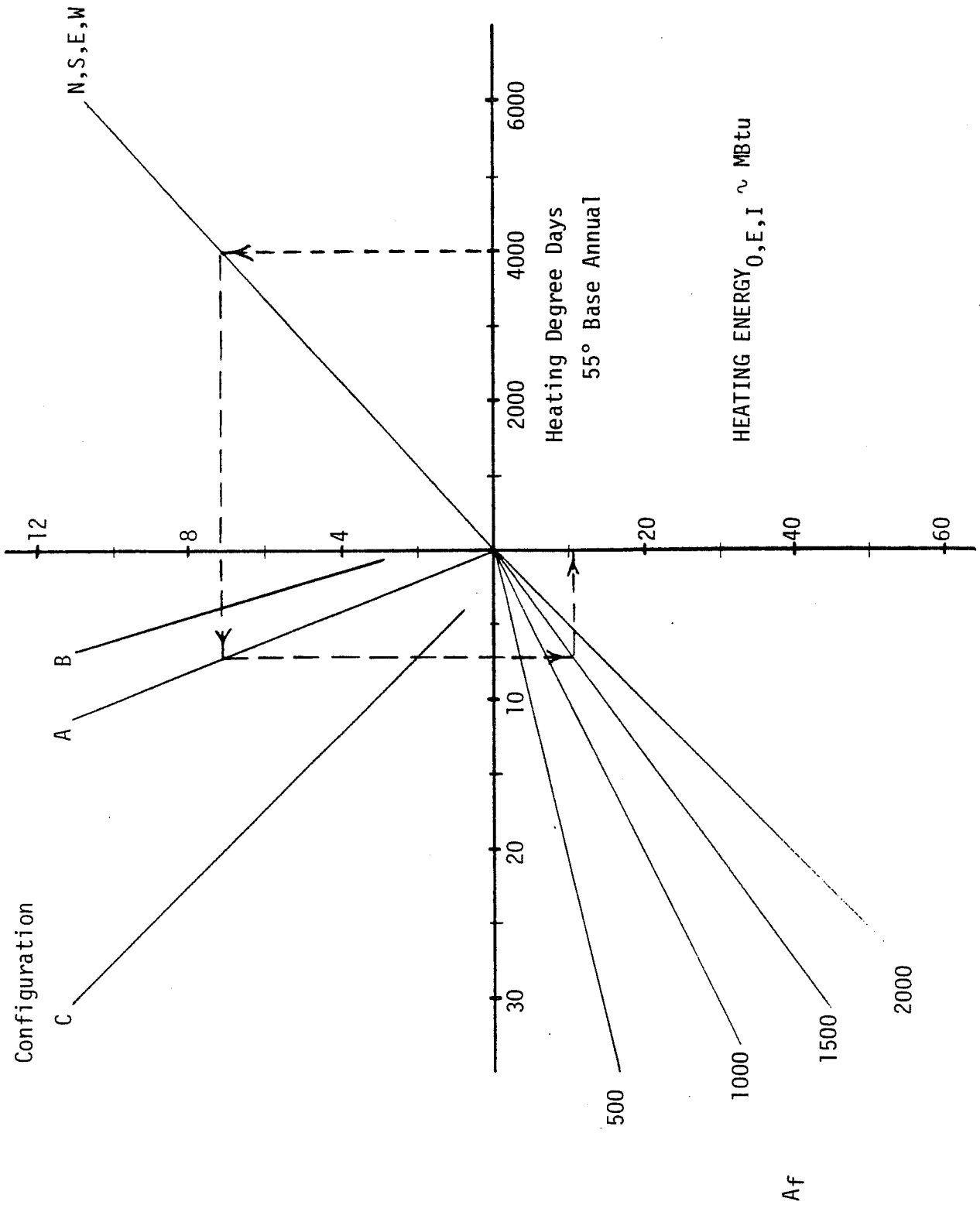
FIGURE 6.31 COOLING PEAK DUE TO CONDUCTION - ROOFTOP
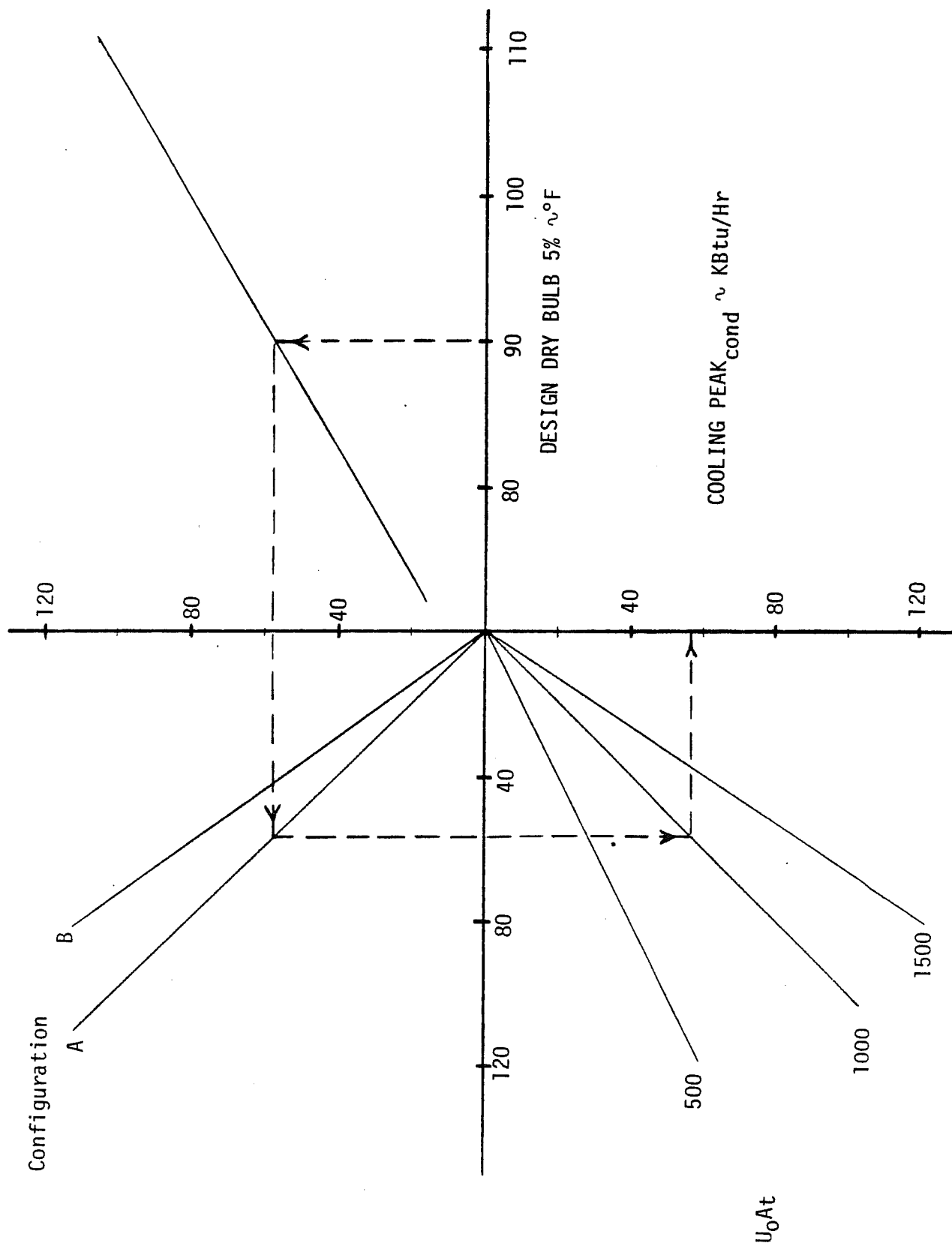
FIGURE 6.32   COOLING PEAK DUE TO SOLAR RADIATION - ROOFTOP
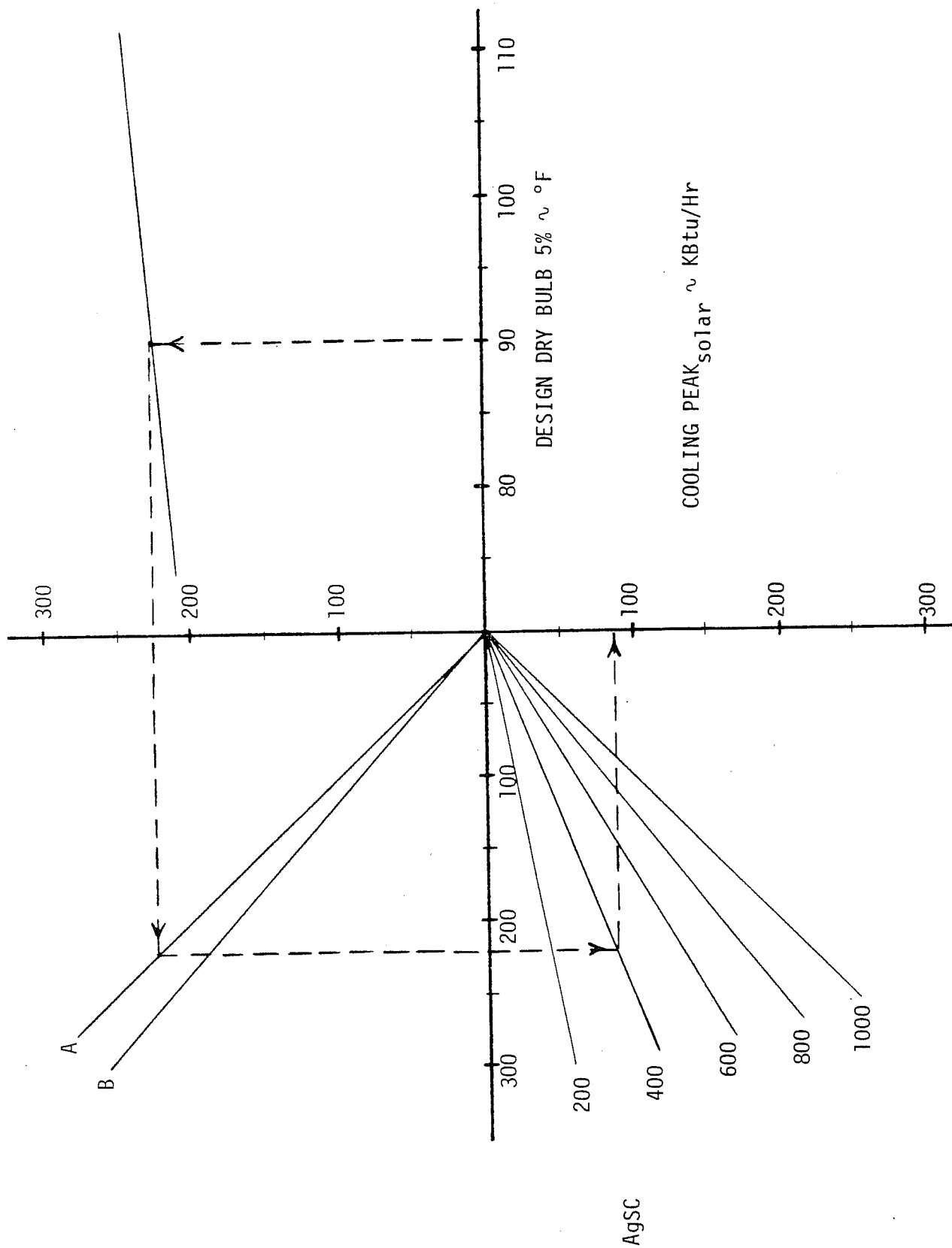
FIGURE 6.33   COOLING PEAK DUE TO OCCUPANTS, EQUIP, INF/VENT - ROOFTOP
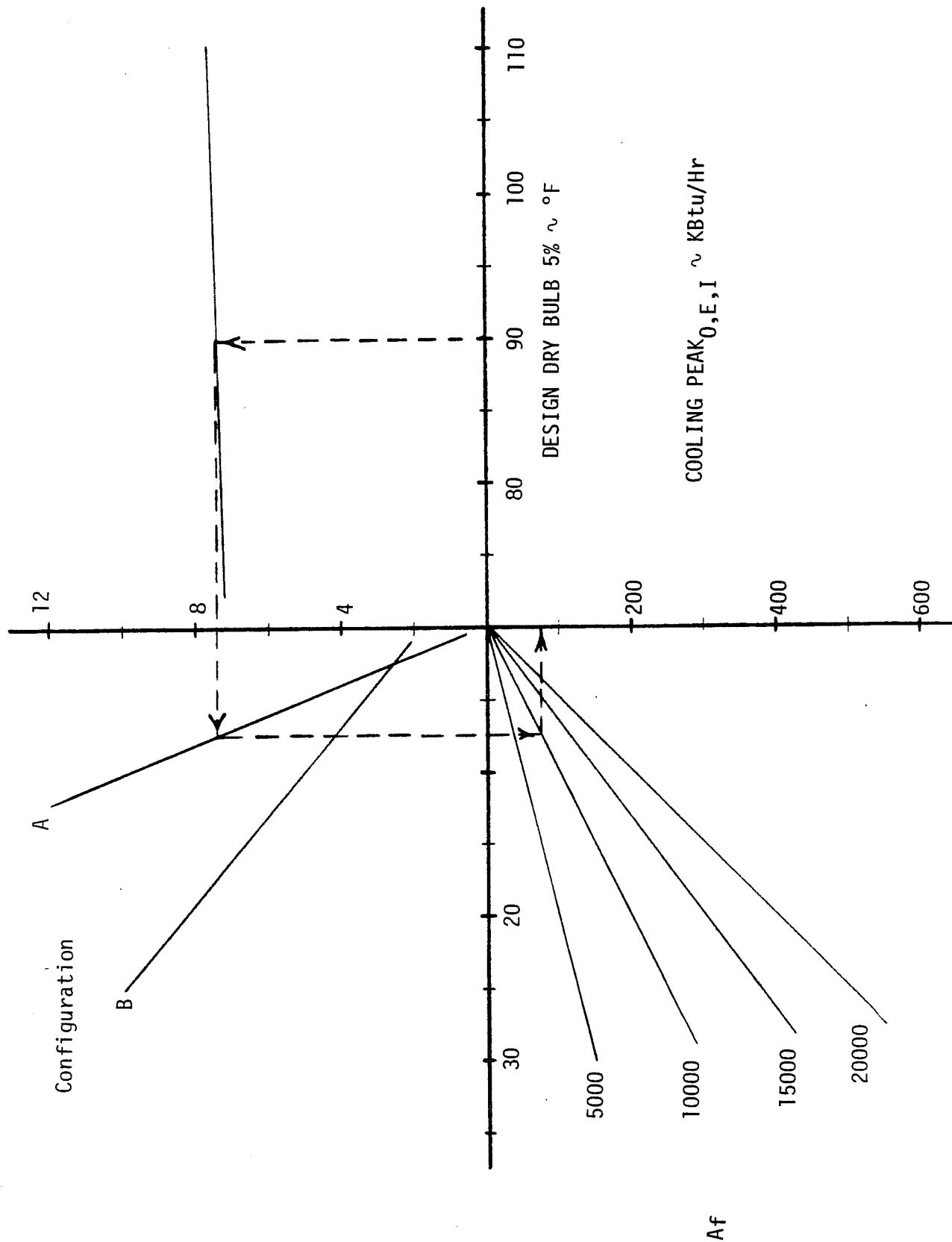
FIGURE 6.34   COOLING PEAK DUE TO LIGHTING - ROOFTOP
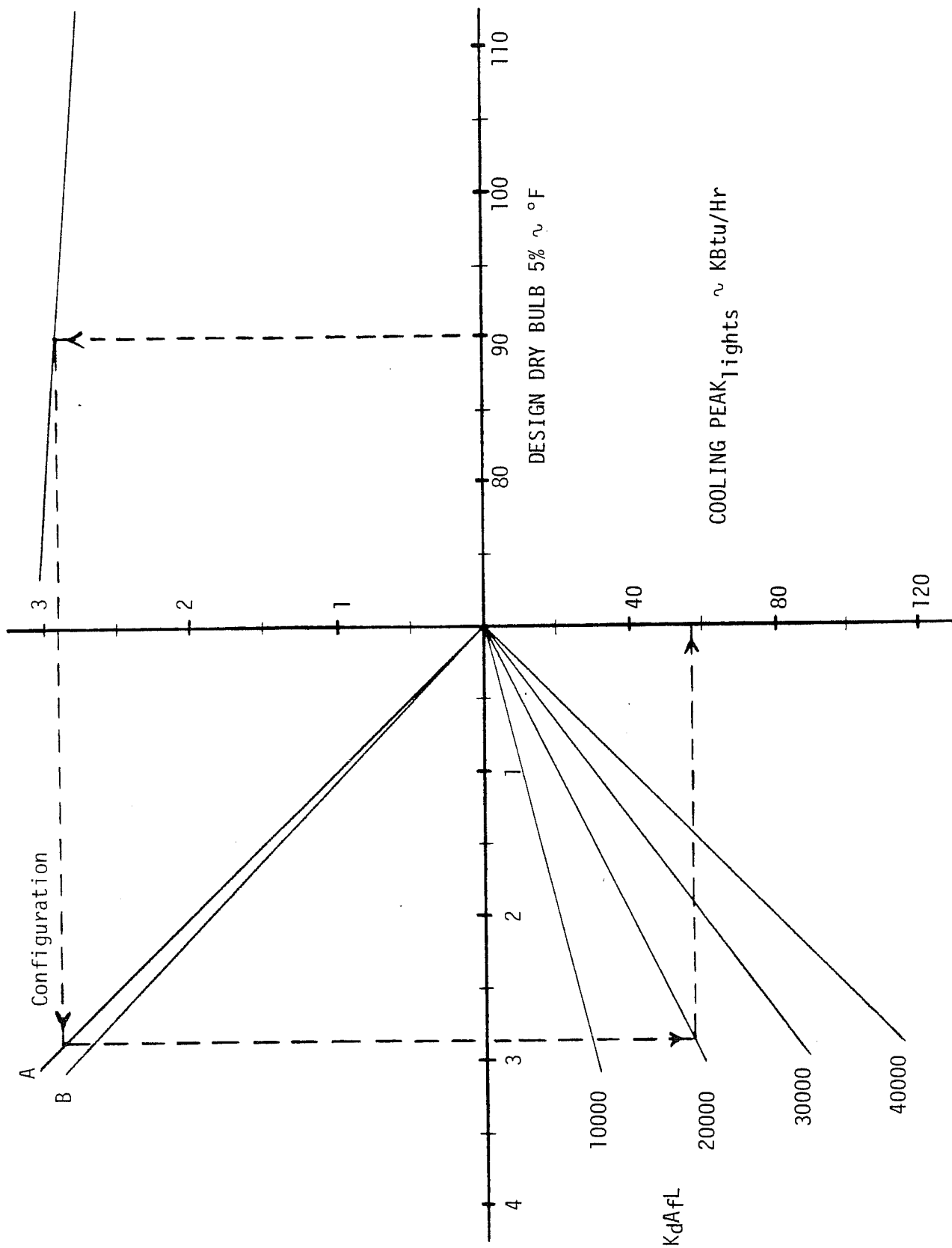
FIGURE 6.35   COOLING ENERGY DUE TO CONDUCTION - ROOFTOP

FIGURE 6.36   COOLING ENERGY DUE TO SOLAR RADIATION - ROOFTOP

FIGURE 6.37   COOLING ENERGY DUE TO LIGHTING – ROOFTOP

FIGURE 6.38 COOLING ENERGY DUE TO OCCUP, EQUIP, INF/VENT - ROOFTOP

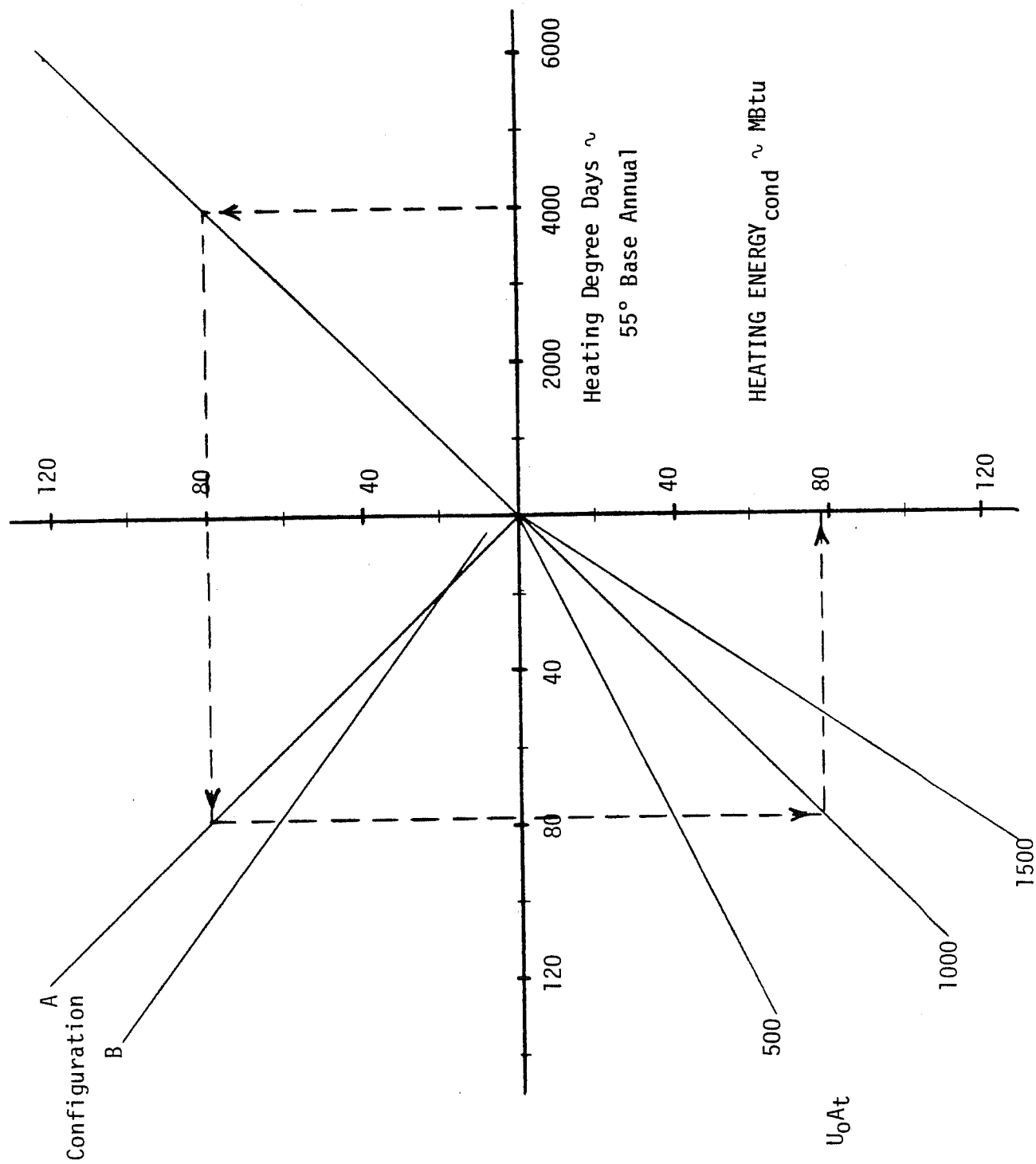FIGURE 6.39   HEATING ENERGY DUE TO CONDUCTION - ROOFTOP

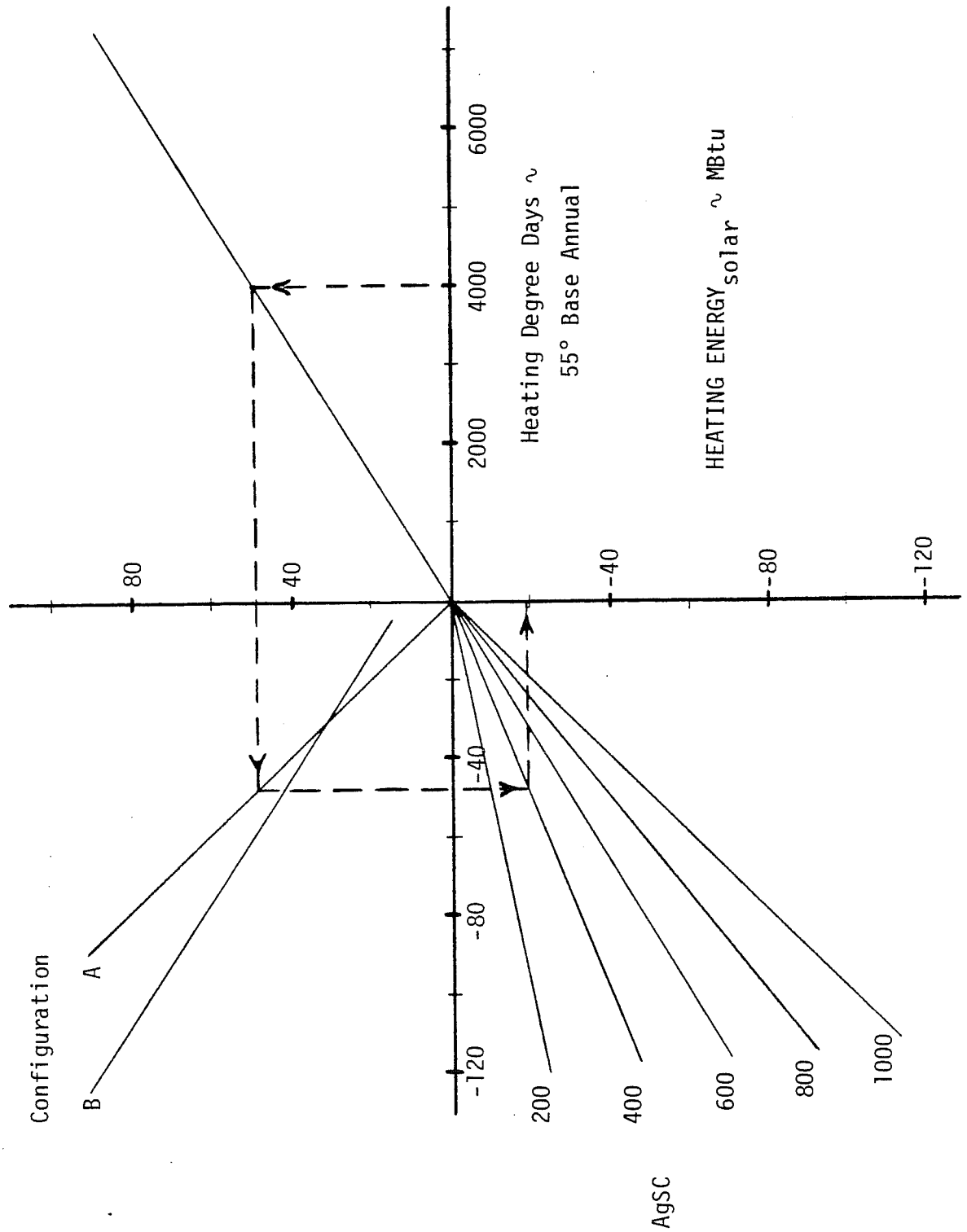FIGURE 6.40   HEATING ENERGY DUE TO SOLAR RADIATION - ROOFTOP
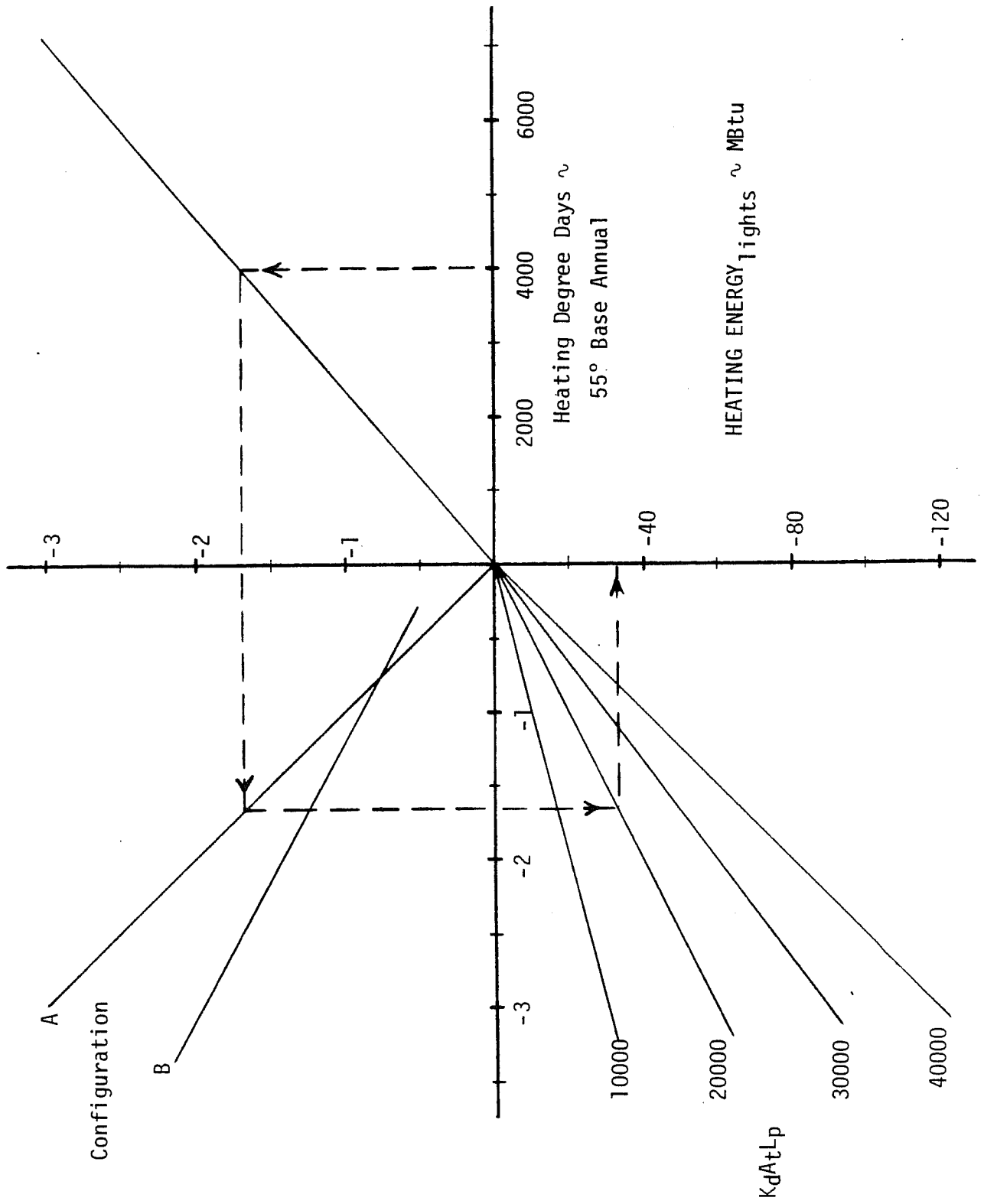
FIGURE 6.41   HEATING ENERGY DUE TO LIGHTING - ROOFTOP

FIGURE 6.42   HEATING ENERGY DUE TO OCCUP, EQUIP, INF/VENT - ROOFTOP